12-2007

A Generic Prognostic Framework for Remaining Useful Life Prediction of Complex Engineering Systems

Alexander V. Usynin
University of Tennessee - Knoxville

To the Graduate Council:

I am submitting herewith a dissertation written by Alexander V. Usynin entitled "A Generic Prognostic Framework for Remaining Useful Life Prediction of Complex Engineering Systems." I have examined the final electronic copy of this dissertation for form and content and recommend that it be accepted in partial fulfillment of the requirements for the degree of Doctor of Philosophy, with a major in Nuclear Engineering.

J. Wesley Hines, Major Professor

We have read this dissertation and recommend its acceptance:

Laurence F. Miller, Belle R. Upadhyaya, Lynne E. Parker, Aleksey M. Urmanov

Accepted for the Council:

Carolyn R. Hodges

Vice Provost and Dean of the Graduate School

(Original signatures are on file with official student records.)

To the Graduate Council:

I am submitting herewith a dissertation written by Alexander V. Usynin entitled "A Generic Prognostic Framework for Remaining Useful Life Prediction of Complex Engineering Systems." I have examined the final electronic copy of this dissertation for form and content and recommend that it be accepted in partial fulfillment of the requirements for the degree of Doctor of Philosophy, with a major in Nuclear Engineering.

_____

J. Wesley Hines, Major Professor

We have read this dissertation
and recommend its acceptance:

Laurence F. Miller
_____

Belle R. Upadhyaya
_____

Lynne E. Parker
_____

Aleksey M. Urmanov
_____

Accepted for the Council:

Carolyn R. Hodges
_____

Vice Provost and Dean of The
Graduate School

(Original signatures are on file with official student records)

A GENERIC PROGNOSTIC FRAMEWORK FOR REMAINING USEFUL LIFE PREDICTION OF COMPLEX ENGINEERING SYSTEMS

A Dissertation
Presented for the
Doctor of Philosophy
Degree
The University of Tennessee, Knoxville

Alexander V. Usynin
December 2007

ACKNOWLEDGMENTS

I want to thank and acknowledge all those who helped me in completing the Doctor of Philosophy in Nuclear Engineering. First, I thank my advisor, Dr. J. Wesley Hines, for scientific supervision and professional assistance throughout the course of my study. He freely shared his knowledge, his time, his guidance and support.

I would like thank my professors at the University of Tennessee, Knoxville. I am grateful to Dr. Miller and Dr. Upadhyaya for serving on my committee. I would like to express my sincere thanks to Dr. Lynne E. Parker for introducing me to reinforcement learning-based methods and for her willingness to serve on my committee.

A special note of thanks goes to Dr. Aleksey Urmanov for the time he spent discussing and shaping many of the ideas presented in this dissertation. I also would like to thank Dr. Andrei Gribok for useful and encouraging discussions.

I would like to take this opportunity to thank Dr. Dodds for fostering a friendly and creative environment in the department.

I want to express my profound gratitude to my family for their constant love and support.

BRIEF ABSTRACT

Prognostics and Health Management (PHM) is a general term that encompasses methods used to evaluate system health, predict the onset of failure, and mitigate the risks associated with the degraded behavior. Multitudes of health monitoring techniques facilitating the detection and classification of the onset of failure have been developed for commercial and military applications. PHM system designers are currently focused on developing prognostic techniques and integrating diagnostic/prognostic approaches at the system level. This dissertation introduces a prognostic framework, which integrates several methodologies that are necessary for the general application of PHM to a variety of systems. A method is developed to represent the multidimensional system health status in the form of a scalar quantity called a health indicator. This method is able to indicate the effectiveness of the health indicator in terms of how well or how poorly the health indicator can distinguish healthy and faulty system exemplars. A usefulness criterion was developed which allows the practitioner to evaluate the practicability of using a particular prognostic model along with observed degradation evidence data. The criterion of usefulness is based on comparing the model uncertainty imposed primarily by imperfectness of degradation evidence data against the uncertainty associated with the time-to-failure prediction based on average reliability characteristics of the system. This dissertation identifies the major contributors to prognostic uncertainty and analyzes their effects. Further study of two important contributions resulted in the development of uncertainty management techniques to improve PHM performance. An analysis of uncertainty effects attributed to the random nature of the critical degradation threshold, , was performed. An analysis of uncertainty effects attributed to the presence of unobservable failure mechanisms affecting the system degradation process along with observable failure mechanisms was performed. A method was developed to reduce the effects of uncertainty on a prognostic model. This dissertation provides a method to incorporate prognostic information into optimization techniques aimed at finding an optimal control policy for equipment performing in an uncertain environment.

ABSTRACT

Prognostics and Health Management (PHM) is a general term that encompasses methods used to evaluate system health, predict the onset of failure, and mitigate the risks associated with the degraded behavior. The term was coined by the U.S. military to include diagnostics, prognostics, and health management.

Multitudes of health monitoring techniques facilitating the detection and classification of the onset of failure have been developed for commercial and military applications. However, the techniques have traditionally focused on fault detection and isolation (FDI). PHM system designers are currently focused on developing prognostic techniques and integrating diagnostic/prognostic approaches at the system level. Of primary interest is the ability to detect degradation, identify failure modes, and predict how they evolve in time, given the current system health status in the form of various diagnostic measurements. PHM systems should also update their prediction in an online manner.

A systematic approach to fault detection/isolation/ and prognosis problems should be available for practitioners to meet the need for PHM systems that can be integrated into various engineering systems and that can function autonomously. This dissertation introduces a prognostic framework, which integrates several methodologies that are necessary for the general application of PHM to a variety of systems. One of the major hurdles in providing a usable PHM system is the fusion of multidimensional health status indicators. To solve this problem, a method is developed to represent the multidimensional system health status in the form of a scalar quantity called a health indicator. Reducing the dimensionality of the vector representing the system health status greatly facilitates development and practical use of prognostic models in the PHM framework. This method is able to indicate the effectiveness of the health indicator in terms of how well or how poorly the health indicator can distinguish healthy and faulty system exemplars. Using this method, the practitioner is able to intelligently select diagnostic information (degradation evidence) pertinent to the failure mechanisms present in the system of interest.

A multitude of prognostic models are currently being researched, but there is little guidance on which types of PHM systems should be used for different applications in which various types of sensed information are available. To fill this gap, a usefulness criterion was developed which allows the practitioner to evaluate the practicability of using a particular prognostic model along with observed degradation evidence data. The criterion of usefulness is based on comparing the model uncertainty imposed primarily by imperfectness of degradation evidence data against the uncertainty associated with the time-to-failure prediction based on average reliability characteristics of the system. Using the criterion of usefulness, the practitioner, who is oftentimes limited in the accuracy of the sensory equipment, is able to assess the expected benefit of using a given prognostic model with the uncertain diagnostic information. In the cases where the practitioner lacks prior knowledge of the failure mechanism characteristics, for instance, degradation rates, the criterion of usefulness is used as an indicator of how many degradation evidence data should be collected on the system of interest to provide a reasonable remaining useful life prediction.

The management of uncertainty in prognostic systems has become increasingly important as researchers are moving from general prognostic model ideas to actual applications. This dissertation identifies the major contributors to prognostic uncertainty and analyzes their effects. Further study of two important contributions resulted in the development of uncertainty management techniques to improve PHM performance. First, an analysis of uncertainty effects attributed to the random nature of the critical degradation threshold, which is an important prognostic model parameter, was performed. The revealed dependency between uncertainty in the critical degradation threshold and the model prediction uncertainty allows the practitioner to formulate practical requirements for a given prognostic model in terms of a maximum allowed critical threshold uncertainty. Next, an analysis of uncertainty effects attributed to the presence of unobservable failure mechanisms affecting the system degradation process along with observable failure mechanisms was performed. A method was developed to reduce the effects of uncertainty on a prognostic model. The method transforms the characteristic timescale in a prognostic model built on degradation data observed in the

presence of unobservable failure modes. The use of the transformed timescale effectively causes the prognostic model to approximate damage due to unobservable failure modes as a linear function of time.

The last element of a PHM system is to use the information to make informed decisions. These decisions are usually related to maintenance scheduling, but operational decisions may be even more important in critical applications. Lastly, this dissertation provides a method to incorporate prognostic information into optimization techniques aimed at finding an optimal operational control policy for equipment performing in an uncertain environment. The use of prognostic information greatly facilitates the search for an optimal control strategy in the case where limited information is available regarding the system dynamics and environmental conditions. Reinforcement learning techniques are employed and the integration of prognostic information provides vastly superior performance over strategies that do not use prognostics.

TABLE OF CONTENTS

LIST OF FIGURES

LIST OF TABLES

1. INTRODUCTION

1.1. Background

Real predictive capabilities are the important element among many interrelated functions and routines involved in Prognostics and Health Management (PHM). The term PHM pertains to methods that allow the practitioner to evaluate a system's actual health/damage conditions, and to predict the onset of failure, and mitigate the risks associated with an abnormal system behavior.

In published literature, PHM is traditionally considered to consist of three major components, which are Detection, Diagnostics and Prognostics. While the detection and diagnostics (isolation) portions have been well established for several past decades, the prognostics-related techniques have recently attracted much attention in many research studies. The reason for the growing interest in the development of prognostic methods is that the prognostic requirements for modern engineering systems and mission- and safety-critical components have become quite ambitious and present many challenges to the system design teams.

PHM has emerged as an alternative to traditional reliability prediction, run-to-failure functioning, and fixed-time scheduled maintenance. Traditional approaches to systems and components reliability should be questioned, since in many engineering applications the intrinsic lifespan of components and interconnections becomes significantly shorter than that of the systems within which they are used (Wilkinson et al. 2004). For example, the assumptions of essentially unlimited life and constant failure rate for electronics should be reviewed. System designers traditionally assume that the rising portion of the well-known "bathtub" reliability curve is unreachable enough to be out of concern in life cycle operations. This assumption has been historically correct, since the components' lifetime has been longer than the entire system's expected life. The advent of electronic components whose life is not longer than the system life makes the constant failure rate assumption invalid (Huber 2002).

In maintaining a fleet of complex engineering systems, one can identify many needs such as maximum asset availability, very low rate of “Returned Tested OK” components, minimum or no periodic inspections, low number of spare items, accurate parts lifespan tracking, minimum false alarms, etc. (Hess et al. 2005). Maintainers need to have the ability to accurately predict future health status and to anticipate problems and maintenance routines before downtime events. Predictive capabilities would let the maintainer perform a very beneficial maintenance strategy based on a "not on-failure nor per-schedule" basis. Some of the benefits provided by such an "on-condition" based maintenance are

- less time spent on inspection,
- better ability to plan maintenance,
- improved fault detection,
- increased asset availability.

Condition Based Maintenance (CBM), which is founded in root cause analysis, allows accurate physics-based diagnostic and prognostic determinations for nuclear plant equipment to be derived. Some research studies for understanding and controlling the aging processes of safety-critical nuclear plant components are currently in progress (Bond et al. 2000, Bond et al. 2002).

1.2. Original Contributions

The original contributions of this work lead to a systematic approach for developing data-driven (empirical) models and methods aimed at performing the tasks constituting the PHM framework. Although several approaches to the PHM implementation have been categorized in recently published literature, the proposed work considers degradation-based reliability assessment and prediction models.

This dissertation contains the following original contributions:

1. A method to represent a multidimensional health status of the system in the form of a scalar quantity called a health indicator. Reducing the dimensionality of the

vector representing the system health status greatly facilitates development and practical use of prognostic models in the PHM framework.

2. The criterion of usefulness, which allows the practitioner to evaluate the practicability of using a particular prognostic model along with observed degradation evidence data. The criterion of usefulness is based on comparing the model uncertainty imposed primarily by imperfectness of degradation evidence data against the uncertainty associated with the time-to-failure prediction based on average reliability characteristics of the system.

3. An analysis of uncertainty effects attributed to randomness in the critical degradation threshold, which is an important parameter of a prognostic model. The revealed dependency between uncertainty in the critical degradation threshold and the model prediction uncertainty allows the practitioner to formulate practical requirements for a given prognostic model in terms of a maximum allowed critical threshold uncertainty.

4. An analysis of uncertainty effects attributed to the presence of unobservable failure mechanisms affecting the system degradation process along with observable failure mechanisms. A method has been developed to reduce the uncertainty effects upon a prognostic model.

5. A method to incorporate prognostic information into optimization techniques aimed at finding an optimal operational control policy for equipment performing in an uncertain environment. The use of prognostic information greatly facilitates the search for an optimal control strategy in the case where limited information is available regarding the system dynamics and environmental conditions.

1.3. Organization of Document

The remainder of the dissertation is organized as follows. Chapter 2 gives a literature survey of common methods and models engaged in PHM offerings.

Chapter 3 introduces the notion of a degradation parameter. A few aspects of using a degradation parameter in the prognostic framework are discussed. A method to evaluate the appropriatness of a degradation parameter is developed.

Chapter 4 presents the uncertainty analysis performed with respect to the following sources of uncertainty that are commonly present in a prognostic model:

- imperfectness of reliability-related observations,

- randomness in the critical degradation threshold, and

- uncertainty effects due to unobservable failure mechanisms.

It also includes a method to mitigate the effect of uncertainty due to unobservable failure modes.

Chapter 5 discusses the use of prognostic information for finding an optimal operational control policy for equipment performing in uncertain environment and Chapter 6 concludes the dissertation and presents recommendations for future work.

2. LITERATURE REVIEW

This section provides a literature survey of the most common approaches and models used for Prognostics and Health Management in complex engineering systems. The survey will give a brief description of traditional reliability theory-based approaches, life consumption monitoring methods, stochastic modeling, and machine learning techniques aimed at making a remaining useful life (RUL) prognosis.

2.1. Introduction

A simple form of prognostics known as reliability analysis has been widely used for decades. The commonly utilized definition of engineering reliability is "Reliability is the probability of a device performing its purpose adequately for the period of time intended under operating conditions encountered" (Barlow 1998). Traditional engineering reliability concerns 1) analysis of failure data, 2) decisions regarding planned maintenance, 3) prediction regarding preliminary design (Barlow 1998), (Barlow 1975), (Martz 1982).

Failure data analysis is based on gathering information about how long the item operates before failure. Statistics collected from a large sample of similar items are estimated to draw conclusions regarding time-to-failure for a typical item. In reliability analysis, the object's lifetime is modeled considering only a static probability distribution that does not take into account condition data observed at the particular object of interest. The lifetime probability distribution,

$$F(t \mid \Theta) = P(T \leq t) \tag{2.1.1}$$

where t is some time, T is a random variable representing failure time, and $\boldsymbol{\Theta}$ is a vector of parameters, is the simplest probabilistic model for lifetime in reliability analysis. Often times the lifetime probability distribution is defined as the complement of the survival function

$$F(t \mid \Theta) = 1 - S(t \mid \Theta) \tag{2.1.2}$$

where S(t|Θ) is the probability that the failure time is later than some specified time.

$$S(t \mid \Theta) = P(T>t) \tag{2.1.3}$$

Given that the object of interest has not failed before the time *t'*, one can use the conditional lifetime distribution.

$$F(t \mid T \geq t', \Theta) = P(T \leq t \mid T \geq t', \Theta) \tag{2.1.4}$$

Based on the conditional distribution, the following expression is termed the expected residual life.

$$r(t) = E(T - t \mid T \geq t', \Theta) \tag{2.1.5}$$

The estimation of the expected residual life is performed given the fact that the object of interest has survived at a certain point of time. Any additional information regarding condition-monitoring observations can complement the parameterization of the model (Vlok 2002). A detailed review of the reliability data-analysis methods using degradation measurements rather than time-to-failure data is given in (Lu et al. 1993). In the following discussions, prognostics is defined as methodologies to predict remaining useful life (RUL), time to failure (TTF), or probability of failure (POF).

2.2. Cumulative Damage Models

The idea of using degradation measurements in assessing the item's reliability was pioneered by Gertsbakh and Kordonskiy (Gertsbakh 1969). A rigorous probabilistically founded description of degradation models is given by Bogdanoff and Kozin (Bogdanoff 1985). In this comprehensive study, the authors introduce a cumulative damage model. The cumulative damage is defined to be the irreversible accumulation of damage in components under a cyclical usage pattern. Although only mechanical components and usage are considered, the authors point out that the cumulative damage model is applicable to a variety of systems exhibiting any kind of wear accumulation.

The developed approach, which is called a "phenomenological model", does not explain the nature of failure, which is rarely understood completely in many real-world cases. Rather, the phenomenological model describes observable failure behavior.

In modeling the cumulative damage process, the emphasis is made on the following sources of variability.

- Random initial level of observed component damage.
- Different severity and order of the loads in successive duty cycles.
- Variable states of damage at the moment of retirement.
- Imperfections in inspection procedures causing additional variability in retirement times.

The authors propose using finite state Markov Chains (MC) to model the damage accumulation process over an item's lifetime under cyclic loadings. The possible levels of damage are represented by a finite set of numbers encompassing the state space of the Markov chain. The only allowed transitions are those that lead the MC to higher states. This reflects the fact that the degraded component cannot improve its health condition.

Although both discrete time and continuous MC are considered, the authors stress that the discrete time models are preferable because, from the engineering standpoint, the cumulative damage evolution is best described in terms of the number of load cycles (duty cycles) to which the system or component has been subjected.

The sources of variability are modeled using parameters of the defined MC. Variability in the initial state is given as a probability distribution over the initial state of the MC. Variability in the severity and magnitude of loadings is modeled by varying the transition probabilities with time and the cumulative damage state. Random states of damage at retirement and imperfect inspections are modeled by probability distributions defined over the damage states of the MC.

If a unit step restriction for the damage increments is assumed, the damage accumulation model is a pure birth process (Gross 1998), in which the damage accumulation process begins at State 1, then moves through States 2, 3,...b-1, and finally

ends up at State *b* (the failure state). A study of such processes is given in (Solovyev, 1972), which considers the use of birth-and-death processes in the renewal theory, which is an important part of the reliability analysis.

The study (Bogdanoff 1985) applies the proposed cumulative damage model to nine data sets of lifetime data. The real-world data sets are analyzed and modeled. The modeling routine usually begins with estimating the two parameters of the gamma distribution, either using the maximum likelihood method or the method of moments. If the estimated TTF distribution is not in accordance with the empirical distribution function, the model is extended. In all demonstrated examples, an adequate model was found. In most of the data sets, the simplest 2-parameter model was found to be sufficiently good to model the time-to-failure distribution function. However, a complex 16-parameter model was required to model the fatigue crack growth data (Virkler 1978). The authors also discuss how the cumulative damage model can be manipulated to predict a *typical* item's behavior under spectrum loading and accelerated lifetime testing.

Although the study does not point out how the proposed cumulative damage model can be used to predict a *particular* item's remaining useful lifetime, the mathematical formalism thoroughly described in the book can be adopted in a prognostic framework, which will be shown in Section 4.2.

A study performed by Myotyri et al. (Myotyri 2006) makes use of Markov Chain-based cumulative damage models. The developed model utilizes condition monitoring measurement data in prediction of a technical system's lifetime. The degradation of the system is represented as a stochastic process. A suitable conditional probability distribution serves as a model of the relationship between degradation state and condition monitoring measurements. The estimated degradation state is successively updated using a Bayesian rule as new measurement data become available. A generalized stochastic filtering approach to the RUL prediction problem is considered in (Pulkkinen 1991).

A key component of the stochastic model is a transition probability matrix for the discrete state Markov process. In the performed study the transition probability matrix is estimated using a deterministic model based on the Paris-Ergodan equation (Paris 1963),

which mathematically describes a crack growth process. Thus, the proposed model is based on information obtained from a specifically defined relationship rather than from a generalized source of information. The examples shown in the study are based in simulated data related to the crack length processes that are well studied in reliability literature. It remains unclear how the proposed method could be applied to the cases in which no deterministic model of the underlying phenomenon is available. The authors claim that the study will proceed by developing methods of estimating the model parameters from practical data rather than from a deterministic model. Also, validation of the proposed approach is claimed to be of primary interest in future research.

2.3. Integrating Condition Monitoring Information

The use of condition monitoring measurements in prediction of a system's remaining useful life has attracted much attention in electronics reliability, which is a field in which it is traditionally believed to be difficult to conduct degradation diagnostic and prognostic procedures. A review of the research in the field of prognostics and health management (PHM) for electronics is given in (Vichare 2006). The paper briefly describes the most up-to-date available methods for diagnostics such as built-in tests, canary devices, and mathematical methods dealing with failure precursors. The emphasis in the paper is on a prognostics technique based on the life consumption monitoring (LCM) methodology introduced by Ramakrishnan and Pecht (Ramakrishnanand 2003) The LCM methodology combines in-situ measured loads with physics-based stress and damage models to assess the life consumed.

2.3.1. Life Consumption Monitoring

A brief review of the LCM procedure is given in (Mishra 2004). The LCM is defined to be a prognostic methodology that consists of the following steps:

1. Failure modes, mechanisms and effects analysis,
2. Virtual reliability assessment,
3. Monitoring critical parameters,

4. Raw data simplification,
5. Stress and damage analysis, and
6. RUL prognosis.

Each step is briefly described and references to the mathematical models involved are given. Two case studies were performed to demonstrate the proposed methodology. The objects of interest in both studies were two identical printed circuit boards (PCB) placed under the hood of a car. The PCBs were subject to various stress conditions. Temperature and vibration were identified to be the strongest affecting factors. A failure modes and mechanisms analysis revealed seven different failure modes such as electrical short between traces, short between windings in the inductors populating the PCBs, and change in electrical resistance due to solder joint degradation.

Virtual reliability assessment revealed that the failure mode having the shortest time-to-failure was solder joint fatigue. The conducted assessment predicted 34 days to failure based on solder joint fatigue. The paper thoroughly describes the experiment design and obtained results; however, the following points need more clear explanation.

The authors define the failure moment to be an occurrence of fifteen "resistance spikes", which is an intermittent change in resistance of a solder joint. The choice of this number seems to be arbitrary. The authors assumed that the tested PCB became inoperable after occurrence of 15 spikes. A probabilistic justification of this threshold level was not given. Also, the sensitivity of the entire prognostic model with respect to the chosen threshold parameter was not determined.

The remaining useful life estimation was performed in an iterative manner. The life consumed on a particular day was subtracted from the estimated remaining life on the previous day, as suggested by the following equation.

$$RL(n) = RL(n-1) - Damage(n), \qquad (2.3.1.1)$$

where $RL(n)$ is the estimated remaining life on Day n, and $Damage(n)$ is the damage accumulated during Day n. The paper does not mention the initial value of remaining life RL(0) used in the iterative formula. According to the figures pictorially shown in the

paper, the initial estimates of remaining useful life were 57 and 65 days for the first and second case, respectively. However, it is unclear how exactly these estimates were obtained. Needless to say, in an iterative procedure the initial value is of primary importance in terms of numerical accuracy.

One more example of the usage of in-situ measured loads for electronics lifetime prediction is given by Pecht (Pecht 2004). The study presents a statistical characterization of the temperature profile usage of a notebook computer. Temperature measurements of the CPU heat sink and the HDD were taken for several months. The measurement data were analyzed statistically in terms of a probability density distribution of the following parameters.

- Absolute temperature values,
- Temperature cycle magnitude, and
- Temperature ramp rate.

A few deviations of the actual temperature loads from the worst-case operating conditions were found, for which the modern thermal management solutions are optimized.

Particularly, "the CPU heat sink was found to be 13°C and 8°C lower than its maximum rating (75°C) over 90% and 95% of the monitored time, respectively". The conclusion made here is that the findings can contribute to the design of a less-energy consuming thermal management scheme.

It was discovered that in around 1% of the observed temperature cycles, the temperature cycle magnitude (50°C) exceeded the standards for computer and consumer equipment (which are 30°C and 20°C, respectively). In the authors' opinion, "such a discrepancy between standardized and actual conditions provides a strong motivation for monitoring actual product application environments".

The obtained temperature ramp rate distribution also exhibited deviations from the worst-case ramp rate specifications. It was concluded that monitoring the actual ramp rate distribution would allow more accurate prediction of solder joint fatigue life.

The author's conclusions would be more convincing if the measurements were taken over several exemplars of notebook computers. This would allow the authors to make a statistically significant estimation of the deviations between the actually observed and standard-specified conditions. In the case of CPU heat sink temperature, a deviation of 12-16% seems reasonably conservative since the CPU usage observed in the experimentation was not as intensive as it could be in long-running computations using 100% of CPU time. The conclusions made upon the other parameter distributions seem arguable in terms of their statistical significance since the deviations in the estimated distributions can be due to the characteristics of the particular usage profile observed in the experimentation.

2.3.2. Machine Learning Techniques

In recently published prognostics research, a great deal of attention has been focused on the use of machine learning techniques such as artificial neural networks, fuzzy logic-based models, classification and pattern recognition methods (He 2006), (Zanardelli 2003), (Wegerich 2003), (Wang 2001), (Brotheron 2002).

A variety of neural network modifications have been applied to construct a prognostic framework. Wang and Vachtsevanos (Wang 2001) use dynamic wavelet neural networks as the prognostic system reasoner. A combination of radial basis function neural networks and rule extractors is applied to gas turbine engine prognostics by Brotheron (Brotheron 2002). Research performed by Byington (Byington 2003) makes use of polynomial neural networks that are trained on vibration data obtained from helicopter gearboxes. A Bayesian belief network is a main tool in Health Management System for avionics proposed by Parker (Parker 1993).

Chinnam (Chinnam 1999) proposes an approach that allows "determination of a component's reliability as it degrades with time". The proposed approach makes use of finite-duration impulse response neural networks (FIR-NN) for modeling degradation measures. Variation in the degradation measures is modeled using self-organized maps (SOM) (Haykin 1999). The paper emphasizes that the end user's interest is in the

reliability characteristics of a particular component rather than the population-average characteristics of a typical component.

An illustrative example of high-speed twist drills is given to demonstrate that the dispersion in the drill-bits lifetime is extensively large even though the tested drills came from the same manufacturer in the same box. The author claims that, in the presence of large variability in the drills lifetime, the end user would benefit from an online estimation of the component's reliability.

To justify the use of feed-forward neural networks (FFNN) for the degradation data analysis the author states that the FFNN are very effective for function approximation and time-series forecasting. Inherent properties of FFNNs, such as their ability to adapt to changes in environment via retraining, are claimed to be one of the motivations for using FFNN for individual reliability assessment.

To facilitate dispersion characteristic modeling, the proposed model makes use of self-organizing maps. It is stated that the use of SOMs allows one to estimate the prediction uncertainty without making the assumption of constant variance, which is known in statistics as a homoscedacity assumption. In fact, constant variance assumptions are made within each domain partitioned by the SOM.

The reliability prediction model is formulated to be a non-linear auto-regressive scheme:

$$y_s = f(y_{s-1}, y_{s-2}, \dots y_{s-p}) + \varepsilon_s \qquad (2.3.2.1)$$

The FIR-NN is designed to predict y_s, given the past p measurements. The proposed structure of the FIR-NN tends to be rather complicated since the designed neural network is claimed to have an ability to input many separate degradation signals and provide different prediction orders.

A few assumptions are made in the proposed reliability prediction model. The most important assumption is that the FIR-NN residuals are Gaussian distributed. Upon this assumption the further conclusions regarding the predicted reliability are drawn.

Namely, the predicted reliability function is expressed in the integral form on the degradation measure:

$$R(t \geq T_f \mid T_c) = \int_0^{y^*} g\left[\hat{y}(T_f)\right] dy \qquad (2.3.2.2)$$

where T_c is the current time instant, T_f is the failure time, y* is the critical threshold exceeding which indicates the failure, and $\hat{y}(t)$ is the output of the FIR-NN. The function g(y) is the probability density function of $\hat{y}(t)$, which is assumed to be the Gaussian function.

A real-world example is given to demonstrate the proposed technique. A series of drilling tests was conducted using 16 drill-bits. The obtained drill-bit's lifetime data and performance related measurements were used to train the FIR-NN for time-series forecasting. Two physical quantities, namely, thrust-force and torque, were chosen to be the performance indicators (degradation measures). The critical threshold values for the chosen degradation measures were taken to be precisely determined. The thrust-torque signatures from 12 randomly selected drill-bits were used to train the MIR-NN; the other 4 exemplars were used for testing purposes.

The description of the obtained results exhibits some degree of inconsistency that causes their engineering interpretation to be difficult. The performance of the tested drill-bits is monitored with respect to the number of holes a drill-bit has made. The choice of this type of duty cycle seems to be very reasonable, since the practitioner's primary interest is to know how many duty cycles the drill-bit will survive. However, the final results, presenting a conditional performance reliability of the tested specimens, are given with respect to a number of time intervals, whose relationship to the number of duty cycles is not clearly stated.

The estimated conditional performance reliability for the specimens is given without quantifying the associated uncertainty. This fact also makes the usage of the obtained results in an engineering application difficult. In other words, the practitioner is not supplied with the confidence level at which the provided results can be trusted.

Another serious drawback of the proposed methodology is the fact that the author does not pay much attention to the problem of overfitting, which is common for machine learning techniques such as neural networks. In the neural network-based analysis, neglecting the overfitting phenomena can cause significant deterioration in terms of the validity of the neural network generalization results.

Another example of the usage of neural networks to solve the reliability prediction problem is given in (Girish 2003). Girish et al. investigate an artificial neural network (ANN)-based methodology to predict system remaining useful life. As pointed out by the authors, the major motivation of using an ANN-based approach is that neural networks can usually be used without any assumptions regarding the functional form of the underlying model. Although this no-assumption feature of ANN-based methods makes them different from model-fitting methods, the proposed model includes an autoregressive component to simulate autocorrelation effects that can be observed in degradation data.

A multilayer feed-forward network is used for mapping the estimates of the distribution parameters of the degradation process. The degradation process is treated as a stochastic process, whose parameters are to be estimated. A set of artificial data is used to test and validate the proposed ANN-based technique. The data are generated according to the following expression

$$Y_t = a\, Y_{t-1} + \varepsilon_t + e^{kt} \qquad (2.3.2.3)$$

where Y_t is the degradation parameter value at time t, ε_t is the error term that is normally distributed with mean μ_ϵ and variance σ_μ^2. The non-linear component e^{kt} represents a deterministic trend observed in the degradation process. The parameter *a* is an autoregressive process parameter.

Two different ANNs are used to estimate the mean and variance of the artificial degradation data. The ANN input includes four variables that are time *t* and the lag terms Y_{t-1}, Y_{t-2}, Y_{t-3}. In other words, the proposed method is based on a time-delay-input neural network (Wasserman 1989). The objective is to provide a mapping of the time series

patterns that show autocorrelation properties and a time dependency as well. A detailed illustration of this type of problem can be found in Stern (Stern 1996).

2.3.3. Model Based Prognostic Approaches

Due to inherent drawbacks of artificial neural networks, such as a tendency to overfit data, difficulties in quantifying the model uncertainty, and an absence of strictly formulated methods to select the optimal network architecture, many researchers have focused their attention onto model-based approaches to solve the RUL prediction problem (Loecher 2003), (Xu 2005), (Carey 1991). Bankert et al. (Bankert 1995) propose a model-based diagnosis and prognosis methodology for rotating machinery. A rotor dynamics model is integrated with expert system-based interpretative capabilities to perform a predictive analysis of mechanical vibration data.

A new general purpose machinery diagnostic/prognostic algorithm for tracking and predicting evolving damage is developed in (Chelidze 2001). The algorithm makes use of available "macroscopic" observable quantities. The damage is considered to be a hierarchical dynamic system consisting of a directly observable subsystem featuring fast dynamic behavior and a hidden "slow" subsystem describing damage evolution. The method provides damage diagnostics and failure prognostics given only measurements from the "fast" component and a model of the slow component. The developed, and then extended, methodology is applied experimentally to an electromechanical system with a faulty supply battery (Chelidze 2004).

Carey and Koenig (Carey, 1991) perform a case study involving degradation of an integrated logic family (ILF). The ILF is a component of a Supervisory Logic Circuit, which is used in submarine cables. The case study is performed to evaluate the degradation of an important parameter of ILF. The degradation parameter is taken to be a propagation delay. If the propagation delay of a logic gate exceeds some threshold value, the logic circuit may fail in the system application. To predict changes in the ILF propagation delay characteristics, the authors utilize the following nonlinear regression model

$$y_n - y_0 = \Theta\left(1 - \exp\left(-\sqrt{\lambda t_n}\right)\right) + \varepsilon_n \qquad (2.3.3.1)$$

where y_0 and y_n are the propagation delays measured at t=0 and t=n, respectively, and ε_n is a normally distributed random variable with zero mean and standard deviation of σ. Θ and λ are the model parameters to be estimated.

Parameter Θ is assumed to be related to the concentration of impurities that are piled up at the sensitive area of the logical gate. Numerically, Θ represents the maximum change in propagation delay that will be reached after all impurities have diffused. Using the nonlinear regression model (2.3.3.1) one can predict the degradation level (the propagation delay) at any point in time. The extrapolation results shown in the paper are in accordance with the assumptions made with respect to the physical model of the aging process.

Another important assumption made in the paper is that the parameter Θ changes as temperature increases. This assumption is of importance since the degradation observations are taken at accelerated temperature stress conditions whereas the ultimate goal is to assess the degradation at the normal operating temperature level. The following regression model is proposed to describe the relationship between Θ and the temperature level.

$$\log(\Theta_{ij}) = A - \left(\frac{B}{kT_i}\right) + \eta_{ij} \qquad (2.3.3.2)$$

where Θ_{ij} is the maximum degradation to be reached by the j-th test device from the i-th temperature group, T_i is the value of temperature for the i-th group, k is Boltzmann's constant, A, and B are unknown coefficients to be estimated, η_{ij} is a random variable representing unobserved variability of the Θ_{ij}. Essentially, equation (2.3.3.2) is deduced from the Arrhenius Law (Laidler 1993).

It should be noted that the Θ_{ij} involved in Equ. (2.3.3.2) is not an observable quantity but an unknown parameter. One has to use the estimates of the Θ_{ij} obtained from the regression model (2.3.3.1) as an input for the regression equation (2.3.3.2). Having

estimated parameters *A* and *B* one is able to estimate the maximum degradation at the normal operating temperature level. Though the regression model (2.3.3.2) is evaluated on only three different temperature levels, the estimated confidence interval of the degradation at the normal temperature level allows the authors to conclude that the degradation of propagation delay observed at the normal temperature condition causes no concern for the reliability of the circuit.

Xu and Zhao (Xu 2005) make use of a logistic function to define a probabilistic measure used to quantify a likelihood of a failure given the degradation level of an object. The authors point out that there are many products, such as semiconductors, mechanical systems and microelectronics that exhibit a degradation failure mode. The degradation failure mode essentially means that there is some important degradation parameter gradually moving upward to a predefined threshold level. The degradation-based analysis is especially helpful when the number of hard failures observed in life data is few to none.

The paper considers a vector x of degradation measures:

$$\boldsymbol{x} = (x_1, x_2, \ldots x_m) \tag{2.3.3.3}$$

A degradation failure event is defined to be

$$F = \bigcup_{i=1}^{m} \{x_i > d_i\} \tag{2.3.3.4}$$

where d_i is the critical threshold value for the degradation measure. Since Equation (2.3.3.4) defines a failure event in discrete manner, the authors use a logistic function to quantify the probability of a failure given the degradation vector x defined in (2.3.3.3)

$$P(failure|x) = \frac{\exp\left(\sum_{i=1}^{m} \beta_i x_i\right)}{1 + \exp\left(\sum_{i=1}^{m} \beta_i x_i\right)} \tag{2.3.3.5}$$

The authors present an example where the given data set is of the following form:

{*Object ID, Degradation Parameter* x_1, *Degradation Parameter* x_2, *Failure Status*} (2.3.3.6)

The last column named Failure Status is populated with a boolean quantity indicating whether a failure has occurred (1 corresponding to a failure occurrence, 0 corresponding to no failure event).

Given the set of degradation data one has to estimate the coefficients $\boldsymbol{\beta}=(\beta_1,\beta_2\ldots\beta_m)$. Having obtained estimates of the $\boldsymbol{\beta}$ one is in possession of the probabilistic measure to evaluate the likelihood of a failure.

To describe the dynamics of the degradation process the authors make use of a state-space model of the following form

$$\frac{dx}{dt} = H(x,s) \qquad (2.3.3.7)$$

where $\boldsymbol{x}$ is a vector of degradation parameters, and s is a vector of random stress factors that affect the evolution of the degradation process. The paper considers the linear form of H(x,s). The results of the case study related to the reliability of light emitting diodes (LEDs) are presented in the paper. The proposed techniques are applied to evaluate the stress effect on LEDs and to predict their reliability under operating conditions. The degradation parameter is obviously chosen to be an LED's light intensity. A sample of LEDs is tested under three different stress levels that are the current of the LED.

Particularly, an automatic accelerated testing setup is designed to continuously monitor the failure times and the applied factors such as the current through the LED. Although the proposed method is able to take into account several degradation parameters, only one degradation measure is utilized in the case study. The temperature stress factor remains constant in all performed tests.

The data obtained from testing under stress levels 40 mA and 35 mA are used to estimate the model parameters. The data obtained at the third stress level of 28 mA are used to validate the model. A statistically sufficient number of 192 exemplars are involved in testing at each stress level. The reliability model is evaluated using simplified

equations derived from (2.3.3.5), (2.3.3.7) and the light intensity degradation data obtained in the performed testing. The authors present the estimated reliability of LEDs at the stress factor of 28 mA. However, the validity and uncertainty assessment of the presented results are not given in the paper.

2.4. Concluding Remarks

This section has reviewed several approaches to the problem of reliability assessment and prediction. Various mathematical techniques were shown to be applied to lifetime data as well as to degradation measurement data. Most of the reviewed techniques make use of a degradation evidence indicator, which is either an observable quantity or inferred value reflecting how the item's performance degradation evolves with respect to time units or duty cycles. In some cases the reliability prediction model is based on a deterministically formulated law of physics. Other methods give a purely stochastic description of the degradation process.

Purely stochastic approaches assume the degradation evolution to be a random process with certain parameters. The rigorously developed mathematical formalism related to random processes and Markov chain models allows one to estimate time-to-failure values as well as associated uncertainty. However, a major drawback of the purely stochastic methods is that degradation data exhibiting a complex behavior of degradation indicators require too many stochastic parameters to be estimated.

It has been shown that several machine learning methods, such as a variety of artificial neural networks, have been widely used to model complex relationships observed in reliability testing. However, quantifying uncertainty of the reliability prediction provided by a neural network is often a nontrivial task. More traditional machine learning techniques, such as regression methods, give an easy-to-understand interpretation of result uncertainty, but require strict assumptions in regards to distributions and dependencies observed in the available data.

In the following chapter the notion of a degradation parameter will be discussed. A method to represent a multidimensional health status of the system is introduced. The

following chapter also introduces the major components of the generic prognostic framework developed in the course of this work. An illustrative example is given to demonstrate a typical workflow of a PHM system designer developing a prognostic model. Major types of prognostic models are outlined. These are a linear growth model, and stochastic damage accumulation model.

3. DESCRIPTION OF PROGNOSTIC MODELS

The main motivation of using degradation data in the reliability analysis is that it allows the practitioner to evaluate the system reliability model in the absence of a large amount of failure data. The lack of failure data is the common situation for a) highly reliable components, such as electronic elements, and b) the cases where running the component to a failure is impractical or unsafe.

Another important aspect of degradation-based reliability assessment is that degradation data can be used as a descriptor of a particular degradation profile, thus providing an individualized reliability assessment and prognosis. Of practical importance is the ability to assess and predict the reliability attributes of the system or component at hand. The traditional reliability analysis is mostly based on statistical characteristics, such as central moments and low-level quantiles of the probability distribution function (PDF) formed by available failure data. The assumption made in the traditional reliability analysis is that the conditions, at which the systems or components operate, are relatively homogeneous such that the systems are considered to be a population of items possessing similar reliability properties. The assumed similarity among the population items implies that the reliability properties evaluated as statistical quantities are mostly relevant to the averaged item placed in the averaged operational environment. The individual characteristics tend to be lost in the statistical treatment of the entire population of items.

Degradation-based reliability assessment makes use of the data collected when the operating component is undergoing some degradation of its operational characteristics due to some failure modes. Although the component has not failed yet, it shows some indications of its degraded operational characteristics, which can be considered as a fault. The degradation or damage tends to accumulate in time. Damage accumulation is defined to be the irreversible degradation process that takes place throughout an item's lifespan, and ultimately causes the item to fail. The definition of the accumulated damage includes a variety of phenomena such as corrosion, wear, creep, fatigue, electrolysis, electro-migration, etc. The particular phenomenon to which the damage accumulation is due is

called a failure mechanism. In many practical situations the item exhibits a mixture of failure mechanisms causing the damage accumulation. However, this study assumes the damage accumulation model to be due to the dominant failure mechanism, which produces the fastest damage accumulation rate. The damage accumulation model is considered as a "replacement of the complex physical reality by some more idealized (approximate) hypothetical system" (Bartlett 1975).

When developing such a model several issues should be considered. First, the damage accumulation model should be able to describe the item's behavior in terms of its operational state. The model should include as few parameters as possible, but the number of included parameters should be sufficient to encompass the failure mechanisms in a complete fashion. A model with unnecessary complexity will tend to generalize poorly. Secondly, the model should be easy to implement computationally and lastly the model should be interpretable in terms of known physical laws.

Considering the damage accumulation model, one's primary interest is the evolution in time of the damage accumulated in the item under operational loadings. Of specific interest is the time to reach a predefined level of damage at which the system or component no longer meets it specifications. This time is called the failure time or the item's lifetime. As soon as the component acquires some critical amount of damage the component is said to fail in providing its function and requires an immediate replacement.

It is possible to use the term "degradation model" in describing the damage accumulation model outlined above. In the following sections, the terms "damage accumulation" and "degradation" will be used synonymously. Hence the important element of the degradation-based reliability analysis is the notion of a critical degradation threshold.

The advantages of using the degradation-based reliability prediction is primarily pertinent to the possibility of performing an individually-oriented reliability prognosis. Having observed the degradation profile of a given component placed in particular operational conditions, one is able to predict the reliability characteristics such as the component's remaining useful life and the probability of failure for any given time

instant. However, the ability to predict the individual remaining useful life is achieved at the expense of having some mathematical, usually probabilistic, model for describing the future progression of the degradation process.

This section outlines major approaches to degradation-based reliability assessment and prognosis. In Section 1, the notion of a degradation parameter is defined. Section 2 introduces a method to evaluate the degradation parameter, given a multidimensional vector of health indicators observed at the system of interest.

3.1. Notion of Degradation Parameter

The main aspects of a generic prognostic framework can be outlined as follows. At the basis lies a failure mechanism that affects the component's functionality within some characteristic timescale and eventually causes the component to fail. The characteristic timescale can be expressed in calendar or usage time, numbers of duty cycles, or any other units expressing the component's characteristic age.

The failure mechanism is expected to manifest itself as an observable phenomenon. The indications of the fault progression can be directly observable in the form of quantities closely related to the failure mode. If there are no observable measures pertinent to the failure mode, the indications can be quantified through the use of various observable variables that are distantly related to the failure mode.

The failure progression is to be modeled via the usage of a suitable mathematical model, which is usually of a probabilistic nature. One uses historical data observed on the component of interest or analogous items in past to a) evaluate the assumed model, b) verify the assumptions and c) produce RUL prognosis. Since the mathematical model serves for prediction purposes, it is usually called a *prognostic model*.

Although the prognostic model can be of various forms, it is practical to assume that the model operates in a two-dimensional space R^2: (T,D), where T is the characteristic timescale, and D is a quantity characterizing the component's ability to perform its specified functions properly. The time variable T is assumed to be an

independent parameter. D is a dependent parameter called a *degradation or prognostic parameter*.

The essence of the prognostic parameter is that its value is stochastically related to the probability of failure. Let η(t) denote a random parameter associated with the component reliability. Let τ denote the lifespan of the component; η' is the history of measurements of the η(t) taken up to time *t*. The parameter η(t) is called prognostic parameter if the following equation holds.

$$P(t < \tau \le t + \Delta t \mid \eta', \eta(t) = \eta, \tau > t) = P(t < \tau \le t + \Delta t \mid \eta(t) = \eta, \tau > t) = \\ = \lambda(\eta)\Delta t + o(\Delta t) \qquad (3.1.1)$$

where λ is a certain function which relates the prognostic parameter η(t) to the conditional probability of failure P. Equation (3.1.1) implies that the conditional probability of failure depends only on the currently observed value of η(t) rather than on the entire history of η(t). Generally speaking, λ(t) can be considered as a generalized failure rate. (Gertsbakh 1977)

The basic idea behind the usage of degradation data for reliability prediction is that components sampled from the population tend to degrade differently even if placed in identical operational conditions. In particular, the components tend to degrade at different degradation rates. If the degradation rates are identical for the entire population, the use of a degradation-based prognostic framework will not derive any benefit compared to the case of using the traditional failure time-based approach. In such a case tracking the degradation parameter does not bring any useful information since the degradation paths for different items are identical to each other. This situation is similar to the failure time based reliability analysis which essentially uses the component's age as the prognostic parameter, η(t) ≡ t. In the terms of degradation-based prognostic model, it appears as a degradation path which progresses linearly with the slope value of 1 for each item in the population.

Being capable to monitor indications of the component degradation, one can determine the component's individual response to the various stressors affecting the component reliability. Combining prior knowledge of failure mechanisms contributing to

the component degradation and the component individual degradation profile, one predicts reliability characteristics pertinent to the particular component at hand. The reliability prognosis is no longer treated as a quantity characterizing an average item taken from the population, but rather it produces a reliability estimate for a specific component of interest.

The definition of the prognostic parameter given in Equation (3.1.1) requires that there is some value of the prognostic parameter, called the critical threshold, exceeding which the component exhibits the probability of failure such that it is no longer safe to continue operation. In many applications the critical threshold is considered to be a strictly defined value. This assumption greatly simplifies the reliability computation, and provides a reasonable model for the critical reliability conditions encountered in real-world applications. In some cases the critical threshold cannot be strictly determined. For example, if the designer is not aware of the precise level of degradation that causes a failure, it is appropriate to represent the critical threshold as a probability distribution function that reflects the designer's vague knowledge about possible critical values. Additionally, the system or component may be used in a variety of applications each of which requires some particular level of critical degradation. In such a case, it seems reasonable to define the critical threshold as a range of critical values having certain probabilities. The aspects related to randomness in the critical degradation threshold are considered in Chapter 4. In the following section a method for degradation parameter selection is proposed.

3.2. Selection of Degradation Parameter

Degradation models are based on probabilistic treatment of a collection of degradation paths formed by the dominant failure mechanism that degrades the component reliability. Degradation paths evolve in the space of a degradation measure (indicator) that quantifies the unit's ability to operate in accordance with its specifications. In the literature, sometimes several degradation indicators are considered to quantify the component reliability. To simplify the analysis, the degradation indicators

are usually grouped together to form the health indicator (status), which is usually a scalar rather than a vector quantity.

One of the major difficulties in implementing the generic prognostic framework is to find a practically suitable and mathematically tractable representation of the degradation (damage accumulation) processes. In a simple case, the representation is defined in terms of one-dimensional Markov-type stochastic process. In reality, complex systems are rarely described well enough with a one-dimensional parameter. Usually the state of a system is given in the form of a multidimensional process.

$$\boldsymbol{\eta}(t) = \left(\eta_1(t), \eta_2(t), \ldots \eta_n(t)\right) \qquad (3.2.1)$$

Of practical interest is to develop a strategy in which the practitioner would be able to perform CBM routines given observations of the multidimensional vector process $\boldsymbol{\eta}(t)$. One possible way to accomplish this task is to find interdependencies among the stochastic processes populating the vector process $\boldsymbol{\eta}(t)$. For example, if some processes $\eta_k(t)$ are functionally dependent on the others included in $\boldsymbol{\eta}(t)$, it is possible to reduce the dimensionality of the vector process $\boldsymbol{\eta}(t)$, since only a few independent processes of the vector process $\boldsymbol{\eta}(t)$ provide useful information.

However, in reality, such a dimensionality reduction can be difficult because of the high complexity of the interdependencies, or it may be impossible due to the complete independency of the considered processes.

Another solution to the problem is to consider the processes $\eta_k(t)$ separately. Assuming that each process η_k reflects a damage process affecting a certain part of the system, one monitors damage in the system parts separately. Thus, maintenance decisions are made independently. For example, a system consisting of two major parts may need to have two preventive maintenance schedules developed for the two parts independently.

However, performing several preventive maintenance schedules on a piece of equipment could be difficult and impractical, since each component in the multidimensional stochastic process $\boldsymbol{\eta}(t)$ would require its own probabilistic model. This issue tends to be even more complicated since, in reality, the practitioner can never

observe the multidimensional state of the system perfectly. Observations made on the system of interest are usually disturbed by various random factors such as measurement noise, partial repairs, random breakages, etc.

Formally speaking, the difficulties attributed to the use of a multidimensional state description are due to the fact that a simple notion of critical threshold, which was discussed in previous sections, is replaced with a more complex notion of critical multidimensional region. Dealing with multidimensional entities could lead to a) high-level uncertainties due to imperfect observations available to assess the multidimensional model, and b) an intensive computational burden, which could be highly undesirable in on-line applications.

A simple, yet practical, solution would be to make maintenance decisions primarily regarding one single parameter reflecting the overall "health" status of the system. Such a parameter should account for all the degradation processes $\eta_k(t)$ taking place in the system. The multidimensional vector $\boldsymbol{\eta}(t)$ should be replaced by a scalar process $r(t)$, which is a function of the vector components $\eta_k(t)$, k = 1,2,…n:

$$\mathbf{r}(t) = \phi(\eta_1(t), \eta_2(t), \ldots \eta_n(t)) \qquad (3.2.2)$$

The scalar process $r(t)$ is expected to inherit the properties of the vector process $\boldsymbol{\eta}(t)$ in the sense that observing the process r(t) the operator is able to assess the current health condition of the system as well as if they observe the multidimensional process $\eta(t)$. The important attribute that ensures the ability of the process r(t) to reflect the system health status is the ability to discriminate failed systems from non-failed (healthy) systems. This leads to the idea of using discriminant analysis to find a good transformation of the vector process $\boldsymbol{\eta}(t)$ to a scalar process $r(t)$. (Gertsbakh 2000) proposed to use a linear transformation chosen in a certain manner to evaluate a scalar health indicator. The key idea of using the linear discriminative analysis is outlined as follows.

Consider a population of systems that is divided into two subpopulations A and B corresponding to healthy and failed exemplars. For each exemplar there is an n-dimensional vector snapshot indicating its health status in a particular time instant t.

$$\mathbf{x}_j(t) = (x_{j1}, x_{j2}, \ldots x_{jn}) \qquad (3.2.3)$$

Each part of the population includes a certain number of exemplars, x_k^A, x_l^B, $k=1,2,\ldots N_A$, $l=1,2,\ldots N_B$.

The vector health status snapshot is replaced by a linear combination of the elements x_{ji}.

$$r_j = \sum_{i=1}^{n} w_i x_{ji} \qquad (3.2.4)$$

The scalar value of r_j can be thought of as a weighted average of the elements x_{ji}, which are the degradation indicators attributed to particular components of the system.

The idea of linear transformation is illustrated in Figure 1, which shows a 2-dimensional case of the vector process $\boldsymbol{\eta}(t) = (\eta_1(t), \eta_2(t))$.

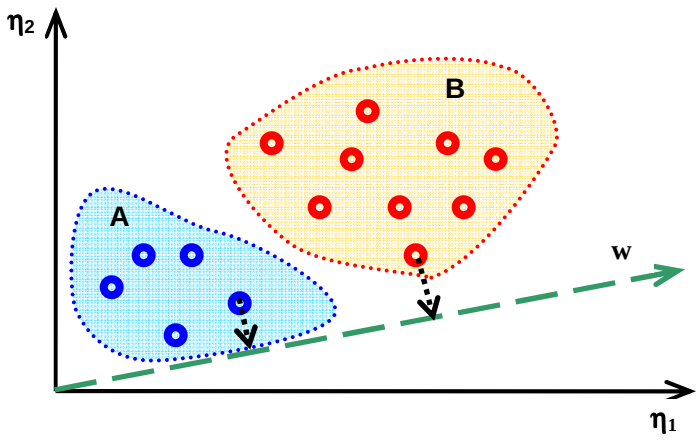

Figure 1. A schematic representation of the vector w that provides a direction, upon which the 2-dimensional vectors of the system health status are projected.

The linear transformation (3.2.4) is essentially a geometric projection onto some line collinear to the vector $\mathbf{w} = (w_1, w_2, \ldots w_n)$. Obviously there are many possible choices for the direction of the vector **w**. However, following the linear discrimination ideas, one seeks the direction that would allow for the best discriminative capability of the new transformed scalar health index r(t).

Studies performed by Fisher (Fisher 1936) suggest that the direction **w** should be chosen such that the following ratio is maximized

$$D = \frac{\mathbf{w}^2(\mu_A - \mu_B)^2}{\mathbf{w}(S_A + S_B)\mathbf{w}^T} \tag{3.2.5}$$

where μ_A, μ_B are the mean values (the mass centers) of Subpopulations A,B, respectively; S_A, S_B are the variances of the samples belonging to Subpopulations A,B. Therefore, the optimal direction **w,** that linearly discriminates the parts A and B is that which maximizes Equation 3.2.5.

It is well known that the maximum of D is attained if the vector **w** takes the following value.

$$\mathbf{w} = \frac{\mu_A - \mu_B}{S_A + S_B} \tag{3.2.6}$$

Another approach to the problem of discriminating healthy and failed exemplars within a population is to apply a more general technique, which is the Neyman-Pearson lemma (Hoel, 1971). The Neyman-Pearson lemma states that the likelihood-ratio test which rejects hypothesis H_0 in favor of hypothesis H_1 when

$$\Lambda(x) = \frac{L(\Theta_0 \mid x)}{L(\Theta_1 \mid x)} \leq k \tag{3.2.7}$$

is the most powerful test of size α (Tamhane 2000)

In practice the likelihood-ratio test is used in the following manner. Let Subpopulations A and B have some probabilistic properties characterized by the density functions $p_A(x)$ and $p_B(x)$. Given a vector x_q, one computes the likelihood ratio

$$\Lambda(x_q) = \frac{p_A(x_q)}{p_B(x_q)} \qquad (3.2.8)$$

If the computed ratio exceeds some predefined level, K, whose magnitude depends on the test's size α, one accepts the hypothesis that the vector x_q was observed at an exemplar belonging to Subpopulation A.

However, it should be noted that the maximal power of the likelihood ratio test is achieved if the probabilistic characteristics p_A, p_B of Subpopulations A and B are known precisely. In practice, it is difficult to estimate density functions of multidimensional data populations, especially if one has limited data available for estimation.

A method to discriminate multidimensional data that reflect the system health status is developed in this work as follows. A non-linear classifier, such as a Support Vector Machine (SVM)-based technique, is applied to construct a classifier, which produces a scalar feature value indicating whether or not a query multidimensional vector **x** is observed at an exemplar belonging to the population of healthy systems. A SVM-based classifier is a function which returns positive or negative values for vectors belonging to the primary or alternative hypothesis class, respectively.

The following is the algorithmic representation of the maintenance routine based on using a SVM-based discriminator.

Step 1. (Collection Phase) One collects observations of the vector process $\boldsymbol{\eta}(t)$ on two samples of the systems. Sample A is composed of systems that exhibit little degradation and can be considered as "brand new". Sample B is composed of the systems that have accumulated a significant amount of degradation and can be considered as being close to failure. It should be noted that the collected data are accompanied with qualitative labels indicating the health status of the monitored system, for instance, "good" and "faulty". These qualitative labels are provided by experts or via off-line inspections that are allowed to be performed in Step 1. Step 1 is essentially a preparation phase for acquiring of initial knowledge that will be used as a basis (training information) for the online SVM classifier. The more

information about the degradation mechanisms that is acquired in Step 1, the better the results that are obtained in the following steps.

Step 2 (Training Phase). One evaluates the SVM classifier parameters using the data collected in Step 1. Essentially this step includes adjusting the SVM parameters (training). Having optimized the SVM parameters, one may need to validate the SVM classifier with respect to its ability to discriminate multidimensional health status vectors. Applying the SVM model to an observed n-dimensional vector **x**, one reduces the observation **x** to one-dimensional feature value *r*. A validation dataset composed of vectors not used for training of the SVM classifier is utilized to evaluate the discriminative ability of the scalar health indicator r(t). Figure 2 shows an comparative example of the histograms of r(t) values computed on Samples A and B, which were introduced in Step 1.

A good health indicator makes a large margin between the new and degraded exemplars, whereas the overlap in the health indicator values index shown in Figure 2b makes it difficult to distinguish exemplars in terms of their health indicator *r(t)*.

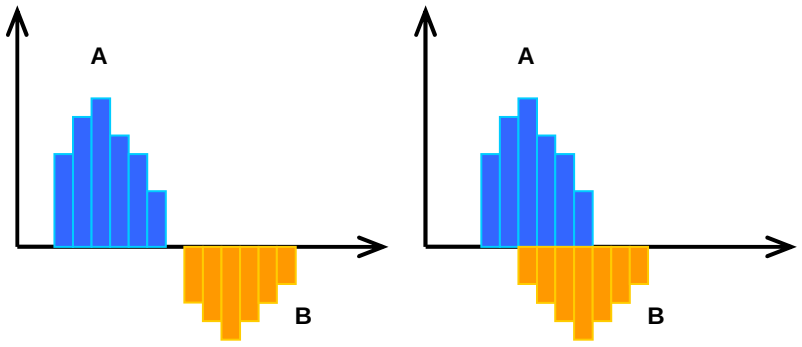

Figure 2. Typical examples of a good (a) and poor (b) discriminative capabilities of a classifier.

Step 3. (Selection of Prognostic Model) One seeks an appropriate probabilistic description of the scalar process r(t). The range of possible candidates is usually wide, starting from linear regression models to stochastic high-order Markovian models. Since the process *r(t)* is of one-dimension it is relatively straightforward to find out which type of model is best suited for the observed realizations of the process *r(t)*. Having defined the probabilistic model for *r(t)*, one introduces set-points for the model. For instance, the first set-point can be the level, exceeding which the process *r(t)* indicates that the system needs preventive maintenance; however, it is still able to function. The second set-point is the level, exceeding which the process *r(t)* indicates that the system's health status is critical, and the system cannot continue functioning within its specifications. The specific values for the set-points are usually case-dependent.

Step 4. (Monitoring Phase) One monitors the health status of the system through observing the multidimensional vector process $\eta(t)$ of the system in operation. Applying the SVM-based transformation defined in Step 2, one evaluates a one-dimensional health indicator *r(t)*. The values of *r(t)* computed through the system's lifespan forms a trajectory in a two-dimensional space of *t* and *r*. The observed trajectory of the health indicator *r(t)* provides information that is used to make a prognosis of remaining useful life of the system. The prognosis is made via evaluating the prognostic model defined in Step 3. The RUL prognosis is utilized for a multitude of purposes primarily aimed to increase assets availability, reduce cost associated with maintenance etc. As soon as the observed process *r(t)* passes the first set-point, preventive maintenance is requested for the particular system where the *r(t)* is observed.

The proposed method for evaluating the scalar system health indicator *r(t)* has advantages over the linear discriminator proposed in (Gertsbakh 2000) in the sense that the margin area, which divides healthy and faulty exemplars, can appear to be non-linear.

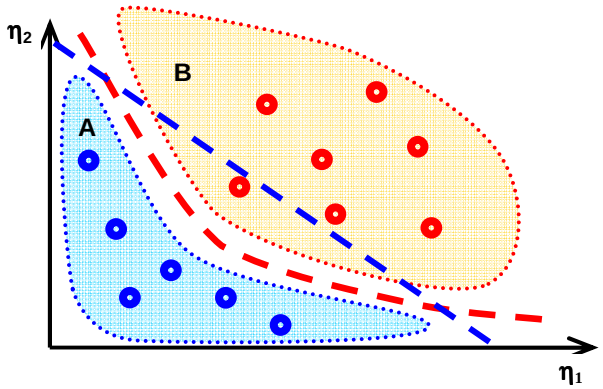

Figure 3. A schematic representation of linear and non-linear discriminators.

The cause of the margin non-linearity can be explained in the following qualitative example. Consider a system whose health status is characterized with two indicators, η_1 and η_2 (Figure 3). Essentially, the health indicators η_1 and η_2 correspond to two failure mechanisms H_1, H_2 observed in the system of interest. The values of η_1 and η_2 numerically quantify the extent at which the failure mechanisms H_1, H_2 affect the system overall health status.

The blue-colored dashed line is a linear discriminator, which performs acceptably well in the cases where values of either η_1 or η_2 are relatively large. Such cases correspond to the situations where only one of the failure mechanisms H_1 and H_2 is dominating in the system degradation process.

It should be noted that the linear discriminator is expected to work perfectly if the overall damage effect the system receives while in operation is, in fact, a linear combination of the degradation mechanisms η_1 and η_2, as given in the following equation:

$$D(t) = \alpha_1*\eta_1(t) + \alpha_2*\eta_2(t), \quad 0<=\alpha_{1,2}, \ \alpha_1+\alpha_2 = 1 \qquad (3.2.9)$$

where D(t) is the overall degradation effect the system is receiving due to the failure mechanisms.

However, in the case where η_1 and η_2 both exhibit moderately large values, the linear discriminator performs poorly since the true discriminator curve is fairly nonlinear (the red-colored dashed curve). The nonlinearity is due to the fact that if both failure mechanisms appear in a moderately large extent, the degradation effects imposed by the failure modes tend to be amplified because of the failure mechanisms interaction.

Numerically this situation can be expressed as a nonlinear relationship between the overall damage effect and the degradation indicators η_1 and η_2.

$$D(t) = \alpha_1*\eta_1(t) + \alpha_2*\eta_2(t) + \alpha_3*f(\eta_1,\eta_2)\ , \quad 0<=\alpha_{1,2,3},\ \alpha_1+\alpha_2+\alpha_3= 1 \qquad (3.2.10)$$

Where $f(\eta_1,\eta_2)$ is a non-linear function of the degradation indicators.

As can be seen, the nonlinear term in (3.2.10) introduces a good deal of nonlinearity in the behavior of the system with respect to the critical degradation level.

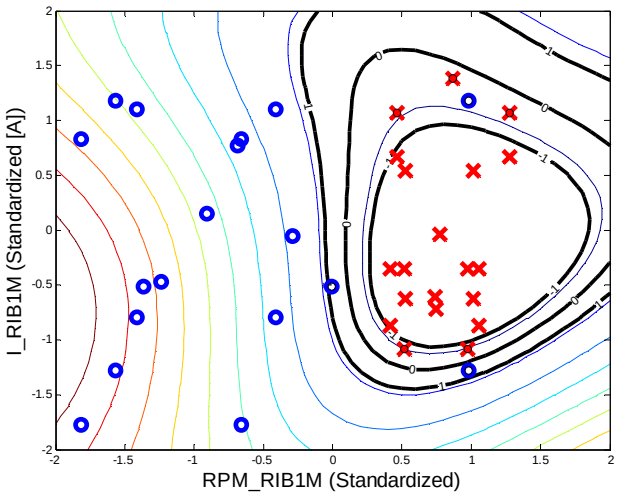

Figure 4. An example of a non-linear margin between healthy and faulty exemplars. The example is based on real-world data

The following example illustrates the use of a non-linear classificator applied to real-world data.

Consider a drilling machine performing a drilling campaign. The operational status of the drilling machine is expressed in terms of 31 parameters; a few of them are given below.

- Hydraulic Unit (HU) Pressure
- HU Target Pressure
- HU Current
- HU Motor RPM
- Annular Pressure
- Borehole Pressure
- Acceleration Sensors X,Y,Z
- Magnetometers X,Y,Z
- Voltage At Alternator
- Temperature
- Stick Slip

The operational parameters are continuously monitored and collected, while the drilling machine is operating.

While in operation, the drilling machine may experience certain faulty conditions, which manifest themselves through the presence of abnormal values in the operational parameters. It has been revealed that a certain fault manifests itself mostly in two particular operational parameters. These are *HU Current* (I_RIB), and *HU Motor RPM* (RPM_RIB).

Figure 4 shows the values of the parameters plotted against each other. Blue-colored circles indicate the states where the drilling machine health status was found to be normal. Red-colored crosses indicate the states where the fault was detected, and the drilling machine health status was no longer normal.

The data shown in Figure 4 were collected on 4 different drilling machines through their operational lifespan. All drilling machines experienced the same type of fault. Although the total number of observations collected on each drilling machine is a large quantity, 5 datapoints were selected as the most representative vectors for normal and abnormal conditions. Thus each drilling machine has provided 10 data points depicted in Figure 4. An SVM-based classifier is applied to the data to evaluate the feature value (system health indicator), according to which one can distinguish healthy and faulty drilling machines.

The scalar health indicator *r(t)* evolves in the domain of values returned by the SVM model. The values of *r(t)* are shown in Figure 4 as contour curves. The value of 1 is the first set-point indicating the need for preventive maintenance. Values of *r(t)* lesser than -1 clearly indicate that the drilling machine is in a faulty state, and should not be operated further.

However, the suggested values for the set-points should be adjusted taking into account the temporal behavior of the scalar health indicator *r(t)*. In some cases, faulty conditions occur in an abrupt manner such that there is not a state that would correspond to a “close-to-fault” condition. In the presented example the scalar health indicator based on two operational parameters I_RIB and RPM_RIB exhibits this type of abruptly changing behavior, which is shown in Figure 5. The blue curve depicts the temporal behavior of the feature value r(t) evaluated for the drilling machine.

The observations in the left-hand side of the plot are situated above the level of 1, which corresponds to normal operational conditions. In the sample interval of 93300 to 93400 the feature value clearly exhibits a decrease below the setpoint of -1, which indicates the onset of fault.

As can be seen the values of *r(t)* do not demonstrate any gradually changing behavior. The appearance of the health indicator *r(t)* suggests that the occurred fault makes the drilling machine proceed into a faulty state immediately.

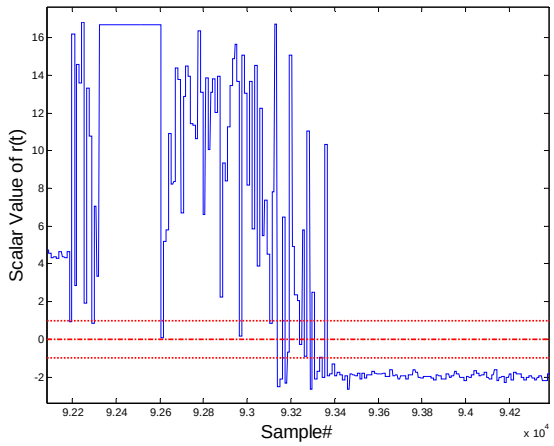

Figure 5. A typical temporal behavior of the scalar system health status.

3.3. Reliability Prediction Approaches

This section provides general recommendations regarding the selection of a prognostic model.

A generic prognostic routine is composed of the following tasks:

- Collect statistical data on the system of interest and the analogous systems.
- Choose a prognostic model to be used for prediction.
- Process the data collected on the system of interest as well as on the analogous systems to estimate unknown parameters of the selected prognostic model.
- Make a reliability prognosis for a given time instant.

The generic prognostic framework is pictorially shown in Figure 6. Statistical data related to the object of interest are obtained through collecting various measurements that will be used to evaluate the technical degradation parameter $\eta(t)$. These measurements, called degradation evidence data, are of major interest in the course of prognostics. Statistical data collected on analogous objects usually bring additional information related to the underlying failure mechanism. The presence of any kind of *a priori* information associated with the objects similar to the to-be-predicted one significantly facilitates the selection of the prognostic model.

An evolution of the degradation parameter is usually represented in the form of a time-series:

$$D = \{Y(t_1), Y(t_2), \dots Y(t_k)\}. \quad (3.3.1)$$

Additional degradation data observed over analogous objects are represented as follows

$$D^j_{add} = \{Y^j(t_1), Y^j(t_2), \dots Y^j(t_n)\}, \quad (3.3.2)$$

where *j* is the index of the object and *n* is usually greater than *k*.

Generally speaking, the object of interest may undergo several distinct failure modes exhibiting different types of degradation evidence data. The presence of different failure modes in the object of interest causes the simple time-series based representation of the degradation evidence data to not be sufficient. However, in many cases it is reasonable to assume that only one failure mode is dominating, so that the observed degradation evidence data are attributed to the dominant failure mode. This assumption should be made cautiously since in making a long-term RUL prediction the dominant failure mode may change.

The choice of the prognostic model is of primary importance in the prognostic framework. A poorly chosen prognostic model will never produce a good prognosis. In choosing the prognostic function one should take into account the following:

- In what manner the degradation process tends to behave, (gradually or abruptly changing).
- How much variability in the given data can be explained by the to-be-selected model. This aspect is often referred to as computational complexity of the model.
- How well the degradation process can be described by a mathematical apparatus, on which the prognostic model is based.

If the degradation process is poorly understood, one may prefer a simple algebraic form for the prognostic model; otherwise a more complicated form can be chosen, for example, a system of differential equations, or a stochastic Markov process.

Also, a great deal of attention should be given to any kind of uncertainties involved into the degradation evidence data. The uncertainties may include the effect of uncontrollable factors, measurement noise, errors associated with inferring unobservable parameters, etc. Figure 7 shows a simple classification of prognostic functions.

3.3.1. Generic Mathematical Approaches for Prognostics

Mathematical models employed in the prognostics framework are usually aimed at dealing with a time-series-based representation of degradation evidence data. The methods, which will be considered in this section, differ from each other in the ways they take into account any *prior* information, the amount of input information, the functional form of modeled relationships, etc.

3.3.1.1.Weighted Average Methods

The weighted average methods are closely related to filtration techniques. The predicted value is computed as a weighted sum of the degradation evidence data observed to date:

$$\hat{Y}_{k+1} = \sum_{i=1}^{k} W_i Y_i \qquad (3.3.1.1.1)$$

where W_i is the weight of the i^{th} observation, and

$$\sum_{i=1}^{k} W_i = 1 \qquad (3.3.1.1.2)$$

If $W_i = 1/k$ for each *i*, the predicted value of Equ. (3.3.1.1.1) is an average of the preceding k measurements. If the weights are calculated according to the following rules,

$$W_1 = a,\ W_2 = a(1-a),\ \ldots\ W_k = a(1-a)^k \qquad (3.3.1.1.3)$$

for $a < 1$, the weighted average method becomes an exponential smoothing prediction.

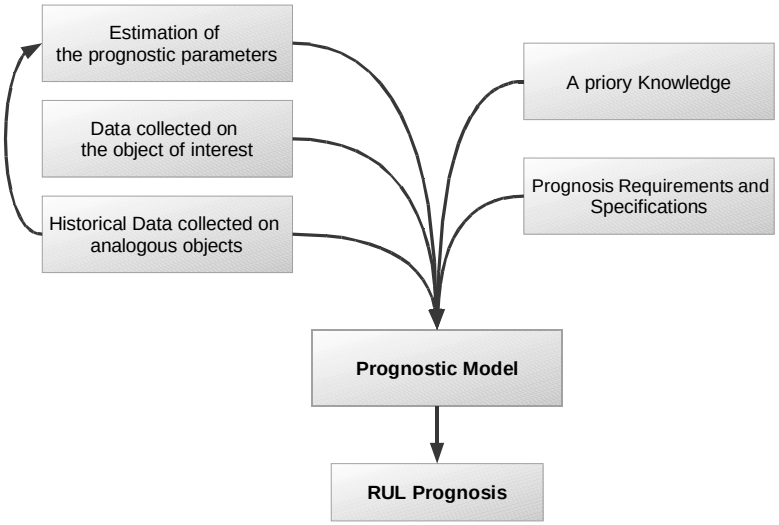

Figure 6. A generic prognostic framework

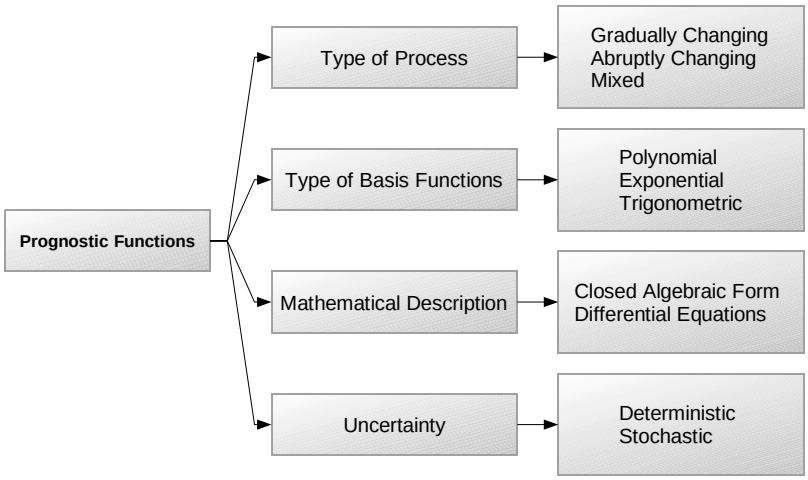

Figure 7. Classification of Prognostic Functions.

The weakness of the weighted average method is that only one time-series can be used to predict future values. The data collected over other objects similar to the one at hand turns out to be useless. However, one can apply a similarity operator (Hui, 2003), (Wegerich, 2004) to all available data to refine the weighting coefficients in Equ. (3.3.1.1.1).

3.3.1.2.Kalman Filtering based Methods

Usage of a Kalman filtering technique requires a solid knowledge of the underlying degradation mechanisms in the object of interest. The prognostic problem is formulated as follows. There is a model of the degradation parameter dynamics

$$\frac{dY}{dt} = F(t)Y(t) + G(t)U(t) \qquad (3.3.1.2.1)$$

where *F(t)* characterizes the dynamic behavior of the degradation parameter *Y(t), G(t)* characterizes the pattern of the input control signal *U(t).* The only observable values are the measurements *Z(t)* contaminated by noise.

$$Z(t) = H(t)Y(t) + \varepsilon(t) \qquad (3.3.1.2.2)$$

where H(t) is a measurement model describing a relationship between the unobservable values of Y(t) and observable measurements Z(t), and $\varepsilon(t)$ is the stochastic noise with known parameters.

Given a series of observations Z(t), $t_0 \le t \le t_{cur}$, one needs to find $\hat{Y}(t_{cur} + \Delta t)$ such that the mean value of the estimate is equal to the true value of $Y(t_{cur} + \Delta t)$ and the variance of the error is minimized.

$$E[\hat{Y}(t_{cur} + \Delta t)] = E\left[Y(t_{cur} + \Delta t)\right] \qquad (3.3.1.2.3)$$

$$Var[\hat{Y}(t_{cur} + \Delta t) - Y(t_{cur} + \Delta t)] \to \min \qquad (3.3.1.2.4)$$

Ref. (Luo, 2003) gives an example of the use of Kalman filtering techniques to predict remaining useful life of an automotive suspension system, whose degradation modes are well understood and can be modeled with differential equations.

3.3.1.3.Extrapolation-based Methods

A regression function $\eta(t)$ describes a behavior of a degradation evidence parameter

$$\eta(t) = E[\ Y(t)\ ] \qquad (3.3.1.3.1)$$

where $\eta(t)$ is a prognostic trend. In the RUL prediction framework, the function $\eta(t)$ is defined to be an approximating curve that provides the best fit of the collected measurements. The parameters of $\eta(t)$ are determined using a mean-squared-error-based criterion.

A prognosis is made through extrapolation of $\eta(t)$ in a moment of time in the future. Hence, the function $\eta(t)$ is considered to be a prognostic function. Usually, the prognostic function $\eta(t)$ is characterized by a vector of coefficients $\overline{\alpha}$. In the cases in which the functional form of $\eta(t,\overline{\alpha})$ is known to be linear with respect to the vector $\overline{\alpha}$, the prognostic function can be written in the following form.

$$\eta(t,\overline{\alpha}) = \sum_{i=1}^{n} \alpha_i c_i(t) \qquad (3.3.1.3.2)$$

where $c_i(t)$, $1<i<n$, are pre-determined basis functions. It is possible to analytically obtain estimates of the coefficients α_i, and variance of the predicted Y(t).

If the functional form of the prognostic trend is unknown, one has to choose the best-suited type of trend. To make a proper choice one needs to use the information found in the moment values such as conditional expected values $E[\ Y(t) \mid Y_1, Y_2, \ldots Y_k\ ]$ and conditional variance $Var[\ Y(t) \mid Y_1, Y_2, \ldots Y_k\ ]$. These statistics reflect the evolution of the degradation process in time. Approximation is performed using all available realizations of the degradation process.

3.3.2. Generalized Representation of A Prognostic Model

In developing a prognostic framework, one has to define a collection of candidate models that reflect the revealed properties and characteristics of the analyzed degradation process. The generic form of a candidate model can be expressed as the following.

$$M = \{ \Psi, W_i(t, \bar{\beta}_i) \}, \; i = 1,2,\ldots L \qquad (3.3.2.1)$$

where Ψ is an operator defining the manner in which the model's components are interacting, $W_i(t, \bar{\beta}_i)$ is the i^{th} component of the model M, $\bar{\beta}_i$ is a vector of parameters attributed to the i^{th} component W_i, and L is the number of components constituting the model M.

In a prediction model there are at least two major components: process-related and noise-related components. The former brings the information directly associated with the degradation mechanisms taking place in the object, the latter accounts for various types of noise present in available observations.

The process-related component $W_p(t, \bar{\beta}_p)$ can include several subcomponents that reflect the evolution of the mean value and central moments (variance, skewness, kurtosis) of the degradation process under surveillance. Also, the process-related component can take into account random abrupt changes in the degradation process' characteristics as well as a stationary process noise.

The noise-related component accounts for a stationary random noise and outliers observed in measurements. Usually, outliers are to be removed during early pre-processing stages.

In practice it is difficult to differentiate stationary process noise from stationary random noise. Hence, it is reasonable to consider the two noise components as one single element accounting for a stationary random noise even though the components are due to completely different phenomena.

Abrupt changes in the process characteristics may not be of interest in long-term prediction. However, short-term prediction is greatly affected by rapidly changing

degradation parameters. An excellent study devoted to detection of abrupt changes in time-series data can be found in (Basseville, 1993).

Even if the practitioner is interested in a long-term RUL prediction, in the cases where the prognostic model should account for several degradation modes, it is required to pay attention to abrupt changes in the process. Such a multimodal prognostic model should be able to switch between the various degradation modes as soon as a rapid change in parameters becomes evident.

Table 1 concludes the description of the components that may be included in a prognostic model.

The deterministic component $\eta(t,\boldsymbol{\alpha})$ approximates the conditional expected value $E[Y(t) \mid Y_1, Y_2, \ldots Y_n]$ of the degradation process within the time interval $(t_1, t_2, \ldots t_n)$ corresponding to the observed measurements as well as within the prediction time interval $t_n < t < t_{hor}$, where t_{hor} is the prognosis horizon value. The deterministic component usually takes the following form

$$\eta(t,\boldsymbol{\alpha}) = \sum_{i=1}^{m} \alpha_i F_i(t), \quad t_1 < t < t_{hor} \qquad (3.3.2.2)$$

where $F_i(t)$ is a basis function. A good candidate for the basis functions is a system of polynomial functions.

$$\{ F_0(t) = 1, F_1(t) = t, \ldots F_m(t) = t^m \} \qquad (3.3.2.3)$$

The order of the polynomial of the deterministic component (3.3.2.2) is usually limited by the second order. A more complex deterministic component can introduce unwanted effects similar to the data-overfitting phenomenon that causes an estimator to have poor generalization abilities.

Table 1 Components of the prognostic model.

Component	Description
$\eta(t,\boldsymbol{\alpha})$	A deterministic component describing how the expected value of the degradation parameter evolves in time *t*.
$\varepsilon_\sigma(t)$	A random component characterizing how the second central moment (variance) of the degradation parameter evolves in time
$\varepsilon_S(t)$	A random component characterizing how the skewness of the degradation parameter evolves in time
$\varepsilon_K(t)$	A random component characterizing how the normalized fourth central moment (kurtosis) of the degradation parameter evolves in time

In most cases the following generic model will be sufficient to produce a good result.

$$Y(t) = \eta(t,\boldsymbol{\alpha}) + \varepsilon_\sigma(t) \qquad (3.3.2.4)$$

where $E[\varepsilon_\sigma(t)] = 0$, $Var[\varepsilon_\sigma(t)] = const$, $Skewness[\varepsilon_\sigma(t)] = const$, $Kurtosis[\varepsilon_\sigma(t)] = const$.

The stochastic component is zero-centered. The moment characteristics of the stochastic component are not changing in time.

3.4. Illustrative Example

The methods described in the preceding subsections were applied to simulated data. The following example considers predicting remaining useful life of electronic power supplies employed in high-end computer systems. A set of power supplies underwent accelerated aging tests. Each power supply was tested under cyclic temperature load. The temperature range and the rate of change were within the specification values. The values of the output parameters (such as output current, voltage, and inside temperature) were monitored and collected for a few months.

These tests revealed that a certain power supply fault causes the power supply to fail to provide an output voltage within the specified range. Specifically, the fault presents itself as abrupt and rapid transients in output voltage. The abrupt transients are observed only when the temperature profile exhibits a non-zero gradient.

Eventually the rapid transients or spikes appear frequent and large in their magnitudes so that the power supply undergoes an unrecoverable failure. Figure 8 shows two samples of real-world measurements taken at the faulty power supplies. The end of the shown measurements corresponds to the moment of the unrecoverable failure.

As can be seen, the magnitude of the spikes can be as large as about 50% of the nominal voltage value. Such severe deviations from the specification eventually lead to the power supply's failing.

Assuming that the statistical properties of a sequence of spikes are known, a sizable group of voltage measurements showing abrupt transients similar to the ones observed at the real-world power supplies were simulated. Specifically, the following assumption was made. The number of spikes occurring within a temperature cycle is a random variable distributed according to the Poisson distribution:

$$P_\lambda(n) = \frac{\lambda^n e^{-\lambda}}{n!} \qquad (3.4.1)$$

This assumption is justified as follows. The probability that a spike occurs in a faulty power supply during a small time unit, such as a second, is relatively small. The number of the time units elapsed during a temperature cycle is quite large since a temperature cycle takes usually about 2 hours in the experiment settings. In the field conditions a temperature cycle may take even longer. Hence, it can be concluded that the number of spikes occurring during a temperature cycle is a Poisson distributed random variable.

The parameter $\lambda = \lambda(t)$ is chosen to be a monotonically increasing value that reflects the gradual degradation of the simulated power supply. In other words, the sequence of voltage measurements is assumed to be a non-stationary Poisson process.

The number of observed events (spikes) in a time interval depends upon the length of the interval as well as upon the interval's location on the time axis.

The degradation indicator $Y(t_k)$ is chosen to be a weighted average of deviations from the nominal voltage value.

$$Y(t_k) = \frac{\sum_{i=1}^{k} w_{k\,i}\Delta d_i}{\sum_{i=1}^{k} w_{k\,i}} \tag{3.4.2}$$

where Δd_i is a deviation of the voltage measurement observed at t_i.

$$\Delta d_i = d_i - d_{nom} \tag{3.4.3}$$

w_{ki} is a weighting coefficient calculated according to

$$w_{ki} = \exp\left(-\frac{t_k - t_i}{h}\right), \quad t_k > t_i \tag{3.4.4}$$

where h is a parameter regulating how many historical data points should be accounted.

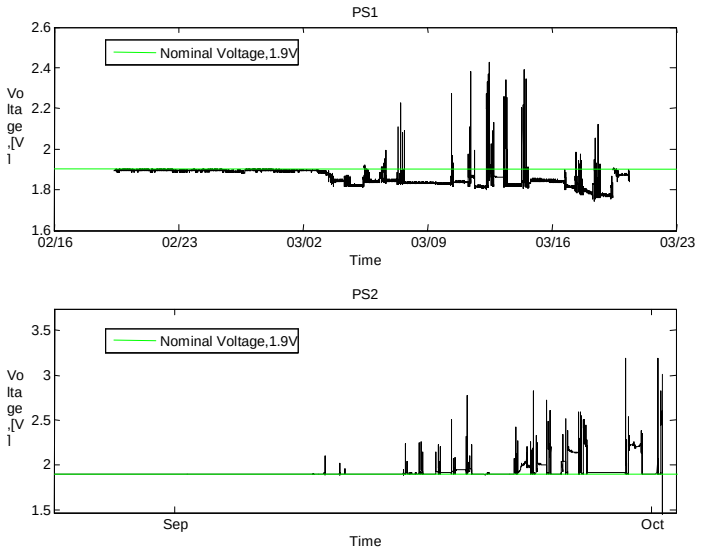

Figure 8. Real-world data obtained from power supplies

If the output voltage of the power supply under consideration does not exhibit any significant deviations from the nominal level, the defined degradation indicator is near zero since the small deviations are likely to be due to measurement noise, which is assumed zero-mean. Figure 9 shows a typical degradation indicator computed on the simulated measurements.

Analysis of the simulated measurements allows for making an appropriate choice of a link function, which will be used to perform a least squares fit of the degradation indicator data. In this example, a log function is a good candidate to provide an adequate prediction model. Figure 10 shows the degradation indicator along with the fitted prediction model whose mathematical expression is given below:

$$p(t) = 4.55^{(t-206.5)} \tag{3.4.5}$$

Figure 10 shows the prognostic trend computed at the moment of time when the fault indication data are available entirely, i.e. the black-dotted prognostic trend corresponds to the time of failure.

In many real-world cases the failure threshold value is not specified in advance. Making use of available historical data one is able to determine the threshold value in a probabilistic manner.

3.5. Linear Growth Model of Cumulative Damage

The simplest form of the damage accumulation model is a linear relationship between the accumulated damage and the time units characterizing the usage of the item. The time units used in the model can be calendar time, usage time, units of cyclic usage such as the number of temperature cycles the item has suffered, or some other units that may be related to wear such as cumulative loading. Usually the time units to use in the model are determined by the time measure with respect to which the observations are made. For example, a well-known data set of fatigue crack growth from Virkler et al. (Virkler 1978) has time units expressed in the number of load oscillations applied to the tested specimens.

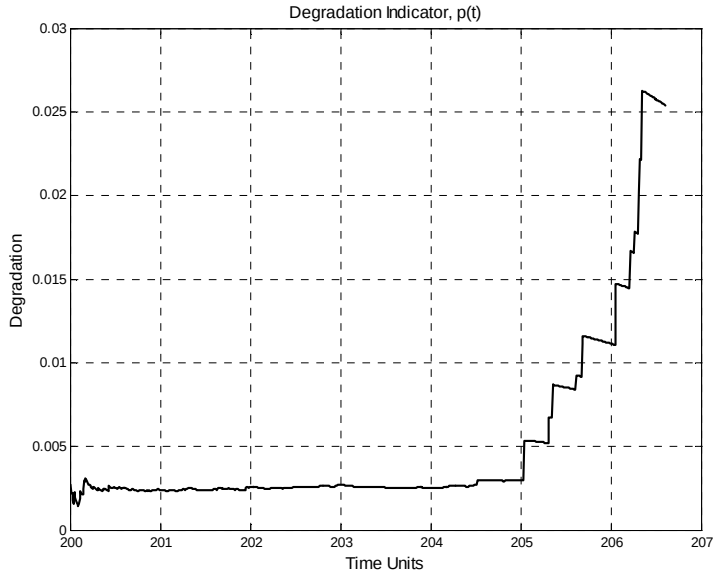

Figure 9. Degradation Indicator computed on the simulated measurements.

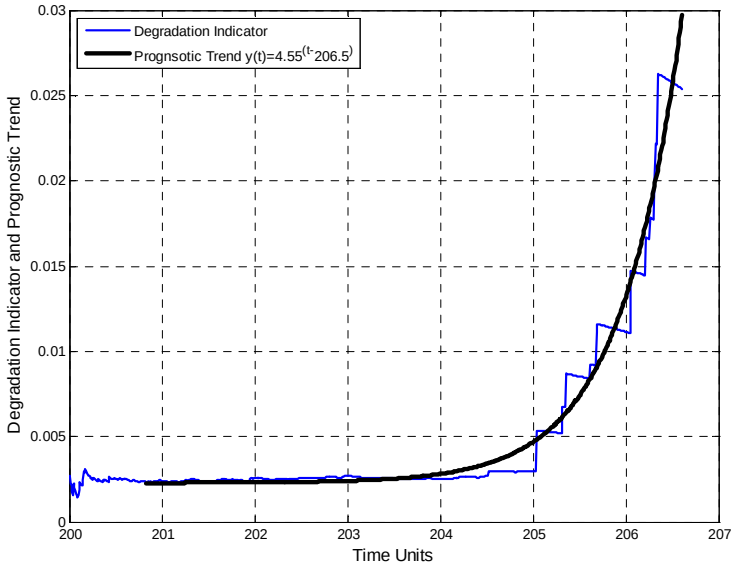

Figure 10. Degradation Indicator and Prognostic Trend.

Although a linear model is assumed, the degradation model can be of any monotonically increasing function. A monotonic transformation is performed to linearize the non-linear model. The selection of the model form should be guided by past experience. Several assumptions are made for use of the linear degradation model:

- The mean degradation rate is constant.
- The damage accumulation process is monotonic.
- A failure occurs as soon as the degradation level exceeds some predefined failure threshold Y*.

The linear degradation model is assumed to be of the following form

$$Y(t) = \beta_1 t + \beta_0 \qquad (3.5.1)$$

where β_1 is the degradation rate, β_0 is the initial level of the item's damage, and t is a time unit. Value Y(t) is the accumulated damage (degradation) observed at time t. An item's lifetime is defined to be the time T such that Y(T) = Y*, the failure threshold.

Since there is no random component dependent on t in (3.5.1), the time to failure (T) can be computed exactly for the linear model, given the values of the β_1 and β_0.

$$T = (Y^* - \beta_0) / \beta_1 \qquad (3.5.2)$$

In a more realistic setting, the degradation model is subject to random deviations, which are due to the random influence of external factors and measurement errors. However, it is reasonable to assume that the mean degradation rate remains constant. An item's lifespan can be partitioned into three main zones with respect to the degradation rate. The zones are pictorially shown in Figure 11. One should be aware that different components have different degradation profiles and this one is chosen for its simplicity and wide range of application. This profile has a relationship to the bathtub curve, which is a profile for a failure rate. The increasing degradation may be thought to be related to the increasing failure rate that occurs during infant mortality and wear out. However, the wear out failure mode is assumed to be the only mode of concern in this study.

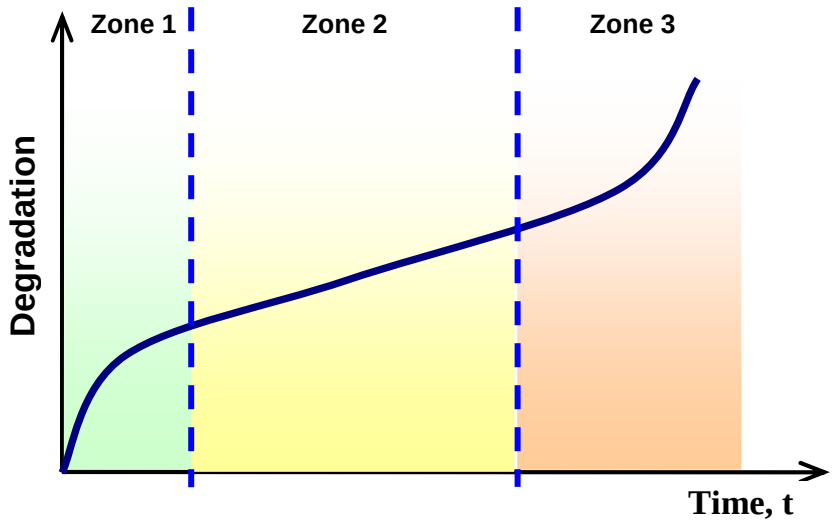

Figure 11. A typical profile of accumulated degradation.

Zone 1 corresponds to intensive degradation, which takes place at the load accommodation phase. A brand new item accommodates itself to the loading conditions in which the item is placed. Zone 1 is characterized by a monotonically decreasing rate of degradation. However, the absolute values of degradation rate are higher than that observed in Zone 2.

Zone 2 corresponds to a steady-state wear process. While in this zone the item acquires certain stable characteristics that allow it to bear the applied loadings in a steady manner. Zone 2 is usually the longest portion of the item's lifetime.

Zone 3 is a zone of catastrophic wear. The rate of wear increases drastically due to a qualitative jump in the item's properties. After accumulating the damage in Zone 2, the item wears out its resource, which is basically a quantitative process reflecting the monotonic degradation of the item. Having accumulated a certain level of damage, the item undergoes a qualitative change, which is usually of structural nature. The qualitative change in the item's properties causes a change in the underlying degradation mechanisms. The degradation rate abruptly becomes much larger than that of steady-state wear. Usually being at Zone 3 is considered as a failure state for an item. The item

undergoing catastrophic wear is no longer capable to function properly. An example of this type of wear would be a bearing that is pitted.

Since the constant degradation rate zone takes the longest time in the item's lifespan, the primary interest of this study is an item's behavior within Zone 2. In applying the linear model (3.5.1) to an individual profile of damage accumulation, the following terms are used: "degradation parameter" and "degradation pathway". The degradation parameter is a scalar value associated with the degradation level at a given point of time, Y(t). The degradation pathway reflects an evolution of the degradation parameter in time. Usually the degradation pathway is represented in the form of a time-series:

$$\mathbf{Y} = \{ Y(t_1), Y(t_2), \ldots Y(t_n) \} \qquad (3.5.3)$$

A typical linear degradation pathway is shown in Figure 12. The random fluctuations about the mean degradation line are usually attributed to random external factors and measurement errors. In this particular example the mean degradation pathway depicted as a dotted line is estimated using a least-squares criterion.

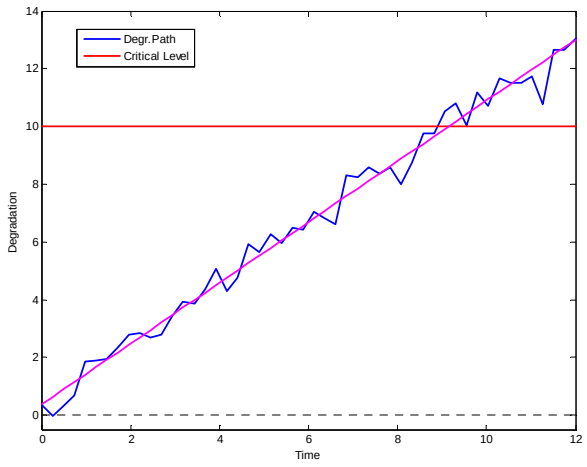

Figure 12. A degradation path is subject to random deviations that are due to process and measurement noise sources.

In the traditional reliability field the main assumptions made in regard to the degradation pathways are that there are no statistically significant differences among the degradation pathways observed for a population of tested items. Assuming homogeneity of the population, one is able to evaluate characteristics of the time-to-failure distribution, such as mean, median, modes, and variance. These characteristics are basically population-averaged estimates of the reliability parameters. A statistical difference in the items due to manufacturing or material differences can be integrated into the model (Ebeling, 2005).

Recent advances in computer and sensor technologies allow the practitioner to monitor critical parameters of the item in field. Measurements associated with the degradation level can be available for a wide range of equipment (Sunghyun 2005), (Lieberzeit, 2006). Even though it is not always possible to directly observe degradation parameter values, a variety of machine learning techniques enable inferring the degradation parameter values at an acceptable level of certainty (Biswas 2006),(Romano 1997). Using modern sensor and micro-processing equipment it is possible to estimate parameters of the degradation pathway in an on-line manner.

Having an ability to assess the degradation level and rate for an individual item, the practitioner is able to perform a time-to-failure prognosis for this particular item. It should be noted that the prognosis made with respect to an individual item is subject to a degree of uncertainty. Needless to say, the individual prognosis makes sense if, and only if, it will provide the practitioner with an uncertainty better than that associated with the population-average-based prognosis.

3.6. Generalized Cumulative Shock Models

The generalized cumulative shock model is the most general mathematical representation of the degradation processes, which evolves in time primarily in a random manner. The generalized cumulative shock model has been considered in the reliability analysis literature for decades (Sumita 1985), (Gut 1990) and is defined as follows.

Let {N(t), t>0} be a point process with sequence of jump times T_1, T_2,… Each jump time T_i has a corresponding random variable C_i. The stochastic process {X(t), t ≥ 0}

$$X(t) = \sum_{i=1}^{N(t)} C_i \tag{3.6.1}$$

is called a cumulative shock model. In this setting, the value of C_i is the magnitude of the shock arrived in time T_i. Figure 13 illustrates a typical cumulative stochastic process X(t).

From the reliability analysis perspective, of primary interest is the random time L(*x*) when the accumulated shock magnitude X(*t*) exceeds a given critical threshold *x* for the first time:

$$L(x) = \inf \{ t, X(t) > x\} \tag{3.6.2}$$

Gut has proven in (Gut, 1990) that the distribution of L(*x*) approaches the normal distribution with the following parameters, if the value of *x* is relatively large:

$$L(x) \sim N\left(\frac{\mu}{\nu}x, \frac{\gamma^2}{\nu^3}x\right) \tag{3.6.3}$$

where $\mu = E(T)$, $\nu = E(C)$, $\gamma^2 = Var(\mu C - \nu T)$

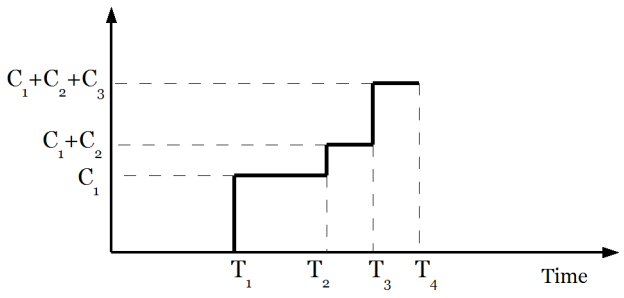

Figure 13. A typical cumulative shock model path with positive increments.

Essentially the normal distribution in (3.6.3) is a limiting case for the TTF distribution implied by a cumulative shock model. The analytical expression for the limiting normal distribution (3.6.3) is of practical importance since it provides information on the time-to-failure distribution for an arbitrary cumulative shock model. In reliability analysis the probability distribution given in (3.6.3) has been known as the Birnbaum-Saunders distribution, which was originally developed to model the rupture time of metals exposed to fluctuating stress and tension (Birnbaum 1967).

The theoretical result provided by Gut (Gut 1990) suggests that any cumulative shock (damage) model implies a TTF distribution that is close to the normal distribution if the critical threshold value is large compared to the damage increments. The mean and variance of the TTF distribution depend on the stochastic parameters of the point process N(t) and the random shock magnitude C_i.

The following subsection outlines the stochastic model of cumulative damage, which is a practical modification of the generalized shock models.

3.7. Stochastic Model of Cumulative Damage

The stochastic model of cumulative damage was originally introduced by Bogdanoff and Kozin in (Bogdanoff 1985). Cumulative damage is defined to be the irreversible accumulation of damage in components under a cyclical usage pattern. The cumulative damage model is applicable to a variety of systems exhibiting any kind of wear accumulation. The cumulative damage evolution is best described in terms of the number of load cycles (duty cycles), to which the system or component has been subjected.

3.7.1. A Stationary Markov Chain-based Model of Cumulative Damage

A finite Markov chain is used to model the degradation accumulation process over the unit's lifetime under cyclic loadings. The possible levels of degradation are represented by a finite set of numbers encompassing the state space of the Markov chain. The only allowed transitions are those that lead the MC to higher damage states. This reflects the fact that the degrading component cannot improve its state.

The simplest cumulative damage model has two parameters. These are the transition probability q and the critical damage state Y^*. The transition probability q characterizes the probability that the damage state receives a unit-size degradation increase during a duty cycle. State Y^* is the critical threshold which causes system failure. The unit-size restriction on the damage increment implies that the time-to-failure is distributed according to a gamma distribution with the shape parameter k and the scale parameter Θ (Tamhane 2000).

The model is based on a Markov chain (MC) representation of the stochastic process imitating the damage accumulation process. The Markov chain transition probability q characterizes the probability that the damage state receives a unit-size increase during a duty cycle. The unit-size restriction implies that the time-to-failure is distributed according to a gamma distribution with two parameters k and Θ. The probability density function (PDF) of the gamma distribution is given by

$$f(t,k,\Theta) = t^{k-1}\frac{\exp(-t/\Theta)}{\Theta^k \Gamma(k)},\ where\ t>0 \qquad (3.7.1.1)$$

where k>0 is the shape parameter, Θ > 0 is the scale parameter.

The Markov Chain-based model of cumulative damage covers many models well known in reliability analysis. The simplest cumulative damage model has two parameters. The damage accumulation is assumed to be a stationary Poisson process beginning at X(0) = 0, which implies that there is no variation in initial damage. The failure is assumed to occur as soon as the MC enters State b. State b and the transition probability, p, are the two parameters of the cumulative damage model. In this case, the time-to-failure is distributed according to a gamma distribution with two parameters.

A generalization of the outlined Poisson process can be derived in the following manner. The damage process evolves as a Poisson process of rate λ_1 up to State k<b. Then, it evolves as a Poisson process at rate λ_2 up to State b, where failure occurs. In this case, the time-to-failure distribution is the sum of two independent gamma distributions. It should be noted that a Poisson process is usually defined in terms of the rate λ whereas

the cumulative damage model is described by the transition probability q. A relationship between the quantities can be established as follows.

$$q = \lambda\tau + o(\tau) \qquad (3.7.1.2)$$

where τ is the time duration of a duty cycle, $o(\tau)$ is a little-o notation.

3.7.2. Use of Degradation Evidence Data in the cumulative damage model

Condition-monitoring observations can complement the parameterization of a prognostic model. Reliability case studies using condition-monitoring measurements can be found in (Vlok 2002), (Carey 1991). A detailed review of the reliability data-analysis methods involving condition measurements rather than time-to-failure data is given in (Lu 1993).

The stochastic cumulative damage model outlined in the previous subsection is primarily focused on using time-to-failure data. However, the inherent properties of the stochastic model allow for utilizing degradation evidence data. Given time-to-failure data, one estimates the parameters of the gamma distribution characterizing the reliability characteristics of the population. The estimated parameters, such as the mean, median and variance, are basic prognostic quantities used to predict remaining useful life of a typical item belonging to the population. However, the RUL prognosis based upon the estimated distribution parameters values is of a static nature since it takes into account only the most general aspects of the item's reliability.

If one is able to accurately assess the item's current damage state, an RUL prediction more certain than the population-average estimates can be obtained. In the following the usage of condition-monitoring measurements in the cumulative damage model is outlined.

Damage is assumed to be a discrete quantity taking the values from Set $d = \{1,2,3,\ldots b\}$, where State b represents a failure state. The damage evolves in the domain of duty cycles. A duty cycle is defined to be a repetitive interval of operation, during which a unit-size damage may accumulate. For example, duty cycles may be given as calendar time units (days, weeks, months), operational time (time in air, mileage), and

usage intervals (number of in-field missions, fuel cycles etc). The damage model is hence a finite-state and discrete-time process.

Let q be the probability that damage takes a unit increment during a duty cycle. The probability that damage remains unchanged is obviously equal to $p = 1 - q$. Damage increases one unit at a time until State b is reached. Once State b is attained, a state of failure is declared and the cumulative damage process is stopped. The probability q is assumed to be constant through the entire evolution of damage. This assumption seems reasonable if the only available reliability information is time-to-failure data observed over a sample of similar items. No other data regarding the trajectory form of degradation evolution are available.

Since the failure event is defined to be the time of entering State b, the time-to-failure is taken to be a random variable distributed according to a gamma distribution, whose PDF is given by (3.7.1).

Apparently, the gamma distribution parameters can be rewritten in accordance with the parameters of the cumulative damage model as follows

$$k = b\ ,\quad \Theta = \frac{1}{q} \tag{3.7.2.1}$$

The mean time-to-failure (MTTF) is expressed using the gamma distribution parameters

$$MTTF = k\Theta = \frac{b}{q} \tag{3.7.2.2}$$

The variance of time-to-failure (TTF) is also easily expressed using the gamma distribution parameters.

$$Var(TTF) = k\Theta^2 = \frac{b}{q^2} \tag{3.7.2.3}$$

Although the variance gives a reasonable representation of uncertainty associated with the predicted time-to-failure, it seems more appropriate to use a percentile-based representation for uncertainty since the gamma distribution tends to be skewed in the case

of small values of *b*. The following interval-based representation of uncertainty is used in this work:

$$PI_{\alpha} = [\ P_{\alpha/2}(b,1/q)\ \ P_{1-\alpha/2}(b,1/q)\ ] \qquad (3.7.2.4)$$

where PI_{α} is the $(1-\alpha)\times100\%$ prediction interval, $P_{\alpha}(b,1/q)$ is the α^{th} percentile of the gamma distribution with parameters *b* and $1/q$.

The developed model is extended with one additional parameter if one is able to observe the current damage state of the item. Let y_{obs} be the observed current damage state of the item. Taking into account the new parameter one can rewrite the mean time-to-failure and the $(1-\alpha)\times100\%$ prediction interval as follows.

$$MTTF = \frac{b - y_{obs}}{q} \qquad (3.7.2.5)$$

$$PI_{\alpha} = [\ P_{\alpha/2}(b-y_{obs},\ 1/q)\ \ P_{1-\alpha/2}(b-y_{obs},\ 1/q)\ ] \qquad (3.7.2.6)$$

Figure 14 illustrates how the RUL prediction is affected by taking into account the unit's current state of damage. The shaded area represents 95% prediction intervals (PI) for the individual RUL obtained using equations (3.7.2.5-3.7.2.6). The dashed lines are the RUL prediction intervals calculated using population average reliability characteristics. It can be easily seen that the individual RUL prognosis tends to be more certain than the average reliability characteristics of the population. At the early phase of the item's operational life the individual RUL prognosis is essentially the same as the population mean time-to-failure. Uncertainty of the initial RUL prediction also coincides with that of the population-based prediction. However, as time proceeds, the RUL prediction becomes more certain compared to the population-based prediction intervals.

It is noteworthy that the individual RUL prediction uncertainty depicted in Figure 14 as a shaded area is only due to variability of operational conditions and randomness of the item's inherent properties. In other words, there is no uncertainty associated with the parameters of the cumulative damage model (b, q, y_{obs}).

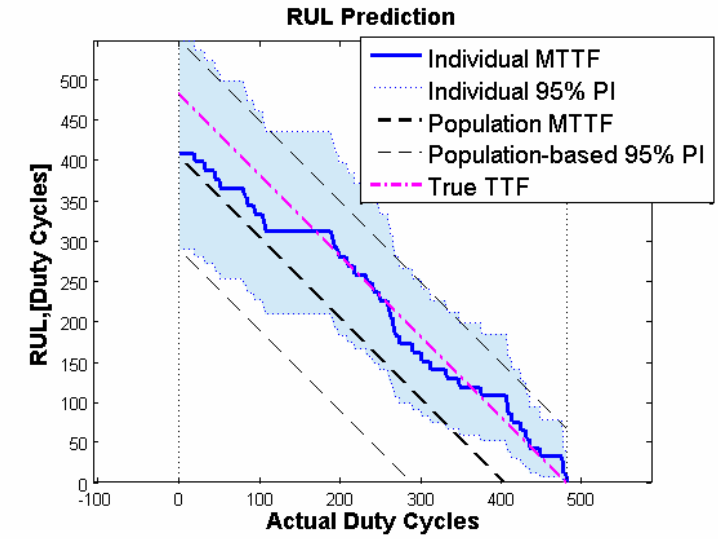

Figure 14 Remaining Useful Life Prediction Intervals calculated using the current damage state of the item.

The RUL prediction uncertainty pictorially shown in Figure 14 is the best uncertainty achievable in the given cumulative damage model. Any additional source of variability causes the final RUL prediction to be more uncertain.

3.8. Concluding Remarks

The criteria and conditions upon which an individual time-to-failure prognosis will give a more certain prediction compared to the population-distribution-based prognosis are of primary interest in performing the remaining useful life (RUL) estimation.

The major sources of uncertainty encountered in performing prognostic routines are outlined in the next chapter. An uncertainty analysis regarding the uncertainty effects upon a prognostic model is performed. Also, the next chapter introduces the criterion, upon which the practitioner can decide whether the individual degradation pathway will provide an RUL prognosis more certain than that based on the population average characteristics.

4. UNCERTAINTY ANALYSIS OF PROGNOSTIC MODELS

The following are the sources of uncertainty which are usually encountered in degradation-based reliability modeling:

- Variability of the severity and order of duty cycles loads.
- Variability of the initial level of component degradation.
- Variability of the degradation state, which is considered to be critical and unsafe for any further use of the component.
- Uncertainties in inspection routines.

Randomness of the severity and order of duty cycles loads is usually the main contributor to the end result uncertainty since the duty cycles loads are likely to be driven by completely random phenomena such as environmental conditions (temperature, humidity, etc.), and operational conditions imposed by the operating regimes that are performed to accomplish the mission. For example, each item may have its own particular environmental and loading conditions. Thus, the item's pathways may exhibit significantly different degradation rates. In practice, one can encounter a situation in which the degradation pathways are subject to a great deal of variation even if the external factors tend to be relatively stable. In such cases the major source of variability is usually due to the complex internal structure of the materials in which the degradation process¸ such as corrosion, creep of metals, etc., takes place. Various particularities of the item's internal properties cause the degradation process to vary from item to item regardless of the external conditions.

Essentially this modeling uncertainty contributor is the goal of a prognostic model. If the prognostic model is able to reasonably reflect the random behavior of the driving forces for the degradation process, the model is expected to provide a good prediction of the reliability characteristics in the future.

Uncertainties in the initial and terminal states of the component's lifespan are closely related to each other, since they quantify the lack of knowledge of the component degradation state at different phases of its operational life. The item's initial level of damage is determined by such factors as differing material intrinsic properties, installation procedures, storage history, and any prior usage.

In many practical situations the initial degradation state is assumed to be of minor importance since brand-new items usually exhibit a relatively small variation of the initial inherent properties. Diversity in the reliability characteristics tends to manifest itself mostly through the variability of the degradation rates.

4.1. Uncertain Measurements of Degradation Parameter

Of practical interest is the uncertainty associated with the condition monitoring observations reflecting the current damage state of the item, y_{obs}. This type of uncertainty is usually determined by the accuracy of monitoring sensor equipment that provides health condition metrics.

Although uncertainty in inspection procedures can be thought of as an uncertainty source similar to the initial and terminal states uncertainties, the origin of the imperfect inspection procedures can be different from that of the initial and terminal states variance. Measurement sensor limitations cause the degradation state estimation to be uncertain. Uncertainty in the estimate of the current degradation state can significantly deteriorate the end result prediction. A reliability prediction model is expected to have a critical level of uncertainty in measurements such that the prediction model supplied with highly uncertain measurements is not able to provide a prediction which would be more certain than that provided by the population average reliability characteristics such as the mean time-to-failure and the associated standard deviation.

Assuming that the current damage state y_{obs} is given with some degree of uncertainty one has to deal with additional source of variability in assessing the final RUL prediction uncertainty. The next section introduces a usefulness criterion for degradation evidence data.

4.1.1. Criterion of Usefulness

Given a stochastic model of cumulative damage one needs to know which certainty level should be attained in measuring the current system "health" status to produce an RUL prediction more certain than the population average characteristics.

The following criterion is developed to assess usefulness of using current "health" condition measurements to predict the system remaining useful life:

$$C(t) = \frac{U_{RUL}(t)}{U_P} \qquad (4.1.1.1)$$

where $U_{RUL}(t)$ is the uncertainty associated with the RUL prediction that takes into account the current damage state at time *t*, U_p is the uncertainty associated with the population average time-to-failure. The latter quantity is usually constant and not time-dependent, whereas the former quantity depends on time since it includes the current damage state y_{obs}, which gradually changes through the system's lifespan.

Apparently, if the criterion value is less than unity the individual RUL prediction produces a result more certain than the population-based reliability characteristics. The values close to unity indicate that the individually made prognosis is comparable to the average time-to-failure in terms of certainty. If the criterion value happens to be larger than unity, the current health condition observations do not benefit the RUL prognosis with respect to certainty.

The criterion can be rewritten in terms of the Markov chain-based cumulative damage model parameters as follows.

$$C(t) = \frac{P_{1-\alpha/2}(b - y(t), 1/q) - P_{\alpha/2}(b - y(t), 1/q)}{P_{1-\alpha/2}(b, 1/q) - P_{\alpha/2}(b, 1/q)} \qquad (4.1.1.2)$$

where $P_\alpha(b,1/q)$ is the α^{th} percentile of the gamma distribution with parameters *b* and $1/q$, $y(t)$ is the damage state observed at time *t*. The following section gives a simulated data example illustrating the behavior of the developed criterion at different levels of degradation state uncertainty.

4.1.1.1.Illustrative Example

This section presents an example of using the cumulative damage model along with the observed current damage state of the system. The following particular values of the cumulative damage model are estimated from the reliability data published in (Bogdanoff, 1985):

$$b = 38,\ q = 0.0933 \qquad (4.1.1.1.1)$$

The data represent lifetimes of test specimens of aluminum strips subjected to cyclic loadings at certain amplitude. The total number of 101 specimens is enough to claim that the parameters (4.1.1.1.1) are estimated certainly. One duty cycle of the lifetime data is taken to be 1000 deflections applied to a specimen.

The estimated parameters imply that the damage space is of 38 different levels of damage from 1 through 38. The probability that the item suffers a unit-size damage during a duty cycle is equal to 0.0933. Figure 15 shows the RUL prediction intervals provided by the cumulative damage model having uncertain estimates of the current damage state. The uncertainty associated with the measurements of the current damage state is expressed in terms of relative accuracy, which is given by

$$A_R = \frac{err}{b} \times 100\% \qquad (4.1.1.1.2)$$

where b is the critical threshold value, which is the maximum achievable damage state; err is the absolute error in estimating the current damage state, $err \in \{0, \pm 1, \pm 2, ...\}$.

Figure 15(a) represents the case where the current damage state is determined at relative accuracy of 5.3%. Figure 15 (b) and 15(c) show the prediction intervals for the cases where the relative accuracy is 10.5% and 18.4%, respectively.

It can be easily seen that a relative accuracy as low as 5.3% hardly affects the RUL prediction. The uncertain estimates of the current damage state have more influence on the RUL prediction at the moments of time close to the failure. However, the RUL uncertainty still remains significantly better than that of the population-based time-to-failure estimate.

In the case of larger uncertainty, the individual RUL prediction becomes as uncertain as the population average reliability characteristics. Figure 15(b) shows such a case. For this particular cumulative damage model the relative uncertainty of 10.5% causes the individual RUL prediction to be comparable to the population-average reliability parameters.

For measurement uncertainty larger than 10%, the cumulative damage model cannot provide a reasonable RUL estimate since the total prediction uncertainty is nearly twice as larger as that of the population-average estimates.

Figure 16 summarizes the usefulness criterion values calculated at different levels of uncertainty. The horizontal line indicates the unity level for the usefulness criterion. Being above the unity level the usefulness criterion suggests that the RUL prognosis should be based upon the population-average reliability estimates rather than upon an individually made prediction. A criterion value below the unity level indicates that the usage of individual health condition data is beneficial in terms of RUL prediction uncertainty.

The simulation was performed for several levels of measurement uncertainty. From visual analysis of Figure 16, it can be concluded that a measurement uncertainty less than 20% does not significantly deteriorate the RUL prognosis. However, if one measures the current health condition of an item at the uncertainty level of 20% or higher, the usage of condition health measurements does not benefit the RUL prognosis in terms of certainty. It should be noted that the particular values of the usefulness criterion were found in conjunction with this particular model of cumulative damage.

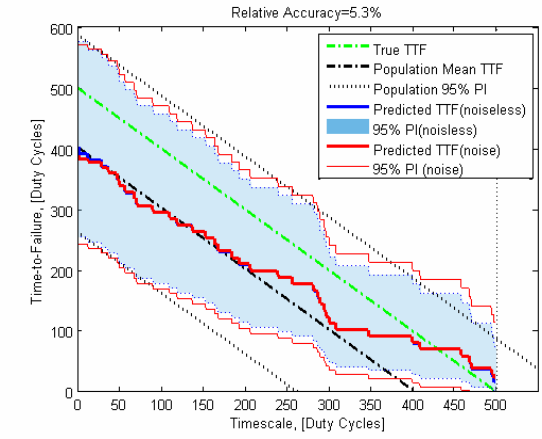

a)

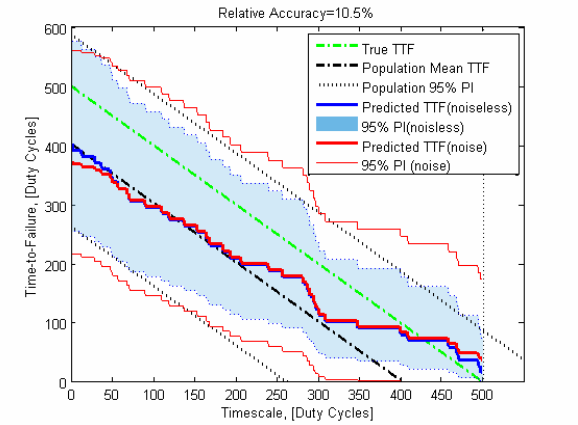

b)

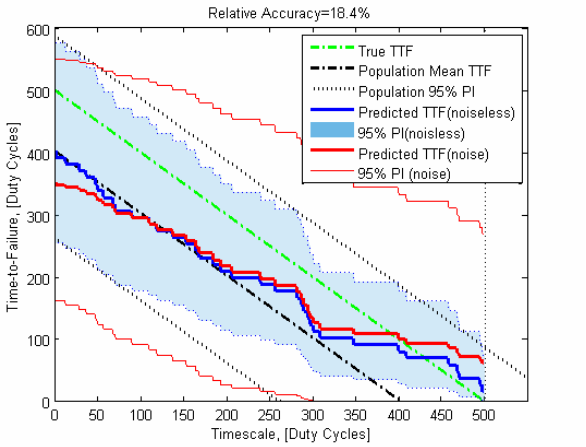

c)

Figure 15. The RUL prediction intervals calculated taking into account the uncertainty associated with the current damage state.

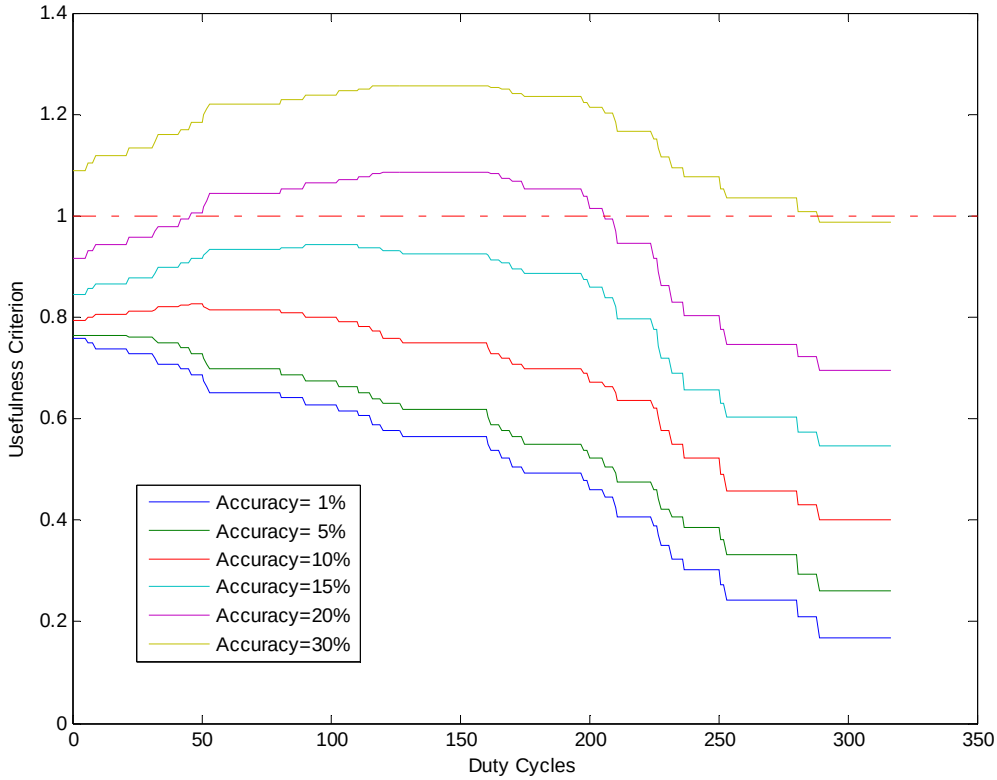

Figure 16. The usefulness criterion evaluated at several levels of current damage state uncertainty.

4.1.2. Usefulness Criterion for a Linear Degradation Model

A linear functional form of an item's degradation pathway is given by

$$Y(t) = \beta_1 t + \beta_0 \qquad (4.1.2.1)$$

Y* denotes the critical threshold of the degradation parameter:

$$Y^* = Y(T^*) \qquad (4.1.2.2)$$

Time T* is defined to be the time of failure for a particular item. To take into account the first two variability sources the parameters of the linear degradation model (4.1.2.1) are taken to be random variables representing random deviations among the items model. The simple assumption in regard the random parameters is that they are Gaussian with mean $\boldsymbol{\mu}_\beta = [\mu_{\beta_0} \mu_{\beta_1}]$, and covariance $\Sigma_{\boldsymbol{\beta}} = \begin{bmatrix} \sigma^2_{\beta_0} & 0 \\ 0 & \sigma^2_{\beta_1} \end{bmatrix}$.

$$\boldsymbol{\beta} \sim N(\boldsymbol{\mu}_\beta, \boldsymbol{\Sigma}_\beta) \qquad (4.1.2.3)$$

A degradation pathway may exhibit random deviations from the linear model. The random deviations can be due to a process noise and random measurement errors. In practice it is difficult to differentiate these noise sources. Hence, it is reasonable to consider the two noise components as one single element accounting for all kinds of random deviations.

The degradation model accounting for the random component is given by

$$Y(t) = \beta_1 t + \beta_0 + \varepsilon(t) \qquad (4.1.2.4)$$

where $\varepsilon(t)$ is a random Gaussian variable, $\varepsilon \sim N(0, \sigma_\varepsilon^2)$

Figure 17 shows a typical example of a collection of degradation pathways. The times that the degradation pathways cross the critical threshold form a time-to-failure distribution, which gives the experimenter an estimate of the time-to-failure and associated prediction uncertainty. The mean-time-to-failure and its 95% confidence interval are shown in Figure 17 by the dotted vertical lines.

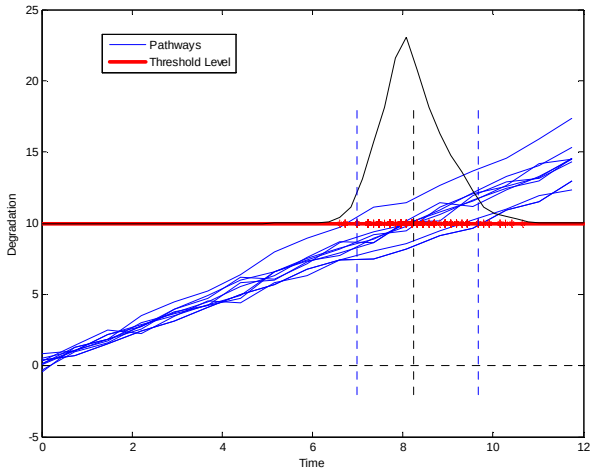

Figure 17. Collection of degradation pathways (random processes) forms a time-to-failure distribution if the failure event is defined to be the time moment of crossing the critical threshold

The model uncertainty associated with the critical threshold is assumed to be negligible. Uncertainty effects attributed to the random threshold will be considered in Section 4.2. In this setting, it is intuitively understandable that the potential benefit of an individual prognosis completely depends upon the uncertainty associated with the entire collection of degradation pathways $(\sigma_{\beta_1}^2, \sigma_{\beta_2}^2)$ and that of a single degradation trend (σ_ε^2). A large variance in a single trend may cause extrapolated values to have a prediction interval as large as the variability of the entire collection of degradation pathways. Such a situation is shown in Figure 18. The greenish colored area includes 95% of the degradation pathways observed from the population. The light blue colored area is 95% prediction intervals computed on the particular degradation pathway (prognostic trend).

As can be seen, the uncertainty in the RUL prognosis based upon the individual prognostic trend is comparable to the uncertainty of the RUL prognosis based upon the entire collection of degradation pathways.

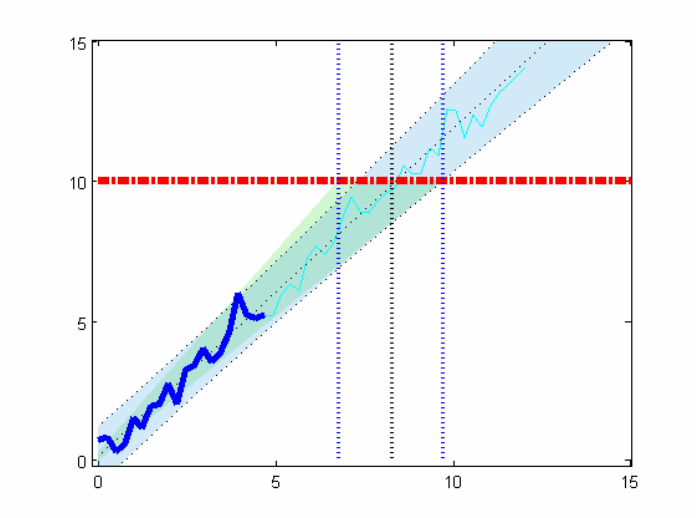

Figure 18 The TTF prediction based upon the individual degradation pathway (the blue shaded area) turns out to be as uncertain as the population average time-to-failure (the green shaded area).

A discussion of similar issues related to lifetime data uncertainties is given in (Gertsbakh, 1967). The authors use the term "signal-to-noise ratio", which is the ratio of mean lifetime to standard deviation of lifetime. The signal-to-noise ratio serves as a criterion in determining if a deterministic model should be used to make the time-to-failure prediction. Large values of the signal-to-noise ratio imply that the random fluctuations from the mean are minor so that a deterministic model is appropriate for time-to-failure prediction. Otherwise, a stochastic model is more appropriate since it accounts for random fluctuations that affect the item's degradation.

The cross-section of the green-shaded area along the axis Y (Figure 18 and Figure 19) can be expressed as

$$U^2_Y = (t_{1-\alpha,\,n})^2 \left(\sigma^2_{\beta_1}\, t + \sigma^2_{\beta_2}\right) \qquad (4.1.2.5)$$

where $t_{1-\alpha,\,n}$ is $(1-\alpha)^{th}$ percentile of the t-distribution with the degree of freedom n, which is the number of pathways observed.

Equation 4.1.2.5 determines the uncertainty associated with the mean degradation level attained by an average item up to time t. The uncertainty associated with an individual degradation pathway is given by

$$U_k^2 = (t_{1-\alpha,\,k})^2\,\sigma^2_{\varepsilon}\ (\ \mathbf{I} + \mathbf{X}_p\,\mathbf{V}\,\mathbf{X}_p^{\,T}\ ) \qquad (4.1.2.6)$$

where $t_{1-\alpha,\,k}$ is $(1-\alpha)^{th}$ percentile of the t-distribution with the degree of freedom *k*, *k* is the number of available observations on the individual pathway, **V** is the inverse covariance matrix computed according to $\mathbf{V} = (\mathbf{X}^T\mathbf{X})^{-1}$, and **X** is the design matrix of available measurements on the individual pathway:

$$X = \begin{bmatrix} 1 & 1 & \dots & 1 \\ t_1 & t_2 & \dots & t_n \end{bmatrix}^T \qquad (4.1.2.7)$$

$\mathbf{X}_p = [1\ t_p]$ is the query point for which the uncertainty U_k is calculated.

It is reasonable to assume that the ratio of the two uncertainties (4.1.2.8) can serve as a criterion to determine if an individual degradation pathway produces a RUL prediction that is more certain than the population average time-to-failure:

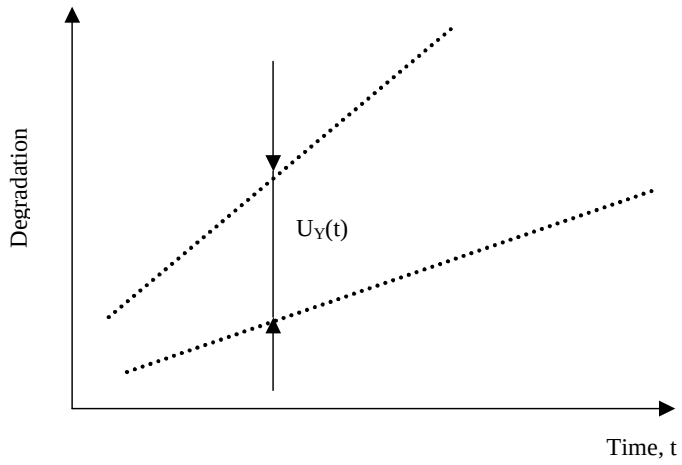

Figure 19. The uncertainty associated with the collection of degradation paths

$$C = U_k / U_Y \qquad (4.1.2.8)$$

If C > 1, the individual degradation pathway uncertainty is larger than the population average uncertainty. This situation can be due to a relatively large value of σ_ε or a great deal of uncertainty related to the term $\mathbf{X}_p\mathbf{V}\mathbf{X}_p^T$. In the latter case it can be expected that more informative observations of the individual degradation process will bring new information sufficient to make a more certain prediction.

An example of a typical behavior of the usefulness criterion is shown in Figure 20. The ratio is evaluated at different moments of time. At the times when few data are available the uncertainty ratio is greater than unity, which implies that the population-average prognosis will produce a more certain result. At time t = 3.18 one has such a number of informative observations that an individual degradation-based prediction made for a time moment later than approximately 3.5 will be certain more than the population-average prediction.

4.1.3. A Bayesian Method to Reduce Uncertainty Effects due to Imperfect Measurements.

This section introduces a Bayesian method developed to reduce uncertainty effects due to imperfect measurements of the system health status. The method is developed in conjunction with a linear degradation model.

The linear degradation model is assumed to be of the following form.

$$y = \beta_1 t + \beta_0 + \varepsilon(t),\ \varepsilon(t) \sim N(0, \sigma_\varepsilon^2) \qquad (4.1.3.1)$$

where β_1 is the average degradation rate, which is assumed to be constant, and β_0 is the initial level of damage attained by the item. The vector notation $\beta = [\beta_0\ \beta_1]$ is used further in the remainder of this section. The random component $\varepsilon(t)$ represents a stationary random noise attributed to measurement errors and random fluctuations of the degradation rate. These two random components are given as one stochastic element since they are difficult to differentiate.

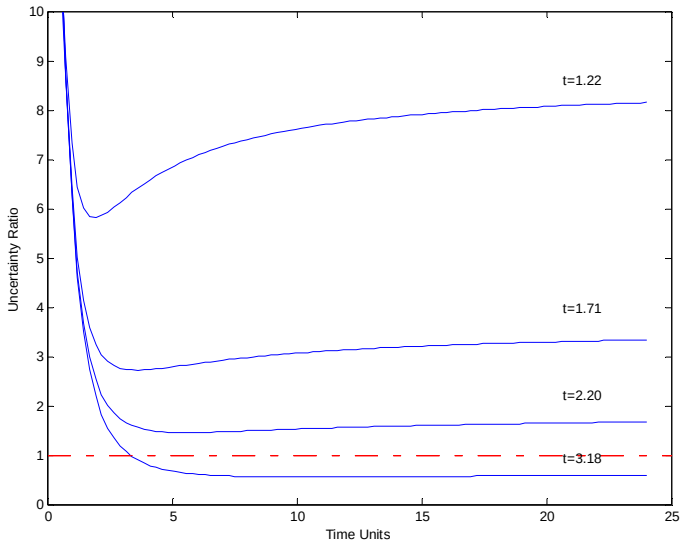

Figure 20. The uncertainty criterion calculated at different time moments.

The elements of the vector **β** are of a random nature attributed to the randomness observed among the items. The random fluctuations in β_0 correspond to random level of initial damage in the item. The random fluctuations in β_1 correspond to a stochastic nature of the item's inherent properties that determine the item's behavior with respect to degradation mechanisms.

Having observed the measurements constituting the particular item's degradation pathway $\boldsymbol{Y}_k = \{y_i: i=1,2,\ldots n\}$ one is able to assess the item's damage accumulation model given by Equation 4.1.3.1. Since the stochastic component ε in the model (4.1.3.1) is assumed to be Gaussian, the estimate of **β** is obtained using the least-squares criterion:

$$\boldsymbol{\beta} = \arg\min_{\beta} \sum_{i=1}^{n} \left(y_i - \left(\beta_1 t_i + \beta_0\right)\right)^2 \qquad (4.1.3.2)$$

Ordinary least squares (OLS) solution to the minimization problem (4.1.3.2) is given by

$$\hat{\boldsymbol{\beta}} = (\mathbf{X}^{\mathrm{T}}\mathbf{X})^{-1}(\mathbf{X}^{\mathrm{T}}\mathbf{Y}), \qquad (4.1.3.3)$$

where the design matrix **X** is of the following form

$$X = \begin{bmatrix} 1 & 1 & \dots & 1 \\ t_1 & t_2 & \dots & t_n \end{bmatrix}^T \qquad (4.1.3.4)$$

The prediction for a query point $X_p = [1\ t_p]$ is made according to the following expression of a (1–α)-level prediction interval:

$$Y_p = X_p\hat{\beta} \pm t_{n-2,\alpha/2} s \sqrt{1 + X_p' \mathbf{V} X_p} \qquad (4.1.3.5)$$

where, $t_{n-2,\ \alpha/2}$ is $(1-\alpha)^{th}$ percentile of the Student-t distribution with n-2 degrees of freedom , $\mathbf{V} = (\mathbf{X}^T\mathbf{X})^{-1}$, s is an estimate of σ_ε.

The prediction given by Equation 4.1.3.5 is derived from the following properties of the least-squares regression coefficients (Tamhane 2000)

$$E(\hat{\beta}) = \beta,\ Var(\hat{\beta}) = \frac{\sigma_\varepsilon^2}{X^T X} \qquad (4.1.3.6)$$

An early prediction of the failure time is subject to a great deal of uncertainty since the data available at the time point when the impending failure indicators just become evident do not suffice to produce a narrow prediction interval in accordance with Equation 4.1.3.5. Such a situation is shown in Figure 21. The thick blue-colored curve is the degradation pathway observed to this point for the particular item. The cyan-colored curve is the pathway along which the item's degradation will proceed. As can be seen, the OLS prediction, which is shown by the green-colored line, gives a relatively good point estimate of the time moment when the item's degradation exceeds the threshold. However, the 95% prediction interval associated with the estimate turns out to be nearly twice as large as that computed using the population-average statistics from Figure 21. The vertical dotted lines indicate the estimate of the population-average time to failure and its 95% confidence interval.

In the case shown in Figure 21 the degradation pathway data observed for the individual item is of no use in terms of obtaining an accurate individual RUL prognosis. Random fluctuations in the individual degradation rate are the main factor contributing to the individual prognosis uncertainty. The obvious approach to make the RUL prediction

more certain is to use prior information about the probabilistic parameters characterizing randomness of the degradation rate β_1 and the initial damage level β_0.

The prior information source is usually given in the form of a collection of historical measurements $\mathbf{D}_{hist}$ taken over several items akin to the to-be-predicted exemplar. The $\mathbf{D}_{hist}$ is usually a collection of measurements obtained from laboratory testing or in-field telemetry equipment. The $\mathbf{D}_{hist}$ can be represented as a $K \times N$ matrix if the same number of measurements are sampled from each item (N is the number of measurements per item, K is the number of observed items). In general, the number of observations may vary for different exemplars.

The collected information is used to estimate the mean value and variation of the degradation rates observed on the collection of items. The following equation assumes that the parameters $\boldsymbol{\beta}$ are normally distributed with mean $\bar{\beta}$ and covariance Σ_β:

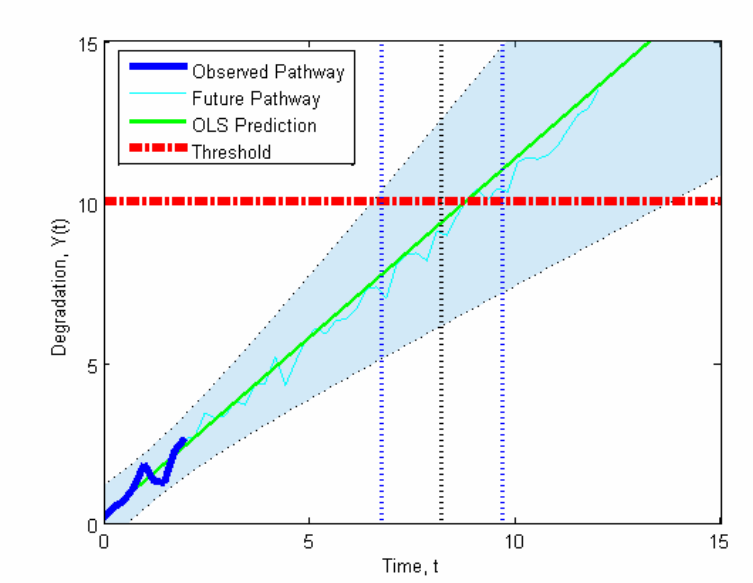

Figure 21. The vertical dotted lines indicate the estimate of the mean time failure obtained from the population-based estimation.

$$\boldsymbol{\beta} \sim N\left(\bar{\beta}, \Sigma_{\beta}\right) \tag{4.1.3.7}$$

The natural estimates of the parameters are the sample mean and variance calculated on historical data $\boldsymbol{D}_{hist.}$:

$$\hat{\beta} = \frac{1}{K}\sum_{i=1}^{K} \beta_i \tag{4.1.3.8}$$

where β_i is an estimate of the model parameters $\boldsymbol{\beta}$ for the i-th exemplar from the collective database $\mathbf{D}_{hist}$. The sample variance is given by

$$S_{\beta}^{2} = \frac{1}{K-1}\left(\tilde{\beta} - \bar{\beta}\right)^{T}\left(\tilde{\beta} - \bar{\beta}\right) \tag{4.1.3.9}$$

where $\tilde{\beta} = [\boldsymbol{\beta_1}, \boldsymbol{\beta_2}, \ldots \boldsymbol{\beta_K}]^T$ is a K × 2 matrix of estimated parameters $\boldsymbol{\beta}_i = [\beta_{i0}\ \beta_{i1}]^T$ of the initial damage level and the degradation rate at the collection of items similar to the to-be-predicted object. Usually the number of items *K* can be large enough to provide accurate estimates of the parameters $\bar{\beta}, \Sigma_{\beta}$.

Using the estimates, Equ. 4.1.3.8, and 4.1.3.9, one is able to use the estimated parameters as a prior knowledge in the degradation model given by Equ. (4.1.3.1). The mathematical formalism used to integrate the prior parameters into the linear model is Bayesian Linear Regression. This technique is described in the following subsection.

4.1.3.1.Bayesian Linear Regression

The objective of the Bayesian methodology is to construct a model for the relationship between parameters $\boldsymbol{\Theta}$ and observable data **Y**, and to estimate the probability distribution of parameters given the data **Y**. Also, Bayesian analysis can provide the predicted distribution of unobserved data.

Bayesian analysis starts with a model for the joint probability distribution of $\boldsymbol{\Theta}$ and **Y**, p($\boldsymbol{\Theta}$,**Y**). The simplest example of such a model is the normally distributed population, in which p($\boldsymbol{\Theta}$,**Y**) is the Gaussian probability distribution function with mean

and variance given by the parameter $\boldsymbol{\Theta} = (\mu, \sigma^2)$. **Y** is a sample of independent measurements. The $p(\boldsymbol{\Theta},\mathbf{Y})$ can be decomposed into two elements:

$$p(\boldsymbol{\Theta},\mathbf{Y}) = p(\boldsymbol{\Theta})\, p(\mathbf{Y}|\boldsymbol{\Theta}) \qquad (4.1.3.1.1)$$

Conventionally, $p(\boldsymbol{\Theta})$ is called the prior distribution of $\boldsymbol{\Theta}$, $p(\mathbf{Y} \mid \boldsymbol{\Theta})$ is called the likelihood function, which is the probability of observing the data **Y** given a particular value of $\boldsymbol{\Theta}$. The well-known Bayes theorem gives the posterior probability distribution $p(\boldsymbol{\Theta} \mid \mathbf{Y})$:

$$p(\boldsymbol{\Theta} \mid \mathbf{Y}) = p(\boldsymbol{\Theta})\, p(\mathbf{Y}|\boldsymbol{\Theta}) / p(\mathbf{Y}) \qquad (4.1.3.1.2)$$

where $p(\mathbf{Y})$ is the integral of $p(\boldsymbol{\Theta})\, p(\mathbf{Y}|\boldsymbol{\Theta})$ over all possible values of $\boldsymbol{\Theta}$.

To perform the Bayesian analysis it is convenient to represent the linear regression model in the following form:

$$\left(\mathbf{Y}|\boldsymbol{\beta}, \boldsymbol{\Sigma}_{\beta}, \mathbf{X}\right) \sim N\left(\mathbf{X}\boldsymbol{\beta}, \boldsymbol{\Sigma}_{\beta}\right) \qquad (4.1.3.1.3)$$

Given parameters $\boldsymbol{\beta}$ and $\boldsymbol{\Sigma}_{\beta}$ and predictors **X**, the distribution of the response **Y** is a normal distribution with the mean value of $\mathbf{X}\boldsymbol{\beta}$ and variance $\boldsymbol{\Sigma}_{\beta}$. If a univariate response is considered, the variance matrix is taken to be equal σ^2.

The next step is to formulate the prior distribution of the parameters $\boldsymbol{\beta}$ and σ^2. A commonly adopted approach is to use a non-informative prior distribution:

$$p(\boldsymbol{\beta},\sigma^2) \propto 1/\sigma^2 \qquad (4.1.3.1.4)$$

When using a non-informative prior, one assumes that the joint probability distribution of the parameters is a flat surface with a level proportional to $1/\sigma^2$. In Bayesian analysis-related literature, it is stated that the choice of a non-informative prior does not greatly affect the outcome in many real-world cases (Gelman 1998). The effect of a large prior σ^2 tends to be overshadowed by that of the likelihood function computed over many informative observations. The posterior distribution of $\boldsymbol{\beta}$ given σ^2 is expressed as

$$\boldsymbol{\beta} \mid \sigma^2, \mathbf{Y} \sim N(\beta_E, V_\beta \sigma^2) \quad (4.1.3.1.5)$$

where $\beta_E = (\mathbf{X}^T \mathbf{X})^{-1} \mathbf{X}^T \mathbf{Y}$, $\mathbf{V}_\beta = (\mathbf{X}^T \mathbf{X})^{-1}$.

The marginal posterior distribution of σ^2 is

$$\sigma^2 \mid \mathbf{Y} \sim \text{Inverse } \chi^2 (n\text{-}k, s^2) \quad (4.1.3.1.6)$$

where n is the number of observations and k is the number of parameters to be estimated. The inverse χ^2 distribution (Hogg 1978) is defined by two parameters, which are the degrees of freedom ν and the scale factor γ^2. The density probability function of the inverse chi-square distribution is given by

$$f(x;\nu,\gamma^2) = \frac{(\gamma^2\nu/2)^{\nu/2}}{\Gamma(\nu/2)} \frac{\exp\left(-\frac{\nu\gamma^2}{2x}\right)}{x^{1+\nu/2}} \quad (4.1.3.1.7)$$

where $x > 0$, ν is the degree of freedom, γ^2 is the scale factor. The inverse chi-square probability distribution characterizes the random variable

$$y = \frac{\gamma^2\nu}{x} \quad (4.1.3.1.8)$$

where x is a chi-square distributed random variable with ν degrees of freedom, $x \sim \chi^2(\nu)$

The scale factor s^2 in (4.1.3.1.6) is estimated according to

$$s^2 = \frac{1}{n-k}(\mathbf{Y} - \mathbf{X}\beta_E)^T(\mathbf{Y} - \mathbf{X}\beta_E) \quad (4.1.3.1.9)$$

The marginal posterior distribution of the parameters $\boldsymbol{\beta}$ given the data $\mathbf{Y}$ is

$$\boldsymbol{\beta} \mid \mathbf{Y} \sim \text{Student t } (n\text{-}k, \beta_E, s^2) \quad (4.1.3.1.10)$$

where Student_t(k, μ, σ^2) is the Student's t-distribution characterizing the random variable

$$T = \frac{\bar{x}_n - \mu}{S_n/\sqrt{n}} \quad (4.1.3.1.11)$$

where $\bar{x}_n$ is the sample mean, S_n is the sample variance. The sample is assumed to be taken from the normal distributed population $N(\mu,\sigma^2)$.

The predictive distribution given a new predictor point $\mathbf{X}_p$ is characterized by the following mean and variance.

$$E[\mathbf{Y}_p|\ \mathbf{Y}] = \mathbf{X}_p\ \boldsymbol{\beta}_E \qquad (4.1.3.1.12)$$

$$\mathrm{Var}(\mathbf{Y}_p|\ \sigma^2,\ \mathbf{Y}) = (\mathbf{I} + \mathbf{X}_p\mathbf{V}_\beta\mathbf{X}_p{}^T)\ \sigma^2 \qquad (4.1.3.1.13)$$

where $\mathbf{I}$ is an identity matrix. The variance is essentially of two components: $\mathbf{I}\sigma^2$, which is the sampling variance characterizing randomness in the available observations, and $\mathbf{X}_p\mathbf{V}_\beta\mathbf{X}_p{}^T\ \sigma^2$, which is the uncertainty associated with the estimates of $\boldsymbol{\beta}$. The marginal posterior distribution of $\mathbf{Y}_p$ is given by

$$\mathbf{Y}_p\ |\ \mathbf{Y} \sim \text{Student\_t}\ (n\text{-}k,\ \mathbf{X}_p\boldsymbol{\beta}_E,\ (\mathbf{I} + \mathbf{X}_p\mathbf{V}_\beta\mathbf{X}_p{}^T)\ \sigma^2\ ) \qquad (4.1.3.1.14)$$

As can be seen, the OLS estimates obtained through the classical regression analysis are similar to those computed according to the Bayesian approach with a non-informative prior. However, the Bayesian regression analysis is aimed at estimating a conditional posterior distribution for the parameters and a predictive distribution for the model, whereas the classical regression analysis is focused on calculating point estimates for parameters and predictions as well as the variances of those estimates. Although classical regression analysis derives the formula through maximization of a likelihood function for model errors, the computations turn out to be similar. The classical estimates of $\boldsymbol{\beta}$ and σ^2 are equal to $\boldsymbol{\beta}_E$ and s^2, respectively. The standard error estimate for $\boldsymbol{\beta}$ is $\mathbf{V}_\beta s^2$.

If one possesses two different sources of information regarding the phenomenon under study, it makes sense to combine the information sources into a single model to estimate parameters and compute predictions. In terms of the damage accumulation model considered in this study, the different sources are the collective historical data observed over a fleet of items and the degradation indicator data observed at a particular item. Possessing information drawn from the collective database of historical

measurements, one is able to formulate and then make use of an informative prior in the Bayesian regression framework.

The Bayesian linear regression with an informative prior assumes two statistically independent data sets to be the prior and the likelihood data set. Conveniently, the informative prior distributions take the following form:

$$\boldsymbol{\beta} \mid h \sim N(\underline{\boldsymbol{\beta}}, h^{-1}\underline{\mathbf{V}}) \qquad (4.1.3.1.15)$$

$$h \sim \Gamma(\underline{\nu}/2, \ \underline{\nu s}^2/2) \qquad (4.1.3.1.16)$$

where $h = 1/\sigma^2$, $\nu = n-k$, $\Gamma(a, b)$ is a gamma distribution with 2 parameters. The gamma distribution is represented by the following probability density function (Tamhane, 2000):

$$\Gamma(x, a, b) = x^{a-1}\frac{e^{-x/b}}{b^a \Gamma(a)} \qquad (4.1.3.1.17)$$

where $a>0$ is the shape parameter and $b > 0$ is the scale parameter.

The underscore notation indicates a parameter for a prior; the upperscore notation indicates a parameter for a posterior. The defined prior distributions (4.1.3.1.15), (4.1.3.1.16) constitute a conjugate prior, which is such a distribution that being combined with the likelihood produces a posterior distribution belonging to the same family of distributions as the prior. In addition to being a conjugate prior, the distributions (4.1.3.1.15) and (4.1.3.1.16) are a natural prior in the sense that the defined prior is of the same form as the likelihood function. The natural conjugate prior is given by

$$\boldsymbol{\beta}, h \sim NG(\underline{\boldsymbol{\beta}}, \underline{\mathbf{V}}, \underline{\nu}/2, \underline{\nu s}^2/2) \qquad (4.1.3.1.18)$$

where $NG(a,b,c,d)$ denotes a normal-gamma joint distribution of the parameters $\boldsymbol{\beta}$ and h. The posterior distribution of the parameters given data $\mathbf{Y}$ is the following.

$$\boldsymbol{\beta}, h \mid \mathbf{Y} \ \sim \ NG\left(\overline{\boldsymbol{\beta}}, \overline{\mathbf{V}}, \overline{\nu}/2, \overline{\nu s}^2/2\right) \qquad (4.1.3.1.19)$$

where

$$\overline{\mathbf{V}} = \frac{1}{\underline{\mathbf{V}}^{-1} + \mathbf{X}^T\mathbf{X}}, \quad \overline{\beta} = \overline{\mathbf{V}}\left(\underline{\mathbf{V}}^{-1}\underline{\beta} + \beta\hat{\beta}(\mathbf{X}^T\mathbf{X})\right) \tag{4.1.3.1.20}$$

$$\overline{\nu} = \underline{\nu} + n, \; \overline{\nu s^2} = \underline{\nu s}^2 + \nu s^2 + \frac{\left(\hat{\beta} - \underline{\beta}\right)^2}{\underline{\mathbf{V}} + \mathbf{X}^T\mathbf{X}} \tag{4.1.3.1.21}$$

The following subsection presents an example illustrating the usage of the Bayesian approach to the RUL prediction for the linear damage accumulation model (4.1.3.1). The priors for the model parameters β_0 and β_1 are estimated from the historical measurements.

4.1.3.2.Example

To simulate the historical measurements, 20 degradation pathways are generated using the following parameters:

$$\boldsymbol{\beta} \sim N\left([0.2 \quad 1.2], [0.08^2 \quad 0.1^2]\mathbf{I}\right), \varepsilon \sim N(0, 0.3^2) \tag{4.1.3.2.1}$$

Observing a particular item's degradation pathway, one needs to extrapolate the trend to estimate the time of failure. A relatively small number of informative observations available at the early phase of the monitoring routine do not allow for an accurate evaluation of the linear model. As can be seen in Figure 22a, not taking into account the historical data observed on other items causes the TTF prediction to be greatly uncertain when compared to the uncertainty associated with the Bayesian prediction. As more observations become available the effect of the prior information becomes weaker. At some point the effect of informative observations outweighs the prior information, so that the OLS regression prediction becomes identical to that of Bayesian regression, as shown in Figure 22b.

To perform a comparison in a quantitative manner, Figure 23 shows the TTF predictions along with their confidence intervals. The population average TTF prediction remains unchanged since it does not take into account the health condition measurements taken at a particular item. The OLS regression TTF prediction is quite uncertain before t = 4. In this case, there is no reason to use the OLS regression-based TTF prediction

before t = 2.5 since it is outperformed by that based on the population average TTF. However, the Bayesian regression TTF prediction provides a result as certain as the average population based TTF even if few observations are available (t<2).

As the data collection proceeds, the difference between the OLS and Bayesian regression predictions becomes smaller. As time nears the actual failure, the two methods provide essentially equal results. The following section considers the notion of a critical degradation threshold given in a probabilistic manner. The uncertainty effect imposed by a stochastically defined critical threshold upon the end result prediction is quantified.

4.2. Random Deviations in Failure Threshold

If the precise critical threshold value is not readily available, one has to estimate it using any available reliability data. When estimating the model parameters that include the critical threshold, one deals with variability in the available data. Since the variability tends to propagate into the estimates, the estimation of the critical threshold is often imperfect. A probabilistic representation of the critical threshold is the only way to numerically express the actual knowledge of the threshold.

The uncertainty associated with the critical threshold is one of the major contributors to uncertainty associated with the RUL estimate provided by the prognostic model. Since uncertainty-related issues are a crucial part of reliability prediction modeling, a particular emphasis should be made in modeling the uncertainty associated with the degradation/health status, which is considered to be critical. Many models used in degradation data analysis make use of the notion of a critical threshold. Oftentimes the critical threshold is assumed to be deterministic, primarily because this assumption simplifies the reliability computation.

Although a deterministic representation of the critical threshold can be absolutely reasonable in some cases, there are situations where a probabilistic description is likely to be more appropriate. For example, if the designer is not aware of the precise level of degradation that causes a failure it is appropriate to represent the critical threshold as a PDF that reflects the designer's vague knowledge about possible critical values.

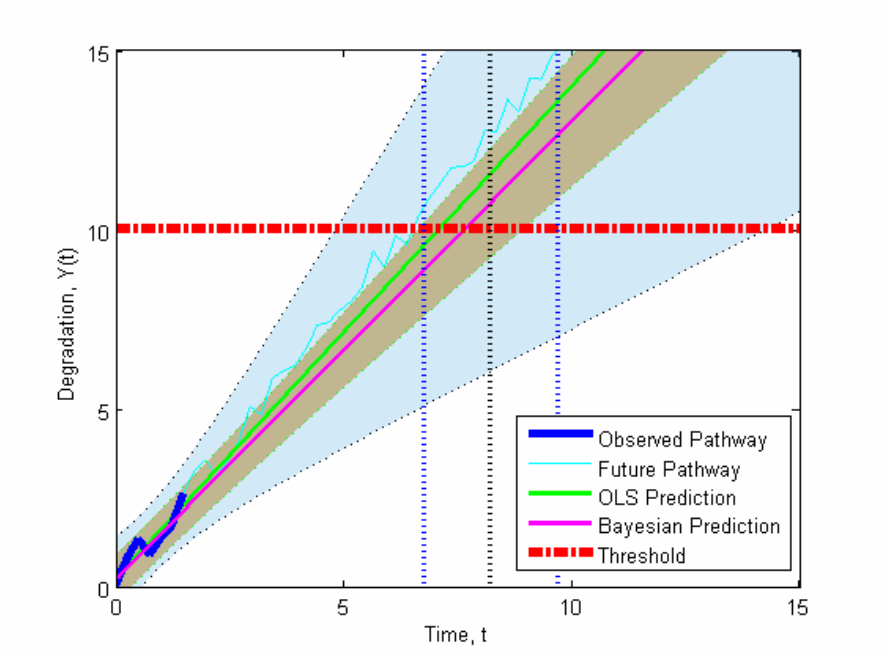

a)

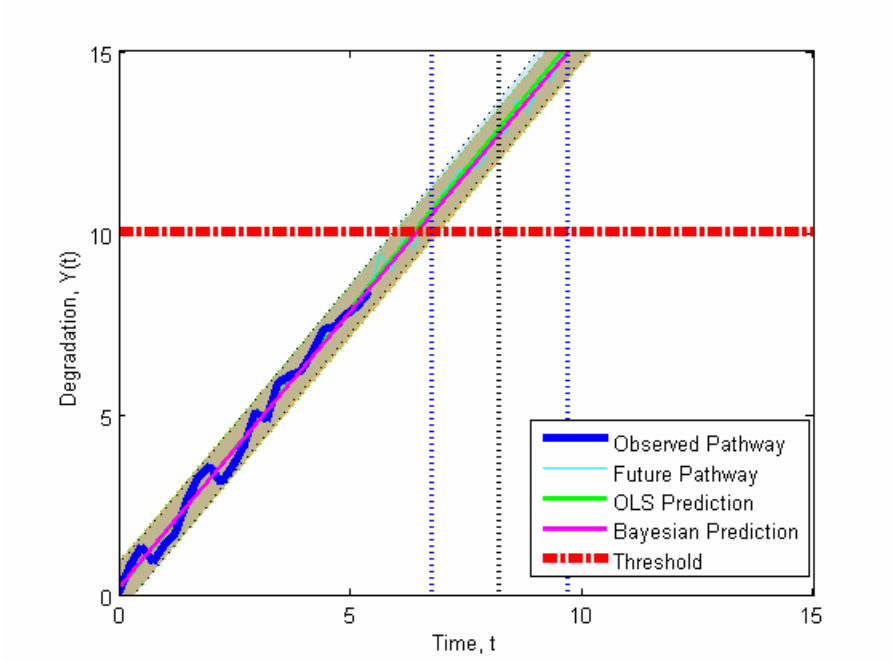

b

Figure 22. OLS prediction versus Bayesian prediction. a) Few observations are available; b) Many observations are available

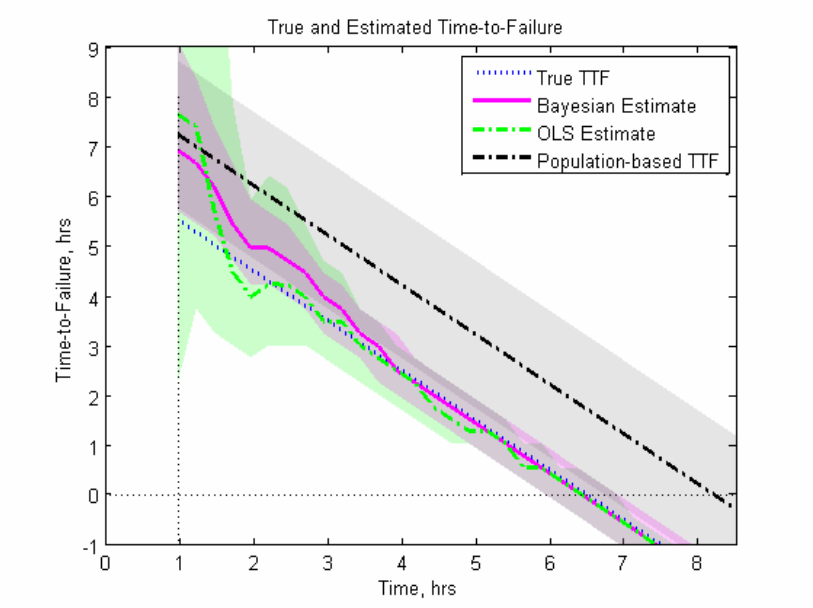

Figure 23. Time-to-Failure values calculated according to three different methods: Population-based Average TTF, OLS regression based TTF and Bayesian regression based TTF.

Additionally, the system or component may be used in a variety of applications each of which requires some particular level of critical degradation. In such a case, it seems reasonable to define the critical threshold as a range of critical values having certain probabilities.

Consider the critical threshold as a random variable distributed according to a certain probability distribution function. Knowledge of the distribution function may come from technical specifications, expert opinions, engineering judgment, experimental data observed in a laboratory and/or in-field testing.

Let $F_Y(y)$ be the cumulative distribution function (CDF) of the random critical threshold.

$$F_{Y^*}(y) = \Pr[Y^* < y] \qquad (4.2.1)$$

where Y^* is the random threshold value for degradation *y*.

$$f_{Y^*}(y) = \frac{dF_{Y^*}(y)}{dy} \tag{4.2.2}$$

is the probability density function (PDF) of the random threshold Y^*.

Let $R_M(\ t \mid \Theta,\ Y^*)$ denote the reliability function predicted by the degradation model $M(\boldsymbol{\Theta},\ Y^*)$, which has a vector of parameters $\boldsymbol{\Theta}$, and critical threshold value Y^*. For the sake of brevity, the parameter vector $\boldsymbol{\Theta}$ will be skipped in the remainder, since the effect of other parameters is beyond the dissertation's scope.

Obviously, to take into account the randomness of the critical threshold, one needs to integrate the parameter Y* out of the reliability function $R_M(\ t \mid \Theta,\ Y^*)$, as shown in the following expression.

$$R_M(t) = \int_{y \in \mathbf{Y}} R_M(t \mid y) \times f_{Y^*}(y) dy \tag{4.2.3}$$

where **Y** is the domain of all possible threshold values.

Uncertainty effects attributed to the random critical threshold will be investigated in the cases of three degradation models. These are

1. Markov chain (MC)-based cumulative damage model,
2. Weiner process with drift, and a
3. Linear Path Model with lognormal random coefficients.

Each of the models belongs to the family of cumulative degradation models, in which degradation is assumed to accumulate through the unit's lifespan. The cumulative degradation eventually causes the unit's failure.

4.2.1. A Markov-Chain based Model

The uncertainty associated with the threshold Y^* is to be expressed as a discrete probability mass function. If the user has an unbiased estimate of the mean threshold value, it is reasonable to use a symmetric probability mass function.

To quantify the effect of the uncertain threshold upon the TTF prediction, the TTF distribution that accounts for the uncertain threshold is given as follows:

$$F(t) = \sum_{k=1}^{\infty} F(t \mid Y^* = k) P(Y^* = k) \qquad (4.2.1.1)$$

where $P(Y^* = k)$ is the probability that the critical threshold value is equal to k, $F(t \mid Y^* = k)$ is the TTF CDF predicted by the MC-based model with the deterministic threshold value of k.

The probability mass function (PMF) characterizing the threshold uncertainty is taken to be a function resembling the Gaussian normal distribution as shown in Figure 24.

The expression for the time-to-failure CDF that takes into account the uncertainty in the threshold is given by:

$$F(t,\Theta) = \sum_{y=1}^{\infty} \frac{\gamma(y_i, t/\Theta)}{\Gamma(y_i)} P(Y^* = y_i) \qquad (4.2.1.2)$$

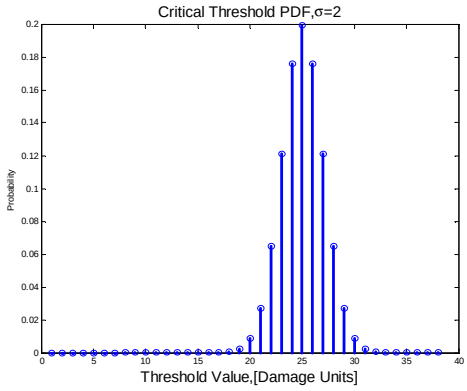

Figure 24. The non-skewed probability mass function that is used to represent the uncertainty associated with the unbiased estimate of the critical threshold.

where $\gamma(y,t)$ is the incomplete gamma function, $\Gamma(y)$ is the gamma function.

$$\gamma(y,t) = \int_0^t x^{y-1}\exp(-x)dx\,,\ \Gamma(y) = \int_0^\infty x^{y-1}\exp(-x)dx \qquad (4.2.1.3)$$

4.2.2. General Path Model (Random Log-normal Coefficients)

A brief description of the general path model is given as follows. The observed sample degradation y_{ij} of unit i at time t_j is

$$y_{ij} = D(t_{ij},\boldsymbol{\beta}_i) + \varepsilon_{ij} \qquad (4.2.2.1)$$

where $D(t_{ij},\boldsymbol{\beta}_i) = D(t_{ij}, \beta_{1i}, \beta_{2i}, \ldots \beta_{ki})$ is the actual degradation level of Unit i at time t_{ij}, and ε_{ij} is a normally distributed variable representing random deviations for Unit i. The vector $\boldsymbol{\beta}_i = [\beta_{1i}, \beta_{2i}, \ldots\beta_{ki}\ ]$ is composed of unknown parameters characterizing the degradation of Unit i. Some of the parameters $\boldsymbol{\beta}_i$ are random from unit to unit. The randomness is attributed to unit-to-unit variability within the population. On the other hand, some of the parameters $\boldsymbol{\beta}_i$ can remain constant for all units, thus representing properties common for the entire population.

Let D_f denote the critical degradation level, exceeding which, the unit is said to fail. The critical level can be defined as a precise level of degradation if one is able to accurately define the failure event in terms of the degradation metric. For example, a light emitting diode is said to fail if its emitting power drops below some percent of the initial power (Fukuda 1988). This type of failure event is called a soft failure.

In some situations, failure events cannot be easily defined in terms of a degradation measure. In such cases, the item just stops working. Failure events do not occur at the same level of degradation because of unit-to-unit variability in the population. In this case, the general path model should provide a probability distribution for the critical level D_f.

Given the model for $D(t)$ one is able to derive a failure-time probability distribution implied by the general path model:

$$F(t) = \Pr[T < t] = \Pr[D(t,\beta_1,\beta_2, \ldots \beta_k) > D_f)\ ] \qquad (4.2.2.2)$$

In this example a linear degradation model of the following form is considered.

$$D(t) = \beta_1 + \beta_2 t \qquad (4.2.2.3)$$

where β_1 is the constant parameter representing the initial degradation in the unit. The initial degradation level is assumed to be identical for each unit in the population. In practice this assumption is reasonable if the initial degradation variability is small compared to the variability in operating conditions the items will encounter in their operational life. β_2 is the random parameter representing the degradation rate, which varies from unit-to-unit. The distribution of the β_2 is taken to be lognormal, since the lognormal distribution assumption allows for deriving a closed-form expression for the TTF distribution.

As shown in (Meeker 1998), the linear degradation model with a lognormal rate implies that the failure times are distributed according to a lognormal distribution given by:

$$F(t \mid \beta, D_f) = \Phi_{norm}\left(\frac{\log(t) - [\log(D_f - \beta_1) - \mu]}{\sigma}\right) \qquad (4.2.2.4)$$

where t>0, and (μ,σ) are the parameters of the lognormal degradation rate distribution, and $\Phi_{norm}(x)$ is the standard normal CDF (Abramowitz, 1972).

As can be seen in (4.2.2.4) the TTF distribution is also lognormal with the parameters $\log(D_f - \beta_1) - \mu$ and σ. Assuming the critical threshold to be random one comes up with the following expression for the TTF distribution,

$$F(t \mid \beta_1) = \int_0^{\infty} \Phi_{norm}\left(\frac{\log(t) - [\log(y - \beta_1) - \mu]}{\sigma}\right) \times f_{D_f}(y)dy \qquad (4.2.2.5)$$

where $f_{Df}(y)$ is the probability density function of the random threshold.

4.2.3. A Wiener process-based model

A stochastic process $\{W(t),\ t \geq 0\}$ is called a Wiener process with drift if the following expression holds:

$$W(t) = \mu t + X(t) \qquad (4.2.3.1)$$

where $\{ X(t),\ t \geq 0 \}$ is a Wiener process with σ^2 = Var(X(1)). The constant μ is called drift parameter.

Wiener processes with drift are used for modeling degradation parameters, (Tseng 2004), (Whitmore 1995), (Doksum 1992), as well as for other applications such as maintenance cost of engineering systems, modeling physical noise processes. A strict mathematical description of Weiner processes may be found in (Beichelt 2002). As can be concluded from Equ.(4.2.3.1), the Wiener process with drift is a superposition of a Wiener process $X(t)$ and a function m(t) = μt representing a deterministic linear trend.

Let y denote the critical level, entering which the Wiener process with drift undergoes a failure event at time T_y. Since the process increments are independent and Gaussian, the probability densities of T_y and y are related as follows:

$$f_{T_y}(t) = \frac{y}{t} f_W(y),\ y > 0, t > 0 \qquad (4.2.3.2)$$

Thus, the probability density of T_y is given by

$$f_{T_y}(t \mid y, \mu, \sigma) = \frac{y}{\sqrt{2\pi}\sigma t^{3/2}} \exp\left(-\frac{(y-\mu t)^2}{2\sigma^2 t} \right),\ t > 0 \qquad (4.2.3.3)$$

The probability density (4.2.3.3) represents that of the inverse Gaussian distribution with parameters μ, σ^2, and y. The CDF of the inverse Gaussian distribution takes the following form

$$F_{T_y}(t \mid y, \mu, \sigma) = 1 - \Phi\left(\frac{y-\mu t}{\sigma\sqrt{t}} \right) + \exp(-2y\mu)\Phi\left(-\frac{y+\mu t}{\sigma\sqrt{t}} \right),\ t > 0 \qquad (4.2.3.4)$$

The expected value and variance of T_y are given by

$$E[T_y] = \frac{y}{\mu}; Var(T_y) = \frac{y\sigma^2}{\mu^3} \quad (4.2.3.5)$$

The distribution of T_y that takes into account the uncertainty in the critical threshold value y is given by

$$F(t \mid \mu, \sigma) = \int_0^\infty F_{T_y}(t \mid y, \mu, \sigma) \times f(y) dy \quad (4.2.3.6)$$

where $f(y)$ is the probability density of the critical threshold.

The outlined MC-based model and Weiner process with drift can be represented in the form of a general cumulative shock model. This is a generalization of degradation-based reliability models, in which degradation is thought of as a damage accumulation process evolving stochastically in time and the damage measure domain.

The cumulative damage models outlined in the previous subsections are expected to produce similar TTF distributions if the model parameters are chosen such that the time between damage occurrences is distributed similarly for the models. The mean and variance of damage increments are also chosen to be almost the same for the models.

Resemblance of the TTF distributions in the cumulative damage models implies that the effect of randomness in the threshold is expected to be approximately the same for the cumulative damage models under the assumption of identical threshold uncertainty. In the next subsection a numerical experiment is presented to confirm this conclusion.

4.2.4. Numerical Experiment

This section presents experimental results illustrating the effect of the critical threshold uncertainty in the cumulative damage models outlined in the previous section. Three different types of degradation models are chosen to evaluate the relative uncertainty in the predicted TTF distribution given the relative uncertainty in the critical threshold for each model. The reference point in the experimentation is taken to be the TTF distribution provided by the degradation models with a strictly defined threshold.

Because of different model structures, the model parameters are model-to-model different. However, the model parameters are selected such that the values of mean time-to-failure and variance are to be approximately the same for each model. Figure 25 shows that the reference TTF distributions are almost identical for the tested models.

To characterize the uncertainty in the critical threshold, the value of relative uncertainty, U_Y, is defined as follows:

$$U_Y = \frac{\sigma_Y}{Y^*} \tag{4.2.4.1}$$

where Y* is the deterministic critical threshold value in the reference model, σ_Y is the standard deviation of the random threshold having the mean value of Y^*.

The objective of the experiment is to evaluate the relative uncertainty, U_{TTF}, of the TTF prediction made by the degradation model with a random threshold:

$$U_{TTF} = \frac{\sigma_{TTF}}{\sigma^*_{TTF}} \tag{4.2.4.2}$$

where σ^*_{TTF} is the standard deviation of the TTF distribution provided by the reference model, σ_{TTF} is the standard deviation of the TTF distribution provided by the model with a random threshold.

Figure 26 shows the numerical results quantifying the relationship between the uncertainty in the critical threshold and the uncertainty associated with the predicted time-to-failure. As can be seen, the tested models have shown approximately identical functional forms that quantify the effect of a random threshold. The Weiner process with drift was revealed to be slightly less sensitive to the randomness in the threshold. However, the difference of 4% that was shown by this model could be attributed to the imperfections in the numerical integration.

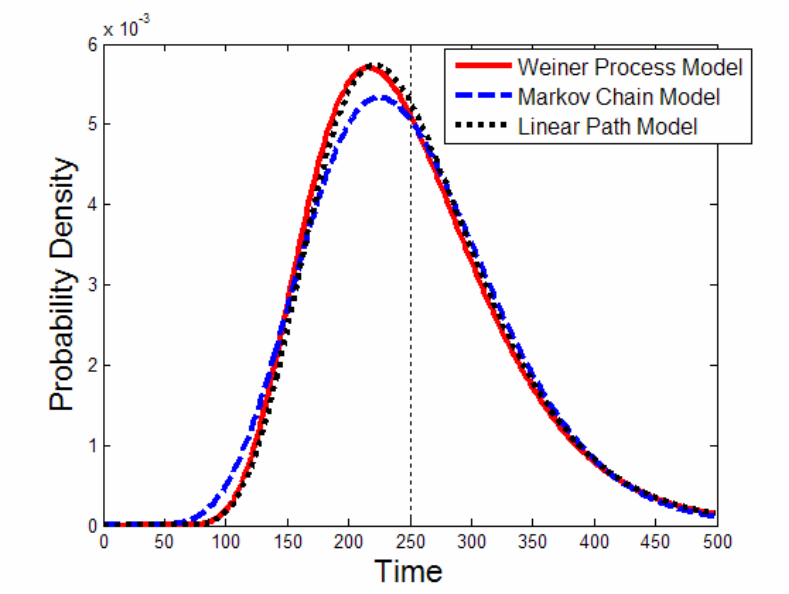

Figure 25. The reference TTF probability densities calculated for the models with a deterministic critical threshold. The vertical black-dotted line indicates the mean time-to-failure, which is identical for the all depicted TTF distributions.

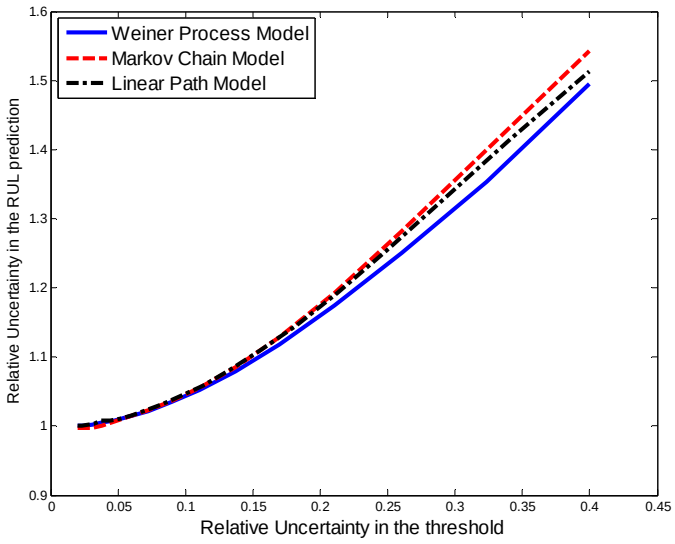

Figure 26. The functional relationship between the relative uncertainty in the critical threshold and the prediction uncertainty associated with the TTF distribution

The results shown in Figure 26 suggest that the manner in which the random threshold affects the TTF prediction does not depend on the particular configuration of the assumed degradation model. The major factor that determines the effect of a random threshold is the shape of the TTF distribution implied by the degradation model, as shown in Equations 4.2.1.1, 4.2.2.5, and 4.2.3.6.

The obtained experimental result is in accordance with the analytical derivations presented in (Gut 1990) where it was shown that for a cumulative stochastic process, the distribution of the first passage time approaches the normal distribution with certain parameters if the critical failure threshold is relatively large (see Equ. 3.6.3).

From the perspective of general cumulative shock models, the tested models can be considered in the following manner. The parameters of the Markov chain-based model are rewritten as follows

$$E(T) = \Theta,\ Var(T) = \Theta^2,\ \ E(C) = 1,\ Var(C) = 0 \qquad (4.2.4.3)$$

Put in words, the time between shocks tends to be distributed exponentially with the mean of Θ and variance Θ^2, where Θ is the MC model parameter (see Equ. 4.2.1.2). The shock magnitude is a deterministic value of 1. According to the limiting distribution (3.6.3) the TTF distribution is given by

$$L(x) \sim N(\Theta x, \Theta^2 x) \qquad (4.2.4.4)$$

where x is the critical threshold value. The distribution parameters given in (4.2.4.4) are in total accordance with the mean and variance parameters of the gamma distribution (4.2.1.2) characterizing the TTF in the MC-based model.

The parameters of the Weiner process with drift can be rewritten as follows:

$$E(T) = 1,\ Var(T) = 0,\ \ E(C) = \mu_{drift},\ \ Var(C) = \sigma^2_W \qquad (4.2.4.5)$$

Put in words, the time between shocks is assumed to be deterministic and unit-sized. The magnitude of shocks is normally distributed with the mean equal to the drift parameter and the variance equal to the variance of the Weiner process. The limiting TTF distribution is of the following form

$$L(x) \sim N\left(\frac{1}{\mu_{drift}}x, \frac{\sigma_W^2}{\mu^3{}_{drift}}x\right) \qquad (4.2.4.6)$$

where x is the critical threshold value. The distribution mean and variance parameters are in accordance with the parameters of the inverse Gaussian distribution, which characterizes the first time the Wiener process with drift exceeds the value of x.

Equations 4.2.4.4 and 4.2.4.6 essentially show that the MC-based degradation model and the Wiener process with drift produce TTF distributions whose dependences upon the critical threshold x are identical. Particularly, the dependence is linear with respect to the TTF mean and variance.

The linear path model with lognormal random coefficients exhibits a stochastic behavior more complex than that of the Markov chain-based model and the Weiner process with drift since the variance of random shock magnitude happens to be not stationary in time, which makes the analysis more difficult compared to the other tested models.

From the identical dependences upon the critical threshold it follows that Equ. 4.2.3 produces identical results for the cumulative degradation models, which possess similar uncertainty in their critical thresholds, and their other parameters are chosen such that the mean values of time-to-failure and variances are approximately the same.

Concluding this section the following statements are made. The investigated degradation models have been considered as general shock models. This mathematical treatment has allowed for deriving a limiting time-to-failure distribution implied by the models. The limiting distribution has been shown to be the same for the models under the assumption of identical mean time-to-failure and variance. Particularly, the limiting distribution is the normal distribution with certain parameters, also known in reliability analysis as the Birnbaum-Saunders distribution, describing the rupture time of metals exposed to fluctuating stress and tension.

Since the degradation models tend to have asymptotically identical time-to-failure distributions, the effect of threshold randomness is approximately the same for the models.

4.3. Uncertainty due to Hidden Failure Mechanisms

This section is concerned with uncertainty issues related to degradation-based reliability models that exhibit a certain pattern in the degradation data available for model evaluation. The essence of the issues to be investigated is illustrated in the following qualitative example.

4.3.1. Illustrative Example

Consider an electronic power supply deteriorating due to two failure mechanisms that are described as follows. An internal defect reinforced by various external stress factors such as temperature and vibration, initiates a crack in the printable circuit board (PCB) so that the crack propagation tends to affect a vitally important electronic component residing on the PCB near the propagating crack. The crack propagates mostly due to temperature gradients suffered by the power supply. The temperature gradients cause certain spots on the PCB to undergo mechanical stresses, which, in turn, cause the crack growth. Eventually the propagated crack deteriorates the electronic element's functioning so that the power supply is no longer capable to provide its output voltage within the specified range. This failure will be attributed to Failure Mechanism 1 (FM_1).

The second failure mechanism is related to corrosion processes mostly affecting the solder joints populating the PCB. Any severely corroded solder joint may cause the power supply to fail (Vichare and Pecht 2006). This failure type will be attributed to Failure Mechanism 2 (FM_2).

The outlined failure mechanisms are assumed to be different with respect to their observability. In the case of FM_1 the mechanical stress reinforcing the crack growth manifests itself as an occurrence of random spikes in the output voltage. By measuring the voltage spikes frequency and magnitude, one is able to assess the damage acquired by the PCB due to FM_1. The assumption made here is that the spike magnitudes and

frequencies are correlated with the crack length. The longer the crack length, the more severe the effect upon the electronic component output voltage. Also there is assumed to be a critical crack length, exceeding which the crack causes the power supply to cease its proper functioning, since the output voltage is no longer stable.

In the case of FM_2,one is not able to perceive online any information related to the level of degradation (corrosion) in the solder joints. The degree at which the corrosion has deteriorated the power supply reliability can be revealed only after a thorough offline inspection, which is usually impractical to perform on a not-yet-failed item.

The absence of perceivable information in regards to FM_2 can hinder the reliability modeling. Figure 27a shows the degradation paths observed in reliability testing of real-world electronic power supplies (Hines and Usynin 2006). Each of the depicted degradation paths has ended with a failure event.

To develop a reliability prediction model, one needs to define a critical degradation threshold, exceeding which, the component is said to fail. If the precise value of the critical degradation threshold is unknown in the initial development phase, it has to be estimated from available degradation and failure observations. However, as shown in Figure 27a the degradation paths can exhibit a great deal of variability in the critical degradation values corresponding to the observed failure moments (Data Points PS1, PS2, and PS3).

As can be seen in Figure 27a, the reason for the large variability in the critical threshold is the fact that Power Supply 3 has degraded in a manner significantly different from those observed at PS1 and PS2. The deviated degradation path can be easily declared to be an outlier since a) its appearance differs from the majority of the tested items (even though the majority is only two items: PS1, PS2), b) the presence of such an anomalous degradation pattern can complicate the reliability model development in the sense that the model would have to account for this unusual degradation path, probably at the expense of the model predictive accuracy.

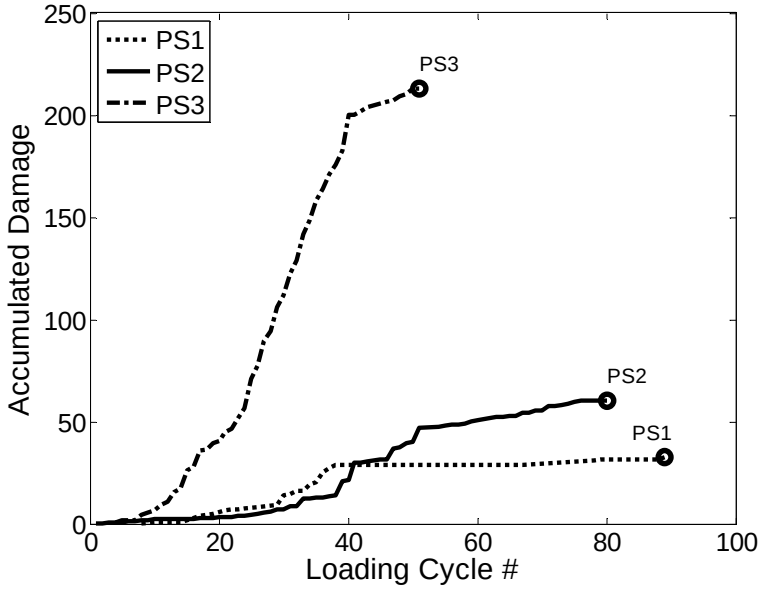

a)

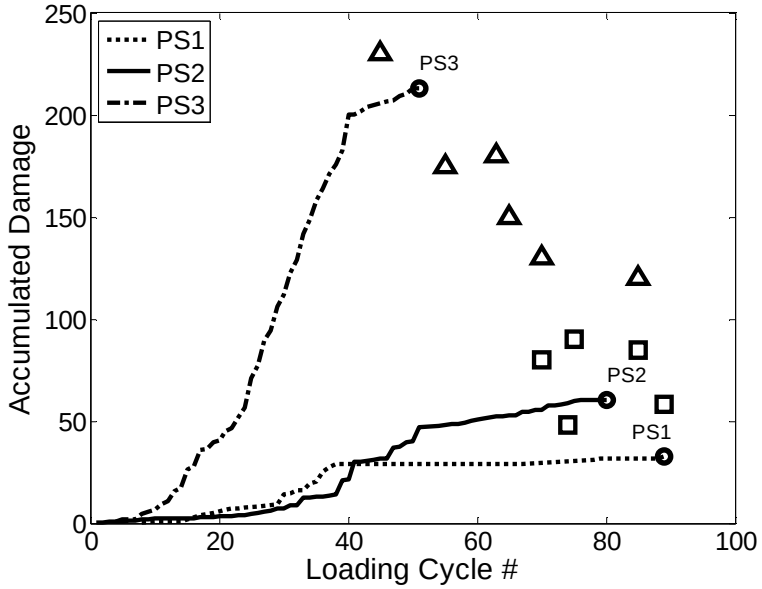

b)

Figure 27. The degradation paths observed from electronic power supplies (a). The triangle and square marks represent imagined power supplies failure points (b). The square-marked failure points are grouped near PS1 and PS2. The triangle-marked failure points are distributed between PS3 and PS2

However the small number of degradation paths obtained in this experiment does not allow one to decide if the PS3 degradation path can be disregarded in the reliability model development because of being an outlier.

If additional degradation paths, which terminated with a failure, were available, and these extra failure observations were situated near the PS1 and PS2 failure points (as is shown in Figure 27b by the black square marks), the PS3 degradation path would clearly be classified as an outlier. On the other hand, if the extra observations were evenly distributed between the PS3 failure point and those corresponding to PS1, PS2 (as shown in Figure 27b by black triangle marks), neglecting the PS3 data would result in an unreasonable loss of information.

If the PS3 data are not to be disregarded, the observed deviation in the PS3 degradation pattern can be explained by the presence of failure mechanism FM_2 associated with corrosion in the solder joints of power supplies PS1 and PS2. The degradation measure (accumulated damage) shown in Figure 27 reflects only the damage the power supplies have acquired due to FM_1. The damage due to FM_2 cannot be accounted for in the observed degradation paths since FM_2 is unobservable. Although the FM_2 cannot be observed, the damage imposed by this hidden failure mode may eventually cause the power supply to fail. From this perspective, the failure mode FM_2 manifests its presence only through the failure events.

The power supplies (real and imagined), whose failure data points are situated at the right-lower side of Figure 27b are likely to have acquired damage mostly due to FM_2, since the damage accumulated due to FM_1 is relatively low, and the lifetimes of these power supplies are relatively large. Corrosion processes are known to proceed in the calendar time domain so that the calendar age of the power supplies is expected to be related to FM_2, in the sense that the calendar age is positively correlated with the probability of failure due to FM_2. However, since FM_2 is unobservable, there is not any numerically expressed evidence of the degradation imposed by FM_2. Hence, in developing the power supply reliability model, one has to deal with degradation data that do not indicate degradation due to FM_2.

The degradation data depicted in Figure 27b show significant variability in the critical damage levels at which the power supplies experienced failure. This variance will primarily affect the estimation of the critical damage level for the degradation-based reliability model.

In this example it is difficult to claim with certainty that the PS3 degradation path in Figure 27b is an outlier. In this situation, the important decision to make is whether to disregard the possible outlier and continue the reliability modeling only with the data that are well fitted to the assumed model, or to adjust the reliability model so that the odd looking data will be a piece of information useful for the reliability prediction.

This work proposes a methodology to deal with such situations where the empirical degradation threshold tends to be uncertain because of variability in degradation and failure data as shown in Figure 27. The study is performed in the framework of shock models that have been used in the reliability analysis for decades (Esary and Marshall, 1973). However the proposed approach is quite general, and can be applied to any degradation-based technique, that utilizes the notion of critical degradation threshold.

4.3.2. A method to mitigate uncertainty effects due to unobservable failure modes

Consider a component subject to several degradation processes, or failure mechanisms, eventually leading to component hard failure. The degradation effects imposed by the failure mechanisms upon the component's reliability are assumed to be approximately equal in their magnitude so that it is difficult to distinguish a dominant failure mode. However, the failure mechanisms can be differentiated with respect their observability.

A failure mechanism is called observable if its effect can be measured directly or inferred through the use of various degradation indicators. For example, an opto-isolator is one of a few critical elements in a switch mode power supply (SMPS). The degradation progression for this component can be detected and tracked through the usage of resonance measurements and the value of current transfer ratio (CTR), which is correlated with the failure progression (Judkins, 2007).

A failure mechanism is called unobservable if its effect upon the component's reliability cannot be measured or even detected because of sensor equipment limitations, or the impracticality of diagnostic and detection routines. While in operation, the component does not manifest the presence of such a failure mechanism in a perceivable manner. The presence and effects of unobservable failure mechanisms can be confirmed and investigated only in a post-mortem analysis. Unobservable failure mechanisms are assumed to make a significant contribution to the component's degradation and fault progression.

Let **F** denote a set of various failure mechanisms that simultaneously affect the component's reliability:

$$\mathbf{F} = \{F_1, F_2, F_3, ...F_n\} \qquad (4.3.2.1)$$

Assume that there is a value of k such that a subset $\mathbf{F}_{obs} = \{F_{i_1}, F_{i_2}, F_{i_3}, ...F_{i_k}\}$ is a set of observable failure mechanisms, and $\mathbf{F}_{hid} = \{F_{i_{k+1}}, F_{i_{k+2}}, F_{i_{k+3}}, ...F_{i_n}\}$ is a subset of unobservable (hidden) failure mechanisms.

Each failure mechanism imposes a certain degradation effect upon the component's reliability. The degradation effect D_i imposed by a particular failure mechanism F_i can be thought of as a function that quantifies the amount of damage suffered by the component solely due to the failure mechanism:

$$D_i = f(T_i, F_i) \qquad (4.3.2.2)$$

where T_i is the timescale associated with the failure mechanism F_i. Apparently, different failure modes can evolve in different timescales. For example, corrosion processes tend to degrade the component in the calendar age timescale, whereas temperature stress-related damage worsens the component's reliability in the operational age timescale.

In this study the overall degradation effect is assumed to be additive so that it is represented by the following expression

$$D_{total} = \sum_{i=1}^{n} D_i \qquad (4.3.2.3)$$

It should be noted that in the case of multiplicative damage, one should perform the log-transformation to use the additive model given in Equation 4.3.2.3.

Since some of the D_i are unobservable, the damage effects can be grouped according to their observability.

$$D_{total} = \sum_{i=1}^{k} D_i + D_{hid} \qquad (4.3.2.4)$$

where D_{hid} is the total degradation effect imposed by the unobservable failure mechanisms. For the sake of brevity, this term is called the hidden damage. The value of hidden damage is assumed to be completely unknown and unobservable.

The presence of the unknown term D_{hid} can be treated as a source of uncertainty in the reliability prediction problem. The influence of the unknown hidden damage cannot be neglected since it is assumed that there is no dominant failure mechanism, so that all of the degradation contributors (observable and hidden as well) play equally important roles in the component deterioration. The uncertainty effect of the hidden damage is illustrated in the following qualitative example.

Assume that the item exhibits two degradation modes F_1 and F_2. F_1 is observable, whereas F_2 is unobservable. The degradation due to the assumed failure mechanisms accumulates linearly in time. The item fails as soon as the total component's damage $D_{total} = D_1+D_2$ exceeds a certain critical threshold D^*, whose value is unknown. Figure 28 shows the observed and true degradation paths, (OA' and OA, respectively) for a particular item, which has suffered some damage due to F_1 and F_2.

The solid line OA' depicts the observable damage D_1 accumulated in the item. The dotted line OA depicts the true (total) damage D_{total} accumulated in the item.

The point A on the critical threshold line is the apparent moment of failure. However, since the only observable damage is due to F_1, one observes the failure moment at the end point A', thus, concluding that the critical damage level is that corresponding to the point A', which seems to be significantly lower than the true critical threshold.

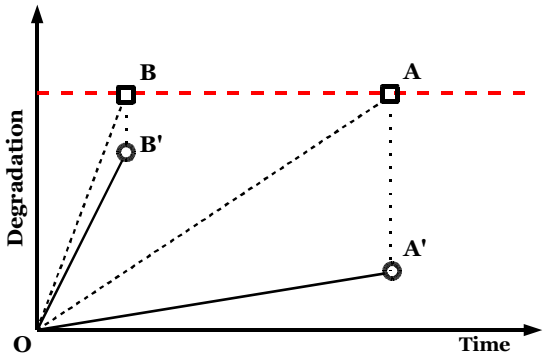

Figure 28. A schematic representation of two observable degradation paths OA' and OB' and their true (yet unobservable) counterparts OA and OB.

This underestimation can be explained by the fact that the item under consideration happens to suffer mostly from failure mode F_2. The ordinates of the points along the degradation path OA' are significantly lower than those of the points along the true degradation path OA.

Degradation paths OB and OB' correspond to an item that suffers mostly due to failure mode F_1. The major portion of the total damage accumulated in this item is observable. Hence the distance between the observed failure point B' and the true failure point B is not significant.

To conclude this qualitative example the following statement is made. The presence of unobservable failure modes introduces uncertainty in the critical degradation level estimation, since the damage levels observed in the moments of failure tend to vary because of variability in the ratio of observable to unobservable failure mechanisms affecting the components.

The problem posed in this study is to reduce the uncertainty effect resulting from the presence of unobservable failure mechanisms in the component degradation process. The uncertainty effect is investigated in the framework of reliability shock models that will be outlined in the following subsection.

The notion of warning setpoint and critical degradation zone is defined as follows. The level of cumulative damage at which the component has the probability of failure (POF), which is assumed to be critical, is called a warning setpoint. Having reached the warning setpoint the component immediately needs preventive maintenance. The notion of warning setpoint is primarily important for determining an optimal preventive maintenance policy.

The critical degradation zone includes the degradation levels starting with the warning setpoint and ending at the damage level where all items from the population are expected to fail. The defined notions of warning setpoint and critical degradation zone are going to be useful in the following subsection that will introduce the methodology.

4.3.3. Optimal Transformation of Degradation Measure

Consider a degradation-based reliability shock model M(T, D), which evolves in the timescale T, and D is defined to be a probability distribution of the critical degradation threshold. The parameters of D are to be estimated from available failure data.

Let $\boldsymbol{\Theta}$ denote the set of available failure data of the following form

$$\boldsymbol{\Theta} = \{ (t_1, d_1), (t_2, d_2), \ldots (t_k, d_k) \} \qquad (4.3.25)$$

where (t_i, d_i) denotes the time and damage level attained by the component *i* at the failure moment.

Assuming that the critical degradation threshold is to be described by the probabilistic model D, one estimates the threshold distribution parameters as the sample mean and variance according to the following formulae:

$$\bar{d} = \frac{1}{k}\sum_{i=1}^{k} d_i , \quad s^2 = \frac{1}{k-1}\sum_{i=1}^{k}\left(d_i - \bar{d}\right)^2 \qquad (4.3.2.6)$$

It is intuitively understandable that a large value of variance in the critical degradation threshold can deteriorate the prediction provided by the model M. In particular, a large variance in the estimate of the critical threshold forces the practitioner to set the warning point too low, thus reducing the component's service life. This

uncertainty effect cannot be smoothed or eliminated completely if the critical threshold variance is mostly due to fully random deviations in the failure moments. However, if the failure data pattern exhibit some systematic regularity, a certain transformation of the available data can be made to reduce the variability in the critical degradation threshold.

The presence of regularity in the failure data can emanate from various origins which are difficult to classify and they are usually highly case-dependent. This research considers regularity due to hidden degradation effects imposed by unobservable failure mechanisms. If the component is subject to at least two different failure modes, and one of the failure modes is unobservable, the degradation data observed on the component may look like that shown in Figure 29. The small circles in Figure 29 represent the time instants and damage levels attained by some components at their failure moments. The origin and particular features of these data will be discussed in detail in the numerical example section.

The degradation data shown in Figure 29 exhibit a certain regular pattern in the failure moments. The items surviving a large number of duty cycles tend to acquire a relatively small amount of damage compared to the items surviving a short number of duty cycles. Hence the failure points form a data cloud inclined downward.

One possible explanation for this appearance can be that the items situated in the right-hand side of Figure 29 (long age survivors) have acquired critical degradation mostly due to the unobservable failure mode. Therefore, their degradation level d_i at the failure moment is relatively low since the observable degradation mode happened to be a minor contributor to the item failure. On the opposite side, the items that are short survivors (situated in the left-hand side of Figure 29) have acquired critical damage mostly due the observable failure mode.

Apparently such regularity in failure data introduces a great deal of variability into the degradation-based reliability model, effectively enlarging the critical degradation zone, which is depicted as a range of damage levels confined between the dotted lines.

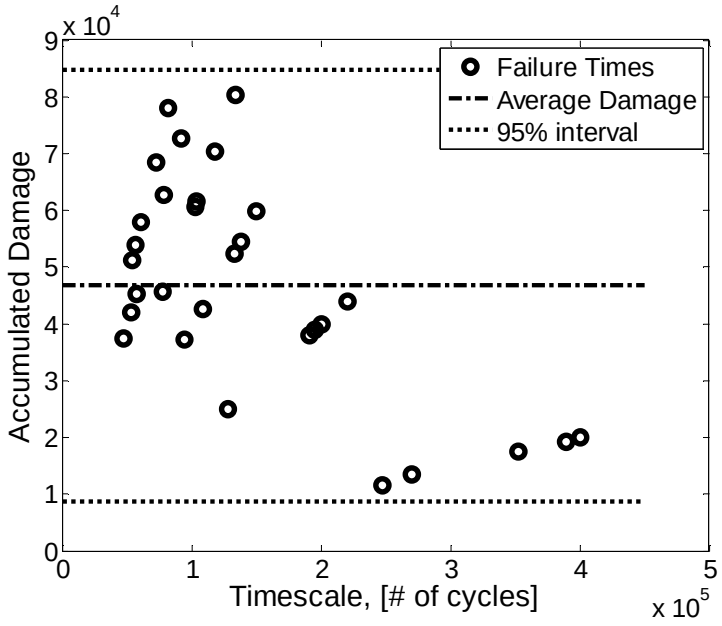

Figure 29. The real-world degradation data exhibiting a certain regularity.

The large critical degradation zone effectively lowers the warning setpoint, approximately depicted by the lower dotted line.

A data transformation method to a new coordinate system is developed to reduce the variability in the critical degradation zone. If failure data exhibit some linearity in the original coordinate system (T, D), a Principal Component Analysis (PCA)-based transformation can be applied to reveal the new coordinate system (T', D'), the usage of which will be more beneficial in terms of the end result uncertainty.

PCA is a useful statistical technique for finding patterns in high-dimensional data. Essentially PCA is an applied-linear-algebra-based method which provides a simple, non-parametric approach for extracting relevant information from confusing data sets. The main question a PCA-based method addresses can be formulated as follows. Is it possible to find a linear combination of the original coordinate basis that best represents the given data (Shlens 2005)?

Let **X** be the original data set, where each column is a multidimensional data point. If **X** is an $m \times n$ matrix, the number of available data points in **X** is n; the dimensionality of the data is m. In this setting the PCA transformation is given by

$$\mathbf{Y}^T = \mathbf{X}^T\mathbf{W} = \mathbf{V\Sigma} \qquad (4.3.2.7)$$

where $\mathbf{V\Sigma W}^T$ is the singular value decomposition (SVD) of **X**, and **Y** is the matrix of transformed data re-expressed in the new coordinate system.

Given the data set **Θ,** one performs the PCA transformation to come up with transformed failure data of the following form:

$$\mathbf{\Theta}' = \{ (t_i', d_i') \},\ i = 1,2,\ldots k \qquad (4.3.2.8)$$

It is well known that PCA transforms data so that the data will have the largest variance along the first transformed coordinate, the second largest variance will be along the second transformed coordinate and so forth. Since the considered data set **Θ** is two-dimensional, the second transformed coordinate *d*' produces the smallest variance in the data. This obviously follows from the fact that the largest variance in the 2-dimensional data set **Θ**' is along the first transformed coordinate *t*'.

Therefore having performed PCA over the original degradation data **Θ** one has the degradation data set **Θ**' such that the transformed degradation measure d' has a minimal possible variability in the given data. Having the minimal variability in the degradation measure is highly beneficial for the reliability modeling. The practical benefits of the minimal variance will be illustrated in the numerical example section.

The performed PCA transformation can be discussed from the perspective of failure mode observability. According to the PCA definition (Equation 4.3.2.7) the transformed degradation measure is represented as

$$d' = w_{12}t + w_{22}d \qquad (4.3.2.9)$$

where w_{ij} is an element of the 2×2 matrix **W**. As can be seen, the degradation measure *d*' is a linear combination of the observable degradation measure *d* and the time measure *t*. Obviously the term $w_{22}d$ accounts for the degradation that is explicitly present in the

original data set **Θ**. The term $w_{12}t$ can be thought of as a linear approximation for the damage acquired due to unobservable failure mechanisms $\hat{D}_{hid}(t) = w_{12}t$.

Goodness of such a linear approximation depends on the regularity pattern the failure data exhibit in the original coordinate system (*t*, *d*). If the exhibited regularity is linear, the PCA transformation is expected to provide a good approximation to the unobservable degradation effects (Equation 4.3.2.4).

In the case of a non-linear pattern in the degradation data, the developed methodology can be generalized through the use of kernel principal component analysis (KPCA). However, this generalized non-linear approach is out of this dissertation's scope and will be considered in future research.

The next subsection presents an example where the developed methodology is applied to real-world data. The example also discusses the practical benefits derived from the usage of transformed degradation data.

4.3.4. Numerical Example

This example considers the fatigue test data originally discussed in (Gertsbakh 2000). A sample of 30 steel specimens was subjected to a series of loading tests until they failed because of fatigue. Each loading test consisted of 5000 fatigue cycles. The magnitude of fatigue loads was chosen such that a specimen underwent $5000\alpha_i$ low-load cycles and $5000(1-\alpha_i)$ high-load cycles in one loading test. Thus the value of α_i represents the ratio of low-load cycles to the total number of cycles applied to Specimen *i* within one load test.

The entire sample was divided into 6 groups G_k k=1,2,..6, each of which was characterized with a certain ratio of $\alpha_{k.}$

Table 2 summarizes the steel specimens failure data. As can be seen the ratio α_k varies from 0.05 to 0.95.

In this study the loading regimes (high-load and low-load) are considered to be two distinct failure mechanisms observed in the tested specimens. Let HL and LL denote

the failure mechanisms associated with high-load and low-load cycles respectively. In this experimentation the cycle frequency is assumed to be 1 load cycle per time unit so that the model timescale is expressed in numbers of cycles.

To apply a shock model-based approach, the loading cycles are assumed to deliver a certain amount of damage to the specimens. Although the original data do not provide any information in regards to how much damage a high- or low-load cycle delivers, for the sake of simplicity the damage delivered by a high-load cycle is assumed to be unit-size. Damage delivered by a low-load cycle is assumed to be unknown (unobservable).

The failure mechanism HL is assumed to be observable. In other words, the damage delivered by high-load cycles is measurable. The failure mechanism LL is assumed to be unobservable due to, for instance, certain limitations in sensor equipment incapable of picking up the degradation indicators of the low-load cycle damage.

Table 2. The fatigue data adopted from (Gertsbakh 2000). The numbers of cycles are given in thousands ($\times 10^3$)

i	α_i	Low-load	High-load	i	α_i	Low-load	High-load
1	0.95	256.8	13.5	16	0.40	32.0	45.7
2		235.8	11.6	17		48.0	70.4
3		370.15	19.25	18		42.0	61.5
4		335.1	17.5	19		42.0	60.6
5		380.3	20.0	20		54.0	80.4
6	0.80	153.0	38.0	21	0.20	10.0	37.5
7		176.2	44.0	22		16.0	62.7
8		160.3	40.0	23		12.0	45.3
9		156.0	39.0	24		19.0	72.6
10		103.0	25.0	25		11.0	42.0
11	0.60	84.0	54.4	26	0.05	3.0	53.9
12		81.0	52.3	27		3.75	68.55
13		90.0	59.9	28		4.25	77.95
14		57.0	37.3	29		3.32	57.95
15		66.0	42.7	30		2.75	51.25

The original data do not provide information as to how the fatigue damage in the specimens evolves in time. In the absence of any knowledge of the damage progression it is assumed that damage accumulates linearly. If this assumption turns out to be unrealistic, the methodology will not suffer, primarily because this assumption of linearity is important only for assessing the efficiency of the particular reliability prediction model, as will be shown later in this section.

From the assumptions, it follows that the original data can be represented as shown in Figure 30. The abscissa represents the total number of load cycles survived by the specimens; the ordinate represents the observable accumulated damage (degradation) which according to the assumption of the unit-size damage increments is the number of high-load cycles suffered by the specimens.

Since the LL damage is assumed unobservable, it is impossible to take into account the effect of the unobservable damage upon the reliability prediction. Computing the mean and variance of the critical degradation values (Equation 4.3.2.6) and assuming the critical probability failure to be 0.025, which corresponds to the 2σ offset in the case of Gaussian distribution, one can estimate the warning setpoint.

$$\textit{Warning Setpoint} = 8.7\times10^{3} \qquad (4.3.4.1)$$

The meaning of the warning setpoint is that any specimen exhibiting the damage level of 8.7×10^{3} has a POF of 0.025, assumed to be unsafe for continuing the specimen's operation. Thus, being at the warning setpoint is the indication that the specimen immediately requires preventive maintenance.

To assess the efficiency of performing preventive maintenance given a value of the warning setpoint, the average useful lifetime metric is introduced. The average useful lifetime metric is defined to be the mean value of a specimen's lifespan given the specimen is to be replaced as soon as its observed degradation reaches the predefined warning setpoint. Figure 30 shows the times of crossing the estimated critical warning setpoint as small squares lined up along the lower dotted line representing the warning setpoint. The times corresponding to the small squares would be the useful lifetimes of

the specimens if they were taken out of service as soon as their observed degradation exceeded the warning setpoint given in Equation 4.3.4.1.

If a PCA-based orthogonal transformation is applied to the data, the transformed warning setpoint will appear as shown in Figure 30 by the dashed line inclined downward.

The times of performing preventive maintenance are depicted as triangle marks lined up along the transformed warning setpoint level. As can be seen the specimens' useful lifespan tends to increase since the transformed warning setpoint takes into account the degradation acquired by the specimen and the time the specimen has been in operation as well.

To quantitatively compare the replacement policies suggested by the original and transformed data, Table 3 summarizes the efficiency metrics corresponding to the replacement policies. The efficiency metric (the average useful life) evaluated for the transformed-data-based policy turns out to be significantly better (longer) than that evaluated for the reliability model built on the original untransformed data.

As can be seen in Table 3, the PCA-based transformation significantly improves the average useful life of the steel specimens. If one follows the preventive maintenance policy based on the warning setpoint evaluated from the transformed data, the expected useful life of the components is almost twice as long as the useful life derived from following the policy based on the original data.

Table 3. The average useful lifetime provided by the preventive maintenance policies based on the original data and transformed data.

	Original Data	Transformed Data
Avg. Service Lifetime [# of cycles]	46.5×10^3	87.0×10^3

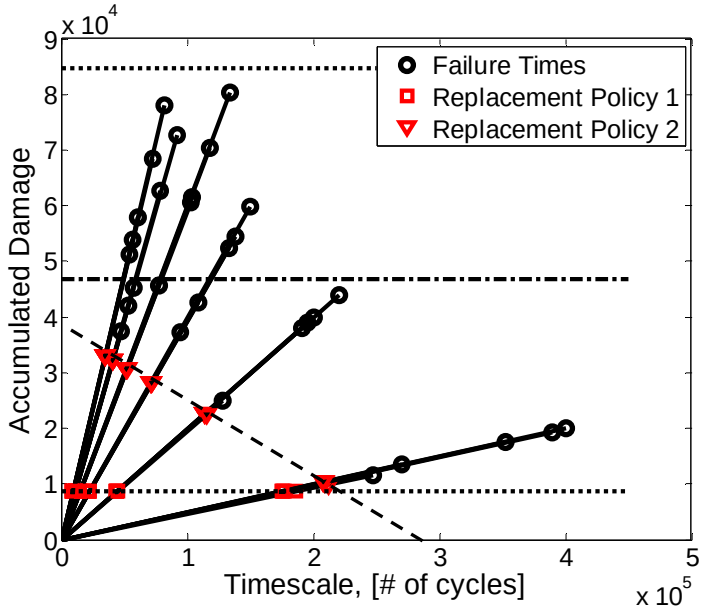

Figure 30. The fatigue data are depicted as degradation paths. The square marks depict the replacement times based on the original warning setpoint (Equ.4.3.4.1). The triangle marks depict the replacement times based on the transformed warning setpoint.

This significant improvement is explained primarily by the fact that the transformed data exhibit a minimal possible variance in the critical threshold. The minimal variation in the model failure threshold in turn provides the most accurate prediction of the TTF distribution, which provides the best achievable preventive maintenance strategy based on the notion of warning setpoint.

The following concludes this section. The presence of unobservable degradation mechanisms can manifest itself as a certain regular pattern in the failure data. The regular pattern can introduce a great deal of variability into the estimated critical threshold involved in the reliability prediction model. A methodology has been developed to reduce possible uncertainty effects of failure data regularity upon the reliability model. The key idea of the methodology is to find a proper data transformation to produce a coordinate system, in which the failure data exhibit minimum variance in the critical degradation threshold. The expected benefit of using the transformed failure data lies in the fact that

the transformation accounts for the regular pattern in the original failure data so that the effect of the regularity in the transformed data is reduced as much as possible.

The case where the regularity is of a linear nature has been illustrated by a numerical example involving real-world data. In the example, a PCA-based transformation was applied to the data. The benefit of using the PCA transformed data was assessed by calculating the efficiency metric, which was defined to be an average useful life. The reliability model built on the PCA transformed failure data has provided an efficiency metric value almost twice that provided by the model using the original failure data.

5. USE OF PROGNOSTIC INFORMATION FOR OPTIMAL OPERATIONAL CONTROL

Most of the published studies devoted to various aspects of PHM have been concerned with health monitoring technologies aimed at scheduling service and maintenance for systems according to their condition as opposed to a fixed time table. Considering capabilities to continuously assess and predict reliability aspects of the system, the practitioner may be interested in how the PHM information can improve the system control in terms of availability and cost reduction.

The research field related to the use of prognostic models for optimal control remains wide-open. Some researchers and practitioners have outlined the main directions to follow and issues to address in regards to the prognostics-based optimal control (Tang, 2006), (Davis, 2006). However, there has been a significant lack of specific control methods and approaches which would be suitable for dealing with uncertain conditions imposed by highly random environmental conditions, variability in operational loadings and imperfect prognostic models.

In the presence of a variety of diagnostic information available online, it would be highly desirable to develop methods and approaches for incorporating prognostic information into the optimal control of the system. The following qualitative example illustrates the idea of prognostic-based control.

Consider a system assigned to complete some mission subject to some time constraints. The system performance is numerically quantified by the system performance rate, which can be thought of as the metric characterizing how fast the system is able to accomplish the mission. Quality-related aspects of accomplishing the mission are out of this simple example's scope.

The system is assumed to be subject to degradation. While in operation, the system degrades at some degradation rate, which is a function of a) the system's current performance rate, and b) the current environmental conditions.

The performance rate, at which the system is operating in particular environmental conditions, imposes some degradation rate that shapes the system degradation profile. Apparently severe environmental conditions and a high-performance rate will cause the system to degrade faster. On the contrary, normal environmental conditions and moderate performance rates cause the system to degrade relatively slowly.

The environmental conditions evolve independently from the system and are assumed to be totally random and uncontrollable. The performance rate is assumed to be the only means to control the system performance.

In this setting, the practitioner wants to accomplish the mission in the required time at the lowest expense in terms of degradation acquired by the system. Running the system at a high performance rate minimizes the time needed to finish the mission, thus meeting the time constraints. However, the high performance rate imposes a high degradation rate, especially in the case of severe environmental conditions. This can cause the system to fail due to wear-out before the mission is accomplished. On the other hand, a low or moderate performance rate can hinder the mission progress, and eventually cause the system to fail in accomplishing the mission if the time constraints are not met. It can be concluded that one should find an optimal performance rate, following which the system will meet the reliability requirements and time-related constraints as well.

Since the degradation rate is subject to random fluctuations, there is no single value of the optimal performance rate that would provide an acceptable result for any sequence of encountered environmental conditions. Rather, the practitioner needs to have an optimal control policy that would optimally select a control action (the performance rate) for each combination of environmental condition and degradation level the system has attained.

The general idea outlined in this discussion will be elucidated in more detail through the following practical examples.

Example 1

A commercial aircraft engine is expected to provide a certain number of "on-wing" hours, which is thought of as the mission to accomplish. Monitoring certain health parameters such as Exhaust Gas Temperature (EGT) margin on a particular engine, the airline operator wants to find Life Extending Control (LEC) to extend the useful life of an engine by modifying control logic or control hardware to smooth dominating life-consuming factors (Wiseman, 2001). One possible method to implement LEC is to improve Active Clearance Control (ACC) systems, which may be beneficial, by compensating for deterioration. The objective is to find a control policy, following which the ACC system prolongs the engine useful life in a long-term run.

Example 2

A drilling machine is going to be employed in a drilling campaign, whose work volume may be defined in terms of the total depth of boreholes to drill. The drilling campaign is to be performed in several runs, which can be thought of as duty cycles. In each run the drilling machine is supposed to complete a certain work volume. The drilling machine acquires certain damage mostly due to wear-out during each run. The magnitude of damage the drilling machine acquires within a duty cycle depends on the rotational speed and other various performance metrics. Additionally, random environmental conditions may introduce stochastic deviations in the damage accumulation process. On the average, the damage accumulation rate tends to be proportional to the performance rate of the drilling machine. This relationship results in the following contradiction. While performing at a high performance speed, the drilling machine is expected to complete the drilling campaign in a short time; however, the degradation may accumulate so intensively that the drilling machine will fail before it completes the campaign.

The objective is to find a policy that would suggest which performance regime should be taken in a particular run to guarantee a successful completion of the entire drilling campaign.

Example 3

Treatments for acutely infected HIV patients utilize certain types of drugs, whose usage has proven to be successful for reducing and maintaining viral loads below the detection limit (Ernst, 2004). However, the long-term effects of using the drugs exhibit substantial complications. Concerns about the long-term use of the drugs have brought attention for the need of a drug-scheduling policy. An ideal drug-scheduling policy would bring the patient's immune system into a balanced state that allows for maintaining the immune control over the virus without using any drug. This balance state can be thought of as the mission goal.. The transfer into the balance state (the mission completion) should be performed with minimal drug-related effects for the patient. Apparently, the minimization of drug-related effects can be thought of as preservation of the patient's health/degradation status.

The systems considered in each of the three examples share one particular feature: the presence of highly uncertain environment. However, despite the uncertainty, the practitioner seeks an optimal control policy, which would ensure that the mission is completed successfully. This dissertation proposes a method in which prognostic information derived for the system of interest can be efficiently used in the search for an optimal control policy.

5.1. Methodology

This section formally introduces the problem of finding an optimal control policy for a system performing in an uncertain environment. The problem is formulated in general terms as well as in a more elaborate form.

Consider a system with discrete time dynamics given by

$$s_{t+1} = f(s_t, a_t), t = 0,1,2,... \qquad (5.1.1)$$

where for all t, s_t is the system state belonging to State Space S, and a_t is the control action belonging to Action Space A.

Let $c(s,a)$ be a real-valued cost function, and γ is a discount factor ($0 \leq \gamma < 1$). Given a stationary control policy $\sigma(\bullet)$: S $\rightarrow$ A, the following equation defines the discounted infinite horizon cost function associated with γ:

$$J_{\sigma}(s) = \lim_{N \to \infty} \sum_{t=0}^{N-1} \gamma^{t} c\left(s_t, \sigma(s_t)\right) \qquad (5.1.2)$$

The objective is to find an optimal policy σ^* such that the cost function *J(s)* is minimized over all s_t.

To evaluate the optimal policy σ^*, one usually does not have to know the system dynamics precisely (Equ. 5.1.1) since a reinforcement learning (RL)-based approach is used to solve the problem. The only available piece of information could be a finite set of system trajectories observed in the past and the associated cost function $c(s,a)$. If system trajectories are not readily available, the RL routine has to learn the system dynamics from the direct interaction with the environment. The learning process can take place in a simulated environment or real-world settings. However, learning in real-world environment is employed usually if some information about system dynamics has been already acquired from simulations.

Given this type of information RL techniques compute an approximation $\hat{\sigma}^*$ to the optimal stationary control policy σ^*. The exact solution, which is the truly optimal policy σ^*, cannot be found given this limited information on the system dynamics.

The above problem formulation is in general terms. In the next subsection, a more elaborate representation will be given.

5.1.1. Minimal-Control-Effort Problem

Consider the following model design. One has to complete a mission whose progress status W_t is characterized numerically with a range of 0 to 100 percent. For the sake of simplicity the range is assumed to be discrete.

$$W_t \in \{0,1,2,...100\}, \quad t > 0 \qquad (5.1.1.1)$$

where *t* is a time in a certain timescale usually expressed in duty cycles. A duty cycle is defined to be a repetitive interval of operation. Thus, t is essentially the number of duty cycles completed since the mission start moment.

The mission is to be accomplished utilizing a system which performs the mission-related task at some performance rates:

$$\mathbf{W}_{perform} = \{w_1, w_2, ...w_k\} \qquad (5.1.1.2)$$

The performance rate w_i is defined to be the portion of the total mission-related work volume performed within a duty cycle.

$$w_i = \frac{\Delta W_i}{\Delta t_i} \qquad (5.1.1.3)$$

where Δt_i is the time length of the i-th duty cycle, ΔW_i is the mission-related work volume performed in the course of the i-th duty cycle.

The system is controlled in terms of its performance rate. Having received a control action a_i, the system will be performing the next duty cycle at the performance rate w_i:

$$\mathbf{A} = \{a_1, a_2, ...a_k\} \qquad (5.1.1.4)$$

where **A** is the set of all possible control actions the system can potentially receive.

Control actions are taken in a discrete manner only upon completion of a duty cycle and before the next duty cycle proceeds. Control actions taken consequently during the course of the mission are called a sequence of control actions

$$\overline{A} = (a_{i_1}, a_{i_2}, ...a_{i_n}) \qquad (5.1.1.5)$$

where a_{ij} is the control action taken at the j-th duty cycle.

The rule that prescribes a control action to be taken in a particular duty cycle in the course of the mission performance, is referred to as a control policy.

The system is assumed to be subject to degradation due to its usage during the mission. Similar to the mission progress, the system health/degradation state is characterized with a numerical range of 0 to 100 percent, where 0 corresponds to an initial "no-degradation" state, and 100% corresponds to a failure state, where the system is not able to perform any longer:

$$D_t \in \{0,1,2,...100\}, \quad t > 0 \tag{5.1.1.6}$$

Degradation accumulates at rates which are assumed to be a function of the performance rate. Apparently, the system is expected to degrade fast when it is performing at a high performance rate. Moderate performance rates tend to impose lower degradation rates. However, the precise relationship between the performance and degradation rates is assumed to be unknown. The uncertainty can be due to random deviations in the degradation rates caused by stochastic factors such as environmental conditions.

The qualitative description of the model design is summarized in the following equations. The system dynamics is given by Equation (5.1.1), where $s_t = \{W_t, w_t, D_t, d_t\}$ is the system state at time t. The precise form of the function $f(s_t,a_t)$ is assumed to be unknown.

The mission is said to be accomplished if the mission progress status is greater than or equal to 100%, while the degradation status is less than 100%. Usually a time constraint complements the definition of the successful completion time.

$$T_{completion} = \inf\{t : W_t \geq 100 \ \wedge \ D_t < 100 \ \wedge \ t \leq T_{\lim}\} \tag{5.1.1.7}$$

where $T_{completion}$ is the mission completion time, T_{lim} is the maximum time allowed to complete the mission.

The mission is said to fail if the mission progress status is less than 100%, while the system degradation exceeds 100% or the time constraint is not met. The failure time T_{fail} is defined as follows:

$$T_{fail} = \inf\{t : [W_t < 100 \wedge D_t \geq 100] \vee [W_t < 100 \wedge t > T_{\lim}]\} \qquad (5.1.1.8)$$

The objective is to find a control policy σ^*, which guarantees that the mission will be completed within the specified time limit T_{lim} and without exceeding the degradation threshold.

The stated problem can be thought of as a minimum-control-effort problem with a time constraint. This type of problem has been extensively studied in the optimal control theory literature (Kirk, 1998). However, in the formulated setting an optimal control theory-based approach cannot be applied because of uncertainty in the functional dependency between the performance and degradation rates. The parametric degradation rate model can be unspecified and unknown because of the high complexity of the degradation mechanisms taking place in the system of interest.

In the absence of a strictly defined parametric model it seems appropriate to use a reinforcement learning (RL) approach, which is a goal-directed learning method based on interaction (Sutton 1998). In the following subsection the idea behind RL approaches is outlined.

5.1.2. Reinforcement Learning

An RL method considers a goal-seeking agent performing within an uncertain environment, which may affect the agent's status in some, possibly random, manner. The agent seeks to achieve a goal despite a complete unawareness of the environment it is placed in. Generally speaking, RL is an algorithmic technique to solve stochastic optimal control problems via a trial-and-error approach (Ernst 2004).

An RL method involves four main components: a policy, a reward function, a value function, and optionally a model for the environment.

A policy determines which control action should be taken by the agent in a given time moment. A policy can be thought of as a mapping from the observed states of environment to actions to be taken. The policy is the major component of an RL agent since the policy suffices to fully determine the agent’s behavior.

A reward function determines the goal to achieve in a RL problem. A reward function assigns a scalar value, a reward, to each state-action pair potentially encountered by the agent. The reward assigned to a particular state-action pair indicates its inherent goodness with respect to the goal the agent seeks. Pursuing the goal, the agent wants to maximize the total reward it receives in a long term run.

A value function specifies the total amount of reward the agent expects to receive in the future if it starts at a particular state. As opposed to the reward function indicating immediate attractiveness of the states, the value function indicates a long-term attractiveness of particular states.

A model for the environment is used for planning, which implies some form of considering possible future states before they are actually encountered. The presence of a model for the environment in an RL-based approach is optional. Early RL systems were fully trial-and-errors learners. However, it has been recognized that RL techniques are tightly related to dynamic programming methods, which utilize models. Modern RL systems enjoy various types of models mimicking the environmental behavior. In the context of this paper, a model for the environment is defined rather vaguely or not given at all.

The agent wants to maximize a long term reward signal. Interacting with the environment the agent is acquiring information, which is received in the form of so-called experience tuples. An experience tuple consists of the following elements: the current state (s), the control action taken (a), the instantaneous reward received (r) and the next state (s') attained due to the performed action.

One of the attractive features of an RL-based approach is that a close-to-optimal control policy can be learnt directly from historical data reflecting the trajectories along which the system of interest progresses (Ernst 2004). Another option is to learn the optimal policy directly from interaction with the environment.

A thorough survey of RL techniques, including temporal difference (TD) learning, the SARSA algorithm, and aspects of exploration versus exploitation can be found in (Kaebling, 1996).

5.1.3. Use of Prognostic Information in an RL routine

This section introduces a method to use prognostic information to facilitate an RL-based search for an optimal control policy.

The RL agent in this study follows an on-policy version of Q learning (SARSA) with the following update rule for the Q-table:

$$Q(s,a) \leftarrow Q(s,a) + \eta(r + \gamma Q(s',a') - Q(s,a)) \qquad (5.1.3.1)$$

where s is the current RL agent state, a is the action taken in State s, r is the immediate reward received for the pair of (s,a), s' and a' are the next state and action to take. The value of γ is called a discount factor, ($0 \leq \gamma < 1$). η is the learning rate which tends to decrease in time for convergence ($0 \leq \eta < 1$).

Equation (5.1.3.1) reduces the difference between the current Q value and the estimate from the previous step. This approach is called a temporal difference algorithm. However, Equation (5.1.3.1) updates only the previous value of state-action pair. To account for past visits eligibility traces are used in the update equation.

Visiting a state-action pair (s,a), the RL agent sets the eligibility trace for the pair (s,a) to 1. The eligibility values of all other pairs are multiplied by $\gamma\lambda$, where λ is called the trace decay parameter. The state-action pairs, that the RL agent has never visited, have eligibilities equal to 0. The visited state-action pairs have non-zero eligibilities decaying in time. The SARSA algorithm takes the following form:

$$\begin{aligned} \delta &\leftarrow r + \gamma Q(s', a') - Q(s, a) \\ Q(s, a) &\leftarrow Q(s, a) + \eta \delta e(s, a) \\ e(s, a) &\leftarrow \gamma \lambda e(s, a) \end{aligned} \qquad 5.1.3.2$$

where δ is the temporal error, e(s,a) is an eligibility of the pair (s,a).

The update rule (5.1.3.2) accounts for all eligible state-action pairs. The update value depends on how far the state-action pairs have occurred in the past. In the literature this algorithm is called SARSA(λ), since the decay parameter λ determines how many previous steps are taken into account. If $\lambda = 0$, only one-step is accounted. If $\lambda = 1$, all previous made steps receives a credit. In the numerical experiment the following values of the RL parameters are used to guarantee convergence:

$$\gamma = 0.9,\ \lambda = 0.9, \eta = 0.9 \qquad (5.1.3.3)$$

For the above formulated problem the RL method makes use of a reward function defined as follows. The RL agent receives a positive reward if the system has completed the mission in time, and the degradation status remains below the critical level. A negative reward is given to the RL agent if the mission fails due to exceeding the degradation threshold or/and the mission time limit. In both cases, the reward is assigned only after the mission is completed, either successfully or not successfully.

The reward function is extended in the following manner. Performing the mission task, the system equipped with a PHM component provides the practitioner with prognostic information that is used to evaluate the probability of a successful mission completion. If the prognosis that is obtained after the system performs a particular action in a particular state suggests that the anticipated failure time is closer than the anticipated completion time, the RL agent receives a negative reward for the particular pair of state and action. The reward is positive if the estimated remaining useful life exceeds the anticipated completion time.

In other words, the RL agent receives an immediate reward based on the prognostic information derived from the current system state and the intrinsic reliability properties of the system. Receiving the immediate prognostics-driven reward is expected to improve the RL routine in terms of convergence time and the end result quality.

The use of prognostic information can be thought of as introducing prior knowledge about the system dynamics into the model-free RL routine. Even if some knowledge of the system dynamic is available beforehand, prognostics can complement

the available information with the data observed or inferred at the system at hand, thus, providing information about individual features potentially affecting the mission accomplishment. The following section presents experimental results obtained in numerical simulations.

5.2. Numerical Results

This section describes the numerical simulation performed to illustrate the benefits of using prognostic information in the reinforcement learning routine. For the sake of simplicity, the problem stated in the previous section is to be reformulated as follows.

A unit is assigned to perform a mission whose completion progress is expressed as an integer within the range of 0 to 30. The unit can operate at 4 different performance rates summarized in Table 4.

The unit is subject to damage accumulation (degradation), whose rate is assumed to be a function of the performance rate. In the numerical simulation the following values of degradation and performance rates are used. However, this relationship is assumed to be unknown to the RL routine.

The time allowed to be spent to accomplish the mission is constrained to T_{limit} = 14 duty cycles. The mission is said to fail due to extensive degradation if the unit's degradation exceeds the damage level of 30, while the mission progress status is still less than 30. If the mission progress status attains the value of 30, but the time constraint T_{lim} is not met, the mission is said to fail as well.

Table 4. The relationship between the performance and degradation rates.

Performance Rates, w_t	1	2	3	4
Degradation Rates, d_t	2	1	3	6

The operator controls the mission progression through varying the unit's performance rate. Having received a control action to perform in a duty cycle the unit completes a certain volume of the mission-related task, and acquires a certain amount of damage (degradation) during the duty cycle.

The operator is interested in having a control policy, which guarantees that the mission will be accomplished while the specified time limit and reliability-related requirements are met. Since the model dynamics (Table 4) are assumed to be unknown, the RL routine is to be performed in a model-free setting.

The system state, s_t, is assumed to contain the following attributes

- Mission Progress, W_t
- Degradation State, D_t
- Performance Rate, w_t
- Degradation Rate, d_t

For each state one should select a control action $a_i \in A$, which determines the performance rate at which the unit will perform in the next duty cycle.

The Q-table, the key component of the RL routine, keeps values for $30\times30\times4\times4\times4=57600$ possible pairs of states and control actions (s_i,a_j) the unit can potentially undergo performing the mission. Being in a particular state the unit can proceed at one of four possible performance rates. This means that the Q-table has the dimensionality of 14400×4.

Starting with completely random Q-values, which implies a completely random control policy, the RL routine is to learn an acceptable control policy.

The reward function employed in the numerical simulation is defined as follows. If the unit has completed the mission successfully, the reward is positive and equals the difference between the time constraint T_{lim} and the actual completion time. If the unit fails to complete the mission, the reward is negative and equals the work volume that yet remains to be done:

$$\text{Reward} = \begin{cases} T_{\lim} - T_{completion} & \text{if success} \\ W_{done} - 30 & \text{if failure} \end{cases} \qquad (5.2.1)$$

This definition of the reward function causes the RL routine to favor control policies that provide a fast and successful completion of the mission, and not to favor those that lead to the mission failure accompanied with the unit's intensive degradation.

Prognostic information derived on the unit complements the reward function in the following manner. Performing the mission one makes a prognosis regarding what would be the anticipated time of the mission completion, and anticipated failure time. If the anticipated failure time happens to be less than the anticipated completion time, the reward function generates a negative reward. In other words, a state and control action pair that produces such an undesirable prognosis is not going to be included in the control policy, since the reward is negative.

Another important aspect of the considered model is the uncertainty associated with the degradation observed at the unit. Until now, it has been assumed that the relationship between the performance and degradation rates is deterministic as shown in Table 4. This means that performing the mission task at any particular performance rate causes the unit to degrade at a particular deterministic degradation rate. However, in reality this may not hold true, since various random factors can affect the degradation process. For example, due to environmental condition variations, a particular performance rate value can lead to a degradation rate value that would vary in different environmental conditions. Performing the mission task in severe environmental conditions is expected to cause the unit to degrade at a greater extent. Since environmental conditions usually are uncontrollable and random in their nature, in this study the effect of random environmental factors is treated as a random noise contaminating the relationship between the performance and degradation rates. Having selected the unit's performance rate for the coming duty cycle the operator expects to observe some random value of damage (degradation) acquired in the duty cycle.

The prognostic model adopted in the numerical simulation is a linear regression-based technique that is applied to evaluate the mean degradation rate exhibited by the

unit. The prognostic information used by the RL agent is the 5th percentile of the estimated time-to-failure (TTF) distribution.

In each duty cycle, the 5th percentile, $\alpha_{0.05}$, of the TTF distribution is compared against the 95th percentile, $\beta_{0.95}$, of the anticipated-completion-time distribution, which is estimated via a linear regression method as well (see Figure 31). The immediate reward is positive, if $\alpha_{0.05} - \beta_{0.95} > 0$, otherwise the reward is negative.

Table 5 summarizes the experimental results obtained in the numerical simulation. Simulations are performed at 4 different levels of degradation rate variability. These levels of relative variability are 0%, 12%, 16% and 25%. Each case is approached with two RL routines, one of which is using prognostic information to compliment the reward function, whereas the other RL routine is not using prognostic information.

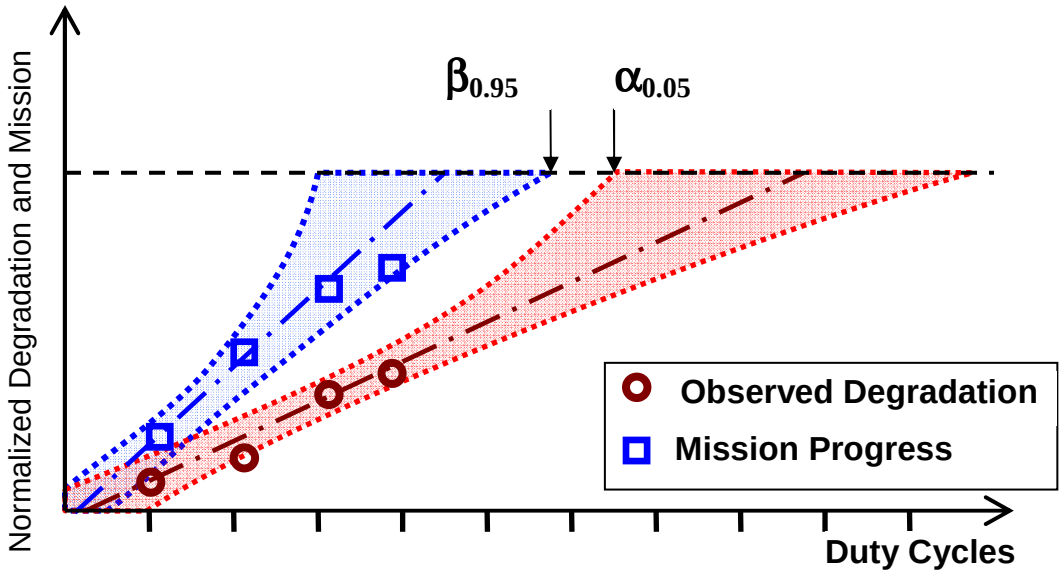

Figure 31. The schematic representation of prognostic information used in the experiment.

Table 5. The experimental results obtained in the numerical simulation.

Variability Level in Degradation Rates	Figures of Merit								
	Probability of Completion, P_s			Mean Completion Time, $T_{complete}$			Mean Health Status at Completion Time, H_s		
	Random	No Prognostics	Prognostics	Random	No Prognostics	Prognostics	Random	No Prognostics	Prognostics
No Variability	0.23	0.96	1.0	13.4(1.4)	12.5(0.9)	14.0(0)	2.9(2.1)	1.1 (1)	5.4 (0.9)
Little	0.22	0.91	0.96	13.4(1.4)	12.3 (1.2)	12.6(0.8)	2.9(2.2)	3.7 (1.4)	5.7 (2.2)
Moderate	0.22	0.71	0.91	13.3(1.5)	12.4 (1.4)	12.6(1.4)	2.9(2.2)	3.5 (2.4)	5.0 (1.8)
Large	0.25	0.57	0.61	13.3(1.4)	13.6 (1.1)	13.3(1.2)	3.0(2.4)	4.3 (2.5)	4.5 (2.3)

To evaluate the derived control policy performance three figures of merit are proposed. These are the probability of successful mission completion P_s, Mean Completion Time $T_{complete}$, Mean Health Status H_s at the mission completion moment. As a reference point in the policy evaluation a completely random policy is introduced. The random policy forces the agent to take control actions in a completely random fashion.

Following a perfect control policy the operator expects a) to have a close-to-one probability of successful mission completion; b) the mission's completion time is expected to be short; and c) the unit's health status is expected to be preserved as high as possible at the mission completion moment.

As can be seen the control policies found by RL provide a probability of successful completion approximately 5 times larger than that based on random control actions. This fact indicates that the implemented RL technique is able to find a satisfactory control policy. The figures of merit evaluated for the random control policy turn out to be almost equal for all levels of variability engaged in the experiment, whereas the learned control policies show a dependency on the variability levels. One possible explanation for this fact is that variability attributed to the random control actions outweighs the variability attributed to the system model (the unit's degradation rates).

Comparing the values of P_s for the learned control policies one can see that the control policies derived using prognostics information provide higher probabilities of successful completion than those policies that do not use prognostic information. However, the difference in this figure of merit, P_s, is significant only in the case of moderate variability in degradation rates. This fact can be explained by the following.

If the relationship between performance and degradation rates is deterministic, the RL agent is able to perfectly learn the model, and come up with a good control policy without using any complementary data such as prognostic information. The slight difference in the values of P_s shown in Table 5 reflects the fact that the use of prognostic information quickens the learning process so that the RL agent reinforced with prognostic information is able to find a good control policy faster than those not using prognostics. If the RL routine without prognostics continued learning for a longer time, a control policy

providing P_s close to 1 would be probably derived. However, in reality, a long learning time could be impractical or safety critical. The ability to shorten the learning time is considered to be a significant benefit derived from using prognostic information. Figure 32 illustrates the learning time spent by the RL routines with and without prognostic information.

As can be seen the use of prognostic information greatly facilitates the RL routine in terms of convergence time. Using prognostics the RL routine converges to an acceptably good policy after approximately 70 training episodes. The RL routine not using prognostics exhibits some convergence as well. However, the learned policy seems less acceptable since the average reward is less than that provided by the prognostics-based policy.

In the case of highly variable degradation rates (the bottom line in Table 5) the small difference in the probabilities of successful completion can likely be explained as due to the prognostic information in these highly noisy models being too uncertain to bring benefits for deriving a good control policy. The prognostic model used in the simulation has a limited ability to handle high-level random noise in input data, which results in prediction uncertainty large enough that the prognostic information becomes useless. Another benefit of using prognostics in the course of RL is that the RL-based policies tend to provide a higher level of remaining health status, H_s, upon completion the mission. This means that the prognostics-based control policies preserve the system health status to a greater extent than those not using prognostics.

The tested policies have not shown a significant difference in the mean completion time metric. However, the values of $T_{complete}$ shown by the prognostics-based control policy are slightly less variable than those $T_{complete}$ shown by "no-prognostics" policies. The experiment has revealed that Probability of Completion exhibits a relatively complex behavior in the sense that the largest difference between the tested RL routines is observed in the case of moderately variable models. The extreme cases where the model variability is low or large have not shown a significant difference between the control policies found by the tested RL routines.

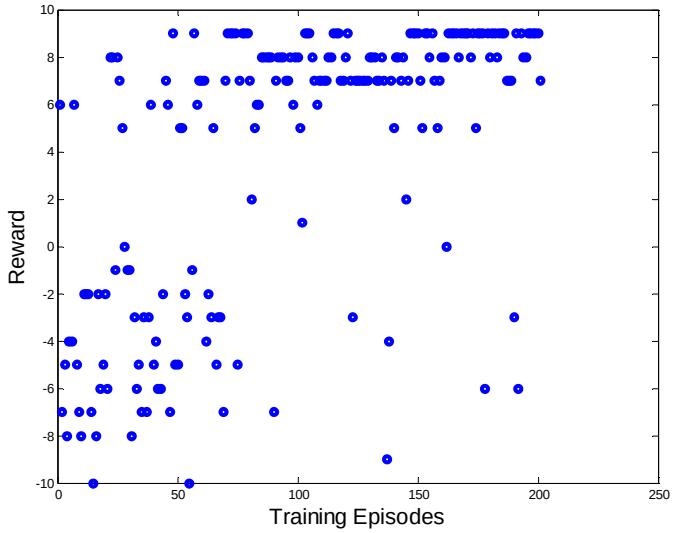

a)

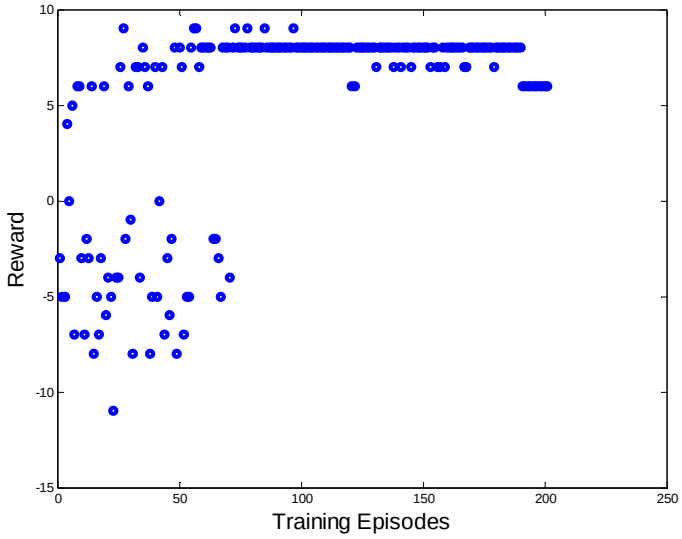

b)

Figure 32. A typical sequence of rewards obtained in the course of reinforcement learning by the agent that does not use prognostic information (a), and does use prognostic information (b).

A prognostic model can be characterized in terms of its informational capacity (computational complexity). This metric is likely to be dependent on the model accuracy, precision, the number of parameters, etc. On the other hand, the model that formulates the setting, in which one should find an optimal control policy, is also characterized in terms of its informational capacity (computational complexity).

The informational capacity of such a model is likely to be dependent on the type of functional dependencies prevailing among the model entities, the level of random noise in the model processes, etc. For example, the model can feature a highly non-linear relationship between the performance and degradation rates, or extensively high variability in the degradation rate values.

From this perspective the following statement is made. There should be a match in terms of computational complexity between the prognostic model employed in the search for optimal control policy and the model describing the setting where the control policy is going to be used. A simple prognostic model may not be able to provide a prognosis that is good enough to be useful for finding the optimal control policy. On the other hand, a simple control model can be easily learned by the RL method without using any prognostic model. A more detailed investigation of this aspect will be investigated in the future.

5.3. Concluding Remarks

A method to incorporate prognostic information into the reinforcement learning routine has been developed. Using prognostic information one can a) improve the RL routine in terms of convergence time, which is a critical issue in real-world applications, and b) reduce uncertainty associated with the derived control policy in terms of stability of system trajectories along which the system proceeds achieving the mission objectives.

6. CONCLUSIONS AND RECOMMENDATIONS FOR FUTURE WORK

This dissertation described a generic prognostic framework developed to provide general guidelines to PHM system designers and practitioners interested in using degradation evidence data for reliability condition assessment and prediction. Within the prognostic framework, the following methodologies were developed:

1. A method to represent a multidimensional health status of the system in the form of a scalar quantity called a health indicator was developed. Reducing the dimensionality of the vector representing the system health status greatly facilitates development and practical use of prognostic models in the PHM framework. The method is capable of indicating the effectiveness of the health indicator in terms of how well or poor the health indicator can distinguish healthy and faulty system exemplars. Using this method, the practitioner is able to intelligently select diagnostic information (degradation evidence) pertinent to the failure mechanisms present in the system of interest.
2. A usefulness criterion, which allows the practitioner to evaluate the practicability of using a particular prognostic model along with observed degradation evidence data was developed. The criterion of usefulness is based on comparing the model uncertainty imposed primarily by imperfectness of degradation evidence data against the uncertainty associated with the time-to-failure prediction based on average reliability characteristics of the system. Using the criterion of usefulness, the practitioner, who is oftentimes limited in accuracy of the sensory equipment, is able to assess the expected benefit of using a given prognostic model with the uncertain diagnostic information. In the cases where the practitioner lacks a priori knowledge of the failure mechanism characteristics, for instance, degradation rates, the criterion of usefulness is used as an indicator of how many degradation evidence data should be collected on the system of interest to provide a reasonable RUL prediction.

3. An analysis of the uncertainty effects attributed to randomness in the critical degradation threshold, which is an important parameter of a prognostic model was performed. The revealed dependency between uncertainty in the critical degradation threshold and the model prediction uncertainty allows the practitioner to formulate practical requirements for a given prognostic model in terms of a maximum allowed critical threshold uncertainty.
4. An analysis of uncertainty effects attributed to the presence of unobservable failure mechanisms affecting the system degradation process along with observable failure mechanisms was performed. A method was developed to reduce the uncertainty effects upon a prognostic model. The method transforms the characteristic timescale in a prognostic model built on degradation data observed in the presence of unobservable failure modes. The use of the transformed timescale effectively causes the prognostic model to approximate damage due to unobservable failure modes as a linear function of time.
5. A method to incorporate prognostic information into optimization techniques aimed at finding an optimal operational control policy for equipment performing in an uncertain environment was developed. The use of prognostic information greatly facilitates the search for an optimal control strategy in the case where limited information is available regarding the system dynamics and environmental conditions.

Through the development of these methods, which are used to select the correct prognostic architecture, manage the effects of uncertainty, produce a health status indicator from multidimensional data, and provide optimal operational control when the system is degraded practitioners will be able to effectively employ prognostic techniques to a multitude of applications. The current gaps in prognostic technologies were identified and techniques were developed to ease the application of prognostic technologies.

There are still several modifications of the framework that would provide additional benefit. These extensions could encompass additional approaches such as

1. A method to fuse information supplied from various sources pertinent to reliability characteristics of the object of interest. The method would smartly manage the uncertainty associated with the information sources. The end result uncertainty should not be greater than those of the information sources involved into the information fusion. The Bayesian technique developed in this work is able to process two informational sources, which are degradation evidence data and prior knowledge of degradation rates, in conjunction with a linear degradation model. A promising area of future research would be to extend the Bayesian technique to process a multitude of data and knowledge sources available from past experience, engineering judgment, empirical evidence, etc.

2. A reliability prediction method that would use empirical degradation evidence data along with a non-parametric empirical model that represents degradation process dynamics. A well known technique to combine system dynamics and empirical data is the Kalman filter. However, to apply the Kalman filter, one needs to know the system dynamics explicitly. Using a non-parametric empirical model for the system dynamics, one would be able to fuse information brought by the system dynamics model and empirical evidence observed at a particular object of interests.

PHM techniques are still in their infancy stage of general application; however, in the future these techniques could provide the "holy grail" to equipment and system survivability.

REFERENCES

Abramowitz, M. and Stegun, I.A., (1972) eds. Handbook of Mathematical Functions with Formulas, Graphs, and Mathematical Tables. NY: Dover,

Bankert, R.J., Singh, V.K., and Rajiyah, H, (1995), "Model based diagnostics and prognosis system for rotating machinery", American Society of Mechanical Engineers, Vol. GT-252, pp. 5-23

Barlow, R.E., and Procshan F.,(1975), *Statistical Theory of Reliability and Life Testing*, Holt, Rinehart and Winston, Inc., NY.

Barlow, R.E.,(1998), *Engineering Reliability*, ASA-SIAM, Philadelphia, Penn.

Bartlett, M.S., (1975), *Probability, Statistics, and Time*, Chapman and Hall, London, p.73

Basseville, M., and Nikiforov, I.,(1993) *Detection of Abrupt Changes: Theory and Application*, Prentice Hall, New Jersey.

Beichelt, F.E., and Fatti, L.P., (2002), *Stochastic Processes and Their Applications*, Taylor&Francis, NY.

Birnbaum, Z.W., and Saunders, S.C., (1969), "A new family of life distributions", *J. Appl. Probability*, 6, pp. 637-52.

Biswas, G., Bloor, G., (2006), "A Model Based Approach to Constructing Performance Degradation Monitoring Systems"**,** Proc. of *IEEE Aerospace Conference, pp. 1-10*, March, 4-11.

Bogdanoff, J.L., and Kozin, F., (1985), *Probabilistic Models of Cumulative Damage*, John Wiley, NY, 1985.

Bond, L.J. et al.,(2000), "Online Intelligent Self-Diagnostic Monitoring For Next Generation Nuclear Plants", *Technical Report for NERI*, DE-FG03-99SF9491.

Bond, L.J., Jarrell, D.B., (2002), "Prognostics and CBM –A Scientific Crystal Ball", *Proc. of ANS Meeting, January*, pp. 9-13.

Brotheron, T., et al, (2002), "A Testbed for Data Fusion for Engine Diagnostics and Prognostics", *Proc. of IEEE Aerospace Conf.*, New York, Vol. **6**, pp.3029-3042.

Brotheron, T., Jahns, G., Jacobs, J., and Wroblewski, D., (2000), "Prognosis of Faults in Gas Turbine Engines", *Proc. of IEEE Aerospace Conf.*, Vol.**6**., pp.163-171.

Byington, C.S., Kalgren, P.W., Johns, R., and Beers, R.J, (2003), "Embedded Diagnostic/Prognostic Reasoning and Information Continuity for Improved Avionics Maintenance", *Proc. of IEEE Systems Readiness Technology Conf.*, pp. 320-329.

Carey, M. B. and Koenig, R. H., (1991), "Reliability Assessment Based on Accelerated Degradation: A Case Study," *IEEE Trans. Reliability*, **40**, No.5, pp.499-506.

Chelidze, D., and Cusumano, J.P., (2004), "A dynamical system approach to failure prognosis", *Journal of Vibration and Acoustics*, **126**, No.1, pp. 2-8.

Chelidze, D., and Cusumano, J.P., (2001), "Failure prognosis using non-linear short time prediction and multi-time scale recursive estimation", *Proc. of the ASME Design Engineering Technical Conference*, **6A**, pp.901-910.

Chinnam, R.B., (1991), "On-line Reliability Estimation of Individual Components, using Degradation Signals", *IEEE Trans. on Reliability*, **48**, No.4, pp.403-412.

Davis, G., et al., (2006), "Predictive and Prognsotic Controller for Wide Band Gap Power Conversion", *Proc. of IEEE Aerospace Conf.*, Big Sky, MT

Doksum, K.A., and Hoyland, A., (1992), "Models for variable-stress accelerated life testing experiments based on Weiner processes and the inverse Gaussian distribution", *Technometrics*, vol. 34(1), pp.74-82.

Ebeling, C.E., (2005), *An Introduction to Reliability and Maintainability Engineering*, Long Grove: Waveland Press, Inc.

Ernst, D., Glavic, M., and Wehenkel, L., (2004), "Power Systems Stability Control: Reinforcement Learning Framework", *IEEE Trans. on Power Systems*, **19**(1), pp.427-435.

Ernst, D., Stan, G.B., Goncalves, J., and Wehenkel, L., (2004), "Clinical Data Based Optimal STI Strategies for HIV: a Reinforcement Learning Approach"

Esary, J.D., and Marshall, A.W., (1973), "Shock Models and Wear Processes", *The Annals of Probability*, 1(4): pp. 627:649.

Fisher, R.A., (1936), "The Use of Multiple Measurements in Taxonomic Problems", *Annals of Eugenics*, 7, pp.179-188.

Fukuda, M., (1988), "Laser and LED Reliability Update", *J. of Lightwave Technology*, vol.6, pp.1488-1495.

Gelman, A., Carlin, J.B., Stern, H.S., and Rubin, D.B., (1998), *Bayesian Data Analysis*, Chapman, London

Gertsbakh, I., (2000), *Reliability Theory with Applications to Preventive Maintenance*, Berlin, Springer

Gertsbakh, I.B, (1977), "*Models of Preventive Maintenance*", North-Holland, Amsterdam

Gertsbakh, I.B., and Kordonskiy, Kh.B.,(1969), *Models of Failure*, Springer, NY

Girish, T., Lam S. W., and Jayaram, J. S., (2003), “Reliability Prediction Using Degradation Data - A Preliminary Study Using Neural Network-based Approach,” *Proc. of European Safety and Reliability Conference (ESREL 2003)*, Maastricht, The Netherlands, Jun. 15-18.

Gross, D., and Harris, C.M., (1998), *Fundamentals of Queuing Theory*, Wiley, NY

Gut, A., (1990), “Cumulative Shock Models”, *Advances in Appl. Probability*, Vol.22(2), pp.504-507.

Haykin, S., (1999), "Ch. 9. Self-organizing maps", in *Neural networks – A comprehensive foundation*, 2nd Edition, Prentice-Hall.

He, D., Wu, S., Banerjee, P., Bechhofer, E., (2006), "Probabilistic Model Based Algorithms for Prognostics", *Proc. of IEEE Aerospace Conf.*, pp.1-10.

Hess, A., Calvello, G., and Frith, P., (2005), "Challenges, Issues, and Lessons Learned Chasing the "Big P": Real Predictive Prognostics", *Proc. of IEEE Aerospace Conference*, pp. 3610-3619.

Hines, J.W., and Usynin, A.V., (2006), Empirical Model Optimization for Computer Monitoring and Diagnostics/Prognostics, Technical Report, Dept. of Nuclear Engineering, Univ. of Tennessee

Hoel, P. G.; Port, S. C.; and Stone, C. J. (1971) "Testing Hypotheses." Ch. 3 in *Introduction to Statistical Theory*, NY: Houghton Mifflin, pp. 56-67.

Huber, S., (2002), "Segmentation and Reliability", *DMSMS 2002 Intel Conference*, New Orleans LA.

Hui, Z., Jianrong, H., Bole, S., Xiaofeng, Z., (2003), "Research on Similarity of Stochastic Non-stationary Time Series based on Wavelet-Fractal", *Proc. of IEEE Conf. on Information Reuse and Integration*, pp. 452-456.

Judkins, J.B., Hofmeister, J., and Vohnout S. (2007), "A Prognostic Sensor for Voltage Regulated Switch Mode Power Supplies", *Proc. of the 2007 IEEE Aerospace Conf.*, Big Sky, MT

Kaebling, L.P., Littman, M.L., and Moore, A.W., (1996), "Reinforcement Learning: A Survey", *J. of Artificial Intelligence Research*, **4**, pp.237-285.

Kirk, D.E., (1998), *Optimal Control Theory. An Introduction*, Prentice, Englewood Cliffs, NJ.

Laidler, K. J., (1993), *The World of Physical Chemistry*, Oxford University Press.

Lieberzeit, P.A**.;** Glanznig, G.; Leidl, A.; Voigt, N.; Dickert, F.L, (2006), "Nanostructured polymers for detecting chemical changes during engine oil degradation", *IEEE Sensors Journal*, **6**, Issue 3, pp. 529-535.

Loecher, M. and Darken, C., (2003), "Concurrent Estimation of Time-To-Failure and Effective wear," *Proc. Maintenance and Reliability Conference (MARCON)*

Lu, C.J., and Meeker, W.Q., (1993), "Using Degradation Measures to Estimate a Time-to-Failure Distribution", *Technometrics*, **35**(2), pp.161-174.

Luo, J., Namburu, K., Pattipati, L., Qiao, L., Kawamoto, M., and Chigusa, S., (2003), "Model-based Prognostic Techniques", *Proc. of IEEE AUTOTESTCON*.

Martz, H.F., and Waller, R.A., (1982), *Bayesian Reliability Analysis*, John Wiley, NY.

Meeker, W.Q. and Escobar, L.A., (1998), *Statistical Methods for Reliability Data*, Wiley, NY

Mishra S., Ganesan S., Pecht M., and Xie J., (2004), "Life Consumption Monitoring for Electronic Prognostics", *Proc. of IEEE Aerospace Conference*

Myotyri, E., Pulkkinen,U., Simola, K., (2006), "Application of Stochastic Filtering for Lifetime Prediction", *Reliability Engineering and System Safety*, **91**, pp.200-208.

Paris, P., and Erdogan, F., (1963) "A Critical Analysis of Crack Propagation Laws", *J. of Basic Engineering, Trans. of ASME*, pp.528-534

Parker, B.E., et al., (1993), "Helicopter Gearbox Diagnostics and Prognostics Using Vibration Signature Analysis", *Proc. of International Society for Optical Engineering*, Vol.1965, pp.531-542.

Pecht M., Vichare N., Rodgers P., Eveloy V., (2004), "In Situ Temperature Measurement of a Notebook Computer – A case study in Health and Usage Monitoring of Electronics", *IEEE Trans. on Device and Materials Reliability*, **4**, No.4, pp.658-663.

Pulkkinen, U., (1991), "A stochastic model for wear prediction through condition monitoring", In: Holmberg, K., Folkeson, A, editors, *Operational Reliability and Systematic Maintenance*, London/New York, Elsevier, pp.221-243.

R. V. Hogg and A. T. Craig.(1978), *Introduction to Mathematical Statistics*, 4th edition. New York: Macmillan, (See Section 3.3.)

Ramakrishnanand A., and Pecht M., (2003), "A life consumption monitoring methodology for electronic systems", *IEEE Trans. on Components and Packaging Technologies*, **26**, no.3, pp. 625–634.

Romano, G.; Sampietro, M., (1997), "CMOS-circuit degradation analysis using optical measurement of the substrate current", *IEEE Transactions on Electron Devices*, Vol 44, Issue 5, pp.910-912

Shlens, J., (2005), *A Tutorial on Principal Component Analysis,* Accessed on July 20, 2007 http://www.cs.cmu.edu/~elaw/papers/pca.pdf

Solovyev, A.D., (1972), "Asymptotic Distribution of the moment of the first crossing of high level by a birth-and-death process", *Proc. of the 6th Berkley Symposium on Mathematical Statistics and Probability*, **6**, pp.71-86.

Stern, H. S., (1996), "Neural Networks in Applied Statistics," *Technometrics*, **38**, No. 3, pp. 205-215.

Sumita, U., and Shanthikumar, J.G., (1985), "A class of correlated cumulative shock models", *Advances in Appl. Probability*, 17, pp.347-366.

Sunghyun, K., Yiseok, K., Jooran Yang; Sangjin Kwon; Sekwang Park, (2005), "Degradation level monitoring sensor for insulating oil of power transformer using capacitive high aspect ratio of electrodes", *The 13th International conference on Solid-State Sensors, Actuators, and Microsystems*, Vol.1, pp.613-616.

Sutton, R., and Barto, A., (1998), *Reinforcement Learning. An Introduction*, MIT Press.

Tamhane, A.C., and Dunlop, D.D., (2000), *Statistics and Data Analysis: from Elementary to Intermediate,* Prentice

Tang, L., Kacprzynski, G.J., Bock, J.R., Begin, M., (2006), An Intelligent Agent-based Self-evolving Maintenance and Operations Reasoning System, *Proc. of IEEE Aerospace Conf.*, Big Sky, MT.

Tseng, S., and Peng, C.Y., (2004), “Optimal burn-in policy by using an integrated Weiner process”, *IIE Transactions*, 36, pp. 1161-1170.

Vichare N.M., and Pecht, M.G., (2006), "Prognostics and Health Management of Electronics", *IEEE Trans. on Components and Packaging Technologies*, **29**, pp.222-229.

Virkler, D.A., Hillberry, B.M., and Goel, P.K., (1978), "The Statistical Nature of Fatigue Crack Propagation", AFFDL-TR-78-43.

Vlok, P.J., Coetzee, J.L., Banejevic, D., Jardine, A.K.S., Makis, V., (2002), "Optimal component replacement decisions using vibration monitoring and the proportional-hazards model", *J. of Operational Research Society*, **53**, pp.193-202.

Wang, P., and Vachtsevanos, G., (2001), "Fault Prognostics using Dynamic Wavelet Neural Networks", *Artificial Intelligence for Engineering Design and Manufacturing*, **15**, pp.349-365.

Wasserman, P. D., (1989), *Neural Computing Theory and Practice*, Van Nostrand Reinhold.

Wegerich, S.W., (2004), "Similarity Based Modeling of Time Synchronous Averaged Vibration Signals for Machinery Health Monitoring", *Proc. of IEEE Aerospace Conf.*, Vol. 6., pp. 3654-3662.

Wegerich, S.W., Wilks, A.D., and Pipke, R.M., (2003), "Nonparametric Modeling of Vibration Signal Features for Equipment Health Monitoring", *Proc. of IEEE Aerospace Conf.*, Vol.7, pp.3113-3123.

Whitmore, G.A., (1995), “Estimating Degradation by a Wiener diffusion process subject to measurement Error”, *Lifetime Data Analysis*, 1, pp.307-319.

Wilkinson, C., Humphrey, D., Vermeire, B., Houston, J., (2004), “Prognostic and health management for avionics”,*IEEE Proc. of Aerospace Conference* , 5, pp. 3435-3447.

Wiseman, M.W., and Guo, T.H., (2001), “An Investigation of Life Extending Control Techniques for Gas Turbine Engines”, *Proc. of the American Control Conference*, Arlington, VA.

Xu, D. and Zhao, W., (2005), “Reliability Prediction Using Multivariate Degradation Data,” *Proc. Annual Reliability and Maintainability Symposium*, Alexandria, VA, pp.337-341.

Zanardelli, W.G., Strangas, E.G., Khalil, H.K. and Miller, J.M., (2003) "Wavelet-based Methods for the prognosis of mechanical and electrical failures in electric motors", *Mechanical Systems and Signal Processing*, 19, pp.411-426

APPENDICES

Appendix 1. The MATLAB Code used to model a Markov chain based degradation model.

```
function [X, T] = simulateTrends(t,b,q,n);
% Simulates a collection of degradation paths
% INPUT: t is a timescale, usually t = 0:1:100
%     b is the critical damage state (critical threshold value)
%     q is the probability of receiving a unit-size damage in a duty
cycle
%     may be either scalar or vector quantity
%     n is the number of paths to generate
% OUTPUT:   X is a matrix of n generated paths
%           T is a vector of failure times (the times when a path
crosses the threshold b)


X = [];
for k=1:n
    x = modelATrend(t,b,q);
    X(:,k) = x;
end

T = [];
for k=1:size(X,2)
    indx = find(X(:,k) == b);
    if ~isempty(indx)
        T(end+1) = t(indx(1));
    end
end
%-------------------------------------------------------------------------
function [x] = modelATrend(t,b,q);
% Simulates a degradation path
% INPUT:
% t is a timescale, usually t = 0:1:100
% b is the critical damage state (critical threshold value)
% q is the probability of receiving a unit-size damage in a duty cycle
% OUTPUT:   x is a degradation path
n = length(t);
x = zeros(n,1);
r = rand(n,1);
x(1) = 1;
if length(q) == 1
    for i=1:n-1
        if r(i) <= q
            x(i+1) = x(i)+1;
        else
            x(i+1) = x(i);
        end
    end
else
    for i=1:n-1
        if r(i) <= q(x(i))
            if x(i) + 1 <= b
```

```
                x(i+1) = x(i)+1;
            else
                x(i+1) = x(i);
            end
        else
            x(i+1) = x(i);
        end
    end
end
%-----------------------------------------------------------------------
```

Appendix 2. The MATLAB Code used to model an RL agent.

```
% An example of a reinforcement learning-based control policy
%

global QTable ETable CompletionReward PrognosisReward DegradationLimit
MissionLimit;


test = 1;
reliability = [];
duration = [];
Rewards = [];
Prcnt = [];
success = 0;

E = 1; % dummy
P = [ 1  2 3 4 ];    % the performance rates
D = [ 2  1 2 6 ];    % the degradation rates
e0 = 1;
CompletionReward = 10;
PrognosisReward = 5;
DegradationLimit = 30;  % the critical degradation threshold
MissionLimit = 30;      % the full ammount of work

numOfEnvCond = length(e0);
numOfActions = length(P);
N = MissionLimit + 10;
% try to open a mat-file with the Q-table saved in previous training
episodes
fid = fopen('qtab2.mat','r');
if fid < 0
      % if there is no Q-table, initialize the Q-table randomly.
    if test == 0
        fprintf('qtab2 not found. Initializing...\n');
        QTable = rand(N,N, numOfActions,
numOfEnvCond*numOfActions,numOfEnvCond,numOfActions);    % init the Q-
table
    else
        disp('Test Mode is on. There is no QTable.');
        return;
    end
else
    fprintf('QTable2 found. Loading...\n')
```

```
    fclose(fid);
    load qtab2
end
IdxTable = zeros(N,N,numOfActions, numOfEnvCond*numOfActions,
numOfEnvCond,numOfActions); % init the E-table
episodes = 0;


% the main loop on the number of episodes
while(1)
    s = initState();
    % Zerofy the eligibility traces
    ETable = zeros(N,N,numOfActions, numOfEnvCond*numOfActions,
numOfEnvCond,  numOfActions);
      % the initial action
    currentAction = actionToDo(s, episodes, numOfActions, P, D, test);
    steps = 1;
    x = [];
    j = [];
    x(steps) = s.degradation;
    j(steps) = s.missionProgress;
    EpisodeRewards = [];
    % the loop for a training episode
    while(1)
        next_s = doAction(currentAction, s, E,D,P);
        next_s = observeState(next_s);
        nextAction = actionToDo(next_s, episodes, numOfActions, P, D,
test);
        % get the reward for the current state and action
        [reward completion] = getReward(next_s, test);
        EpisodeRewards(end+1) = reward;
        % update the Q-table if the test mode is on, otherwise skip the
update.
        if test == 0
            [QTable, ETable] = updateQTable(s, currentAction, reward,
next_s, nextAction, P,D);
        end
        s = next_s;
        currentAction = nextAction;
        steps = steps+1;
        j(steps) = s.missionProgress;
        x(steps) = s.degradation;
        % if the episode is over (either succesfully or not), leave the
loop
        if completion == 1
            break;
        end
    end
    fprintf('steps=%f; reward=%f\n',steps, reward);
    episodes = episodes+1;
    Rewards(end+1) = reward;
    % track the training process statistics
    if test == 1 && reward > 0
        success = success + 1;
```

```
        reliability(end+1) = s.missionProgress - s.degradation;
        duration(end+1) = size(s.history,1);
        Prcnt(end+1) = success/episodes;
        subplot(2,1,1);
        plot(Prcnt);
        subplot(2,1,2);
        plot(duration,'b.');
        drawnow;
    end
    if test == 0
        fprintf('%d episodes done\n',episodes);
        plot(x,'r','linewidth',2); hold on;
        plot(j,'b','linewidth',2);
        plot([0 16], MissionLimit*ones(1,2),'r-.');
        axis([0 16 0 MissionLimit*1.1]); hold off;
        title(sprintf('test=%d;epis.=%2.0f;steps=%2.2f;
reward=%2.2f\n',test,episodes, steps, reward));
        drawnow;
    end
 % save the Q-table every 10 training episodes
    if mod(episodes,10) == 0 && test == 0
        disp('Saving the QTable...');
        save qtab2 QTable
    end
    if test == 0 && episodes > 400
        break;
    end
end
plot(Rewards,'b.');
%--------------------------------------------------------------------------
function [s_new] = doAction(action, s, E, D, P);
% the function does the action suggested by the control policy
% INPUT:    action is the action to do
%                 s is the current state
%                 E is the transition matrix characterizing the
environment
%                 D is the vector of degradation rates
%                 P is the vector of performance rates
% OUTPUT:   s_new is the new state the system goes after the action is
taken.
%

global DegradationLimit MissionLimit;

s_new = s;
%r = rand;
%cs = cumsum(E(s.env,:));
%idx = find(r < cs);
%s_new.env = idx(1);

s_new.PRateIdx = (action);
s_new.DRateIdx = (action);
s_new.history(end+1,:) = [s.missionProgress s.degradation];
s_new.missionProgress = s.missionProgress + P(s_new.PRateIdx);
```

```
r = randn;
level = 4;
if s.degradation + D(s_new.DRateIdx) + r * D(s_new.DRateIdx)/level <=
DegradationLimit
    s_new.degradation = s.degradation + D(s_new.DRateIdx) + r *
D(s_new.DRateIdx)/level;
else
    s_new.degradation = DegradationLimit + 2;
end
%--------------------------------------------------------------------
function [reward completion] = getReward(s, test);
global CompletionReward PrognosisReward DegradationLimit MissionLimit;
% The function assigns a reward value to the RL agent
%  INPUT:
%     s is the current RL agent state
%     test is a flag indicating wether or not the test mode is on
%  OUTPUT:
%     reward is the value of reward
%     completion is a flag indicating the mission completion

completion = 0;
reward = 0;
if s.missionProgress >= MissionLimit && s.degradation <=
DegradationLimit
    completion = 1;
    y = s.history(:,1);
    reward = 20 - size(y,1);
    return;
elseif s.degradation > DegradationLimit
    reward = s.missionProgress - s.degradation;
    completion = 1;
    return;
end

if test == 0
y = s.history(:,1);
if length(y) > 5
    x = [0:1:length(y)-1]' ;
    xtst = [0:1:100]';
    [beta dev stats] = glmfit(x,y,'normal');
    [yhat ylo yhi] = glmval(beta, xtst, 'identity',stats);
    [CompletionTime1, ystar, indx] = findCrossingTime(yhat+yhi,
DegradationLimit, xtst);
    [CompletionTime2, ystar, indx] = findCrossingTime(yhat-ylo,
DegradationLimit, xtst);
    if CompletionTime1 > 14
        reward = -PrognosisReward;
        return;
    end
    y2 = s.history(:,2);
    [beta dev stats] = glmfit(x,y2,'normal');
    [yhat2 ylo2 yhi2] = glmval(beta, xtst, 'identity',stats);
```

```
    [FailureTime1, ystar, indx] = findCrossingTime(yhat2+yhi2,
MissionLimit, xtst);
    [FailureTime2, ystar, indx] = findCrossingTime(yhat2-ylo2,
MissionLimit, xtst);
    Measure = FailureTime1 - CompletionTime2;
    if Measure > 0
        reward = PrognosisReward;
    end
end
end
%---------------------------------------------------------------------
function [s] = initState();
% initializes the RL agent state

s.missionProgress = 1;
s.degradation = 1;
s.PRateIdx = 2;
s.DRateIdx = 2;
s.history = [s.missionProgress s.degradation];
s.env = 1;
%---------------------------------------------------------------------
function sObs = observeState(s)
% returns the state observation (sObs) given the current state s.

sObs = s;
sObs.missionProgress = round(s.missionProgress);
sObs.degradation = round(s.degradation);
%---------------------------------------------------------------------
function [QTable, ETable] = updateQTable(s, currentAction, reward,
next_s, nextAction, P, D);
% the function updates the Q-table using eligibility traces E
% INPUT:    s - the current state
%     currentAction is the action performed in the current state
%     reward is the reward assigned to the RL agent
%     next_s is the next state
%     nextAction is the action to be taken in the next state
%     D is the vector of degradation rates
%     P is the vector of performance rates

global QTable ETable;

lambda = 0.9;
gamma = 0.9;
eta = 0.9;

next_Qval =
QTable(next_s.missionProgress,next_s.degradation,next_s.PRateIdx,next_s
.DRateIdx,next_s.env,nextAction);
Qval = QTable(s.missionProgress,s.degradation, s.PRateIdx, s.DRateIdx,
s.env, currentAction);
TD = reward + gamma * next_Qval - Qval;
ETable(s.missionProgress,s.degradation, s.PRateIdx, s.DRateIdx, s.env,
currentAction) = 1;
```

```
QTable = QTable + (eta * TD) .* ETable;
ETable = lambda.*ETable;

%--------------------------------------------------------------------
```

Appendix 3. An example of a linear degradation model.

```
% this is an example of a linear degradation model
Nt = 50;           % the number of simulated observations in a
degradation path
t = linspace(0,12,Nt)'; % the observations are equidistant in time
RedLev = 10;        % the critical degradation threshold
N = 500;               % the number of degradtion paths to simulate
B0 = [0.2 0.08];    % the probabilistic parameters for the intersect,
[Mean SD]
B1 = [1.2 0.1];     % the probabilistic parameters for the slope, [Mean
SD]

% generate N paths
y = sampleFunctions(t,N,'linear',B0,B1);
sigma = .3;
y = y +  randn(size(y))*sigma;  % contaminate the paths with noise

% find the time momnents of crossing the critical threhsold RedLev
Tstar = [];
for i=1:N
    [crossingTime, ystar, indx] = findCrossingTime(y(:,i), RedLev, t);
    Tstar(i) = crossingTime;
end
Tstar(find(isinf(Tstar))) = [];   % get rid of inf values

% this portion of code requires the KDE toolbox available in the
Internet
k = kde(Tstar,'rot');
p = evaluate(k,t');
MTTF = mean(k);     % calculate the mean time to failure

% find the 2.5-th and 97.5-th percentiles of the time-to-failure
distribution
alpha = 0.95;
P = cumsum(p)/sum(p);
[Tup, Pstar, indxUp] = findCrossingTime(P, alpha+(1-alpha)/2, t);
[Tlo, Pstar, indxLo] = findCrossingTime(P, (1-alpha)/2, t);

figure
plot(t,P); hold on;
a=axis;
plot(ones(1,2)*MTTF,a(3:4),'k:');
plot(ones(1,2)*Tup,a(3:4),'b:');
plot(ones(1,2)*Tlo,a(3:4),'b:');


% take the k-th degradation path, and make a prediction
k=2;
beta = regress(y(1:1:end,k), [ones(size(t)) t]);
```

```
yhat = [ones(size(t)) t]*beta;

figure
plot(t,y(:,k),'b','linewidth',2); hold on;
a = axis;
axis([a(1:2) -0.5 a(4)]);
plot(a(1:2),RedLev*ones(1,2),'r-.','linewidth',2);
plot(t,yhat,'m:','linewidth',2); hold on;
plot(a(1:2),zeros(1,2),'k:','linewidth',1);
xlabel('Time');
ylabel('Degradation');
legend('Degr.Path','Critical Level');

figure
plot(t(1:3:end),y(1:3:end,1:50:end),'b'); hold on;
plot(t,RedLev+20*p,'k');
a = axis;
plot(a(1:2),RedLev*ones(1,2),'r-.','linewidth',3);
plot(a(1:2),zeros(1,2),'k:','linewidth',1);
plot(Tstar,RedLev*(ones(1,length(Tstar))),'r*');
plot(ones(1,2)*MTTF,a(3:4),'k:');
plot(ones(1,2)*Tup,a(3:4),'b:');
plot(ones(1,2)*Tlo,a(3:4),'b:');
plot(t,mean(y'),'r')
xlabel('Time');
ylabel('Degradation');
legend();

T = [ones(size(t)) t];
b = regress( mean(y')', T);

b1 = [];
for i=1:size(y,2)
    b1(:,i) = regress( y(:,i), T);
end

% set the prior values of the degradation rate (Bprior) and associated
stand. deviation
Bprior = mean(b1')'
Sprior = std(b1')'

%-----------------------------------------------------------------
```

Appendix 4. An example of a Bayesian linear regression.

```
% this is an example of Bayesian linear regression

k = 33;
alpha = 0.05;   % (1-alpha)*100% confidence
t_future = linspace(0,24,2*Nt)';
[failureTime, ystar, indx] = findCrossingTime(y(:,k), RedLev, t);
trueTTF = [];  olsTTF = []; bayesTTF = [];
startIndx = 5;
```

```
for i=startIndx:1:Nt
    handydata = 1:i;
    X = t(handydata);
    Y = y(handydata,k);
    X1 = [ones(size(X)) X];
    N1 = size(X,1); P1 = size(X1,2);
    [b bint r rint stats] = regress(Y,X1);
    Yhat = X1*b;
    e = Y - Yhat;
    s2 = sumsqr(e)/(N1-P1);
    Sxx = sumsqr(X-mean(X));

    ta = tinv(1-alpha/2,N1-(P1+1));
    T_future = [ones(size(t_future)) t_future];
    yfuture = T_future*b;
    V = inv(X1'*X1);
    ylo = yfuture - ta*sqrt(s2)*sqrt(1+diag(T_future*V*T_future'));
    yhi = yfuture + ta*sqrt(s2)*sqrt(1+diag(T_future*V*T_future'));

    Thi_i = findCrossingTime(ylo, RedLev, t_future);
    Tlo_i = findCrossingTime(yhi, RedLev, t_future);
    T_i = findCrossingTime(yfuture, RedLev, t_future);

% Bayesian Approach-----------------------------------------------------
-----------
    Sigma = diag(Sprior.^2);
    Bprior = Bprior;

    Vprior = Sigma./sigma^2;
    Vpost = inv(inv(Vprior) + X1'*X1);
    Bpost = Vpost*(inv(Vprior)*Bprior + (X1'*X1)*b);
    NuSprior = (Nt-P1)*sigma^2;
    NuSpost = NuSprior + (N1-P1)*s2 + diag(inv(Vprior+X1'*X1)).*(b-
Bprior).^2;
    VarBpost = Vpost.*NuSpost(1)/(N1-P1);
    Spost = NuSpost(1)/Nt;

    % make a prediction
    y_b = T_future*Bpost;
    yhi_b = y_b+tinv(1-alpha/2,Nt+N1-
P1)*sqrt(Spost.*diag(eye(size(T_future,1)) +
T_future*VarBpost*T_future'));
    ylo_b = y_b-tinv(1-alpha/2,Nt+N1-
P1)*sqrt(Spost.*diag(eye(size(T_future,1)) +
T_future*VarBpost*T_future'));
    %---------------------------------------------------------------
    bayesFailureTime = findCrossingTime(y_b, RedLev, t_future);
    bayesFailureTimeHi = findCrossingTime(yhi_b, RedLev, t_future);
    bayesFailureTimeLo = findCrossingTime(ylo_b, RedLev, t_future);
    olsFailureTime = findCrossingTime(yfuture, RedLev, t_future);
    olsFailureTimeHi = findCrossingTime(yhi, RedLev, t_future);
    olsFailureTimeLo = findCrossingTime(ylo, RedLev, t_future);

    % draw a plot if i = {6, 8, 10, 14}
```

```
    if i == 8 || i==10 || i==6 || i==14
    hndl =[];
    u1 = sigma^2*diag(eye(length(T_future)) + T_future*V*T_future');
    u2 = (B1(2)^2)*t_future.^2 +B0(2)^2;
    utmp = (u1./u2);
    hndl(1) = plot(t_future(1:i), utmp(1:i),'b'); hold on;
    plot(t_future(i), utmp(i),'bo');
    plot(t_future(i+1:end), utmp(i+1:end),'b:');
    a = axis;
    hndl(3) = plot(a(1:2), ones(1,2),'r-.');
    hold on;
    xlabel('Time Units');  ylabel('Uncertainty Ratio');
    t(i)
    axis([a(1:2) 0 10]);
    end
    trueTTF(i) = failureTime-t(i);
    bayesTTF(i,:) = [bayesFailureTime bayesFailureTimeHi
bayesFailureTimeLo] ;
    olsTTF(i,:) = [olsFailureTime olsFailureTimeHi olsFailureTimeLo];
    drawnow;
end

olsTTF = olsTTF - repmat(t,1,3);
bayesTTF = bayesTTF - repmat(t,1,3);
popTTF = repmat([MTTF Tup Tlo],length(t),1) - repmat(t,1,3);
hndl = [];
figure
hndl(1) =
plot(t(startIndx:end),trueTTF(startIndx:end),'b:','linewidth',2); hold
on;
hndl(2) =
plot(t(startIndx:end),bayesTTF(startIndx:end,1),'m','linewidth',2);
hndl(3) = plot(t(startIndx:end),olsTTF(startIndx:end,1),'g-
.','linewidth',2);
hndl(4) = plot(t(startIndx:end),popTTF(startIndx:end,1),'k-
.','linewidth',2);
a = axis;
plot(a(1:2),zeros(1,2),'k:');
plot(t(startIndx)*ones(1,2),a(3:4),'k:');
axis([a(1) 8.5 -1 9]);

indx = t([startIndx:end end:-1:startIndx])';
indx1 = [bayesTTF(startIndx:end,3)' bayesTTF(end:-1:startIndx,2)']';
indx1(find(isinf(indx1)==1)) = 100;
fill(indx,indx1,'m', 'FaceAlpha', 0.2, 'EdgeColor', 'none' );
indx2 = [olsTTF(startIndx:end,3)' olsTTF(end:-1:startIndx,2)']';
indx2(find(isinf(indx2)==1)) = 100;
fill(indx,indx2,'g', 'FaceAlpha', 0.2, 'EdgeColor', 'none' );
indx3 = [popTTF(startIndx:end,3)' popTTF(end:-1:startIndx,2)']';
fill(indx,indx3,'k', 'FaceAlpha', 0.1, 'EdgeColor', 'none' );
xlabel('Time, hrs'); ylabel('Time-to-Failure, hrs');
legend(hndl,'True TTF','Bayesian Estimate','OLS Estimate','Population-
based TTF');
title('True and Estimated Time-to-Failure');
```

Appendix 5. An example of the Bayesian prediction

```
k = 33;
alpha = 0.05;   % (1-alpha)*100% confidence
t_future = linspace(0,24,2*Nt)';
[failureTime, ystar, indx] = findCrossingTime(y(:,k), RedLev, t);
trueTTF = [];  olsTTF = []; bayesTTF = [];
startIndx = 5;

for i=startIndx:1:Nt
    handydata = 1:i;
    X = t(handydata);
    Y = y(handydata,k);
    X1 = [ones(size(X)) X];
    N1 = size(X,1); P1 = size(X1,2);
    [b bint r rint stats] = regress(Y,X1);
    Yhat = X1*b;
    e = Y - Yhat;
    s2 = sumsqr(e)/(N1-P1);
    Sxx = sumsqr(X-mean(X));
    ta = tinv(1-alpha/2,N1-(P1+1));
    T_future = [ones(size(t_future)) t_future];
    yfuture = T_future*b;
    V = inv(X1'*X1);
    ylo = yfuture - ta*sqrt(s2)*sqrt(1+diag(T_future*V*T_future'));
    yhi = yfuture + ta*sqrt(s2)*sqrt(1+diag(T_future*V*T_future'));
    Thi_i = findCrossingTime(ylo, RedLev, t_future);
    Tlo_i = findCrossingTime(yhi, RedLev, t_future);
    T_i = findCrossingTime(yfuture, RedLev, t_future);

% Bayesian Approach-----------------------------------------------------
    Sigma = diag(Sprior.^2);
    Bprior = Bprior;
    Vprior = Sigma./sigma^2;
    Vpost = inv(inv(Vprior) + X1'*X1);
    Bpost = Vpost*(inv(Vprior)*Bprior + (X1'*X1)*b);
    NuSprior = (Nt-P1)*sigma^2;
    NuSpost = NuSprior+(N1-P1)*s2+diag(inv(Vprior+X1'*X1)).*(b-
Bprior).^2;
    VarBpost = Vpost.*NuSpost(1)/(N1-P1);
    Spost = NuSpost(1)/Nt;
    % Make a prediction
    y_b = T_future*Bpost;
    yhi_b = y_b+tinv(1-alpha/2,Nt+N1-
P1)*sqrt(Spost.*diag(eye(size(T_future,1)) +
T_future*VarBpost*T_future'));
    ylo_b = y_b-tinv(1-alpha/2,Nt+N1-
P1)*sqrt(Spost.*diag(eye(size(T_future,1)) +
T_future*VarBpost*T_future'));
    %---------------------------------------------------------------
    bayesFailureTime = findCrossingTime(y_b, RedLev, t_future);
    bayesFailureTimeHi = findCrossingTime(yhi_b, RedLev, t_future);
    bayesFailureTimeLo = findCrossingTime(ylo_b, RedLev, t_future);
    olsFailureTime = findCrossingTime(yfuture, RedLev, t_future);
```

```
    olsFailureTimeHi = findCrossingTime(yhi, RedLev, t_future);
    olsFailureTimeLo = findCrossingTime(ylo, RedLev, t_future);

      hndl = [];
      hndl(2) =  plot(t,y(:,k),'c'); hold on;
    indx = t_future([1:3:end end:-3:1])';
    indx1 = [yhi(1:3:end)' ylo(end:-3:1)'];
    fill(indx,indx1,[.42 .72 .90], 'FaceAlpha',0.3,'EdgeColor','none');
    indx2 = [yhi_b(1:3:end)' ylo_b(end:-3:1)'];
    fill(indx,indx2,[.90 .72 .42], 'FaceAlpha', 0.99, 'EdgeColor',
'none' );
    hndl(3) = plot(t_future,yfuture,'g','linewidth',2);
    hndl(1) = plot(X,Y,'b','linewidth',3); hold on;
    hndl(4)=    plot(t_future,y_b,'m','linewidth',2);
    plot(t_future,ylo_b,'g:');
    plot(t_future,yhi_b,'g:');
    plot(t_future,ylo,'k:');
    plot(t_future,yhi,'k:');
    axis([0 15 0 15]);
    a = axis;
      hndl(5) = plot(a(1:2),RedLev*ones(1,2),'r-.','linewidth',4);    %
threshold level
    plot(ones(1,2)*MTTF,a(3:4),'k:','linewidth',2);
    plot(ones(1,2)*Tup,a(3:4),'b:','linewidth',2);
    plot(ones(1,2)*Tlo,a(3:4),'b:','linewidth',2);
    indx1 = [0 Tlo Tup 0];
    indx2 = [B0(1)+2*B0(2) RedLev RedLev B0(1)-2*B0(2)];
    hold off;
    trueTTF(i) = failureTime-t(i);
    bayesTTF(i,:) = [bayesFailureTime bayesFailureTimeHi
bayesFailureTimeLo] ;
    olsTTF(i,:) = [olsFailureTime olsFailureTimeHi olsFailureTimeLo];
    legend(hndl,'Observed Pathway','Future Pathway','OLS
Prediction','Bayesian Prediction','Threshold');
    xlabel('Time, t'); ylabel('Degradation, Y(t)');
%    title(sprintf('Time=%2.2f, Size:%d',t(i),N1));
    drawnow;
    pause
end

olsTTF = olsTTF - repmat(t,1,3);
bayesTTF = bayesTTF - repmat(t,1,3);
popTTF = repmat([MTTF Tup Tlo],length(t),1) - repmat(t,1,3);

figure
hndl(1) =
plot(t(startIndx:end),trueTTF(startIndx:end),'b:','linewidth',2);hold
on;
hndl(2) =
plot(t(startIndx:end),bayesTTF(startIndx:end,1),'m','linewidth',2);
hndl(3) = plot(t(startIndx:end),olsTTF(startIndx:end,1),'g-
.','linewidth',2);
hndl(4) = plot(t(startIndx:end),popTTF(startIndx:end,1),'k-
.','linewidth',2);
```

```
a = axis;
plot(a(1:2),zeros(1,2),'k:');
plot(t(startIndx)*ones(1,2),a(3:4),'k:');
axis([a(1) 8.5 -1 9]);

indx = t([startIndx:end end:-1:startIndx])';
indx1 = [bayesTTF(startIndx:end,3)' bayesTTF(end:-1:startIndx,2)']';
indx1(find(isinf(indx1)==1)) = 100;
fill(indx,indx1,'m', 'FaceAlpha', 0.2, 'EdgeColor', 'none' );
indx2 = [olsTTF(startIndx:end,3)' olsTTF(end:-1:startIndx,2)']';
indx2(find(isinf(indx2)==1)) = 100;
fill(indx,indx2,'g', 'FaceAlpha', 0.2, 'EdgeColor', 'none' );
indx3 = [popTTF(startIndx:end,3)' popTTF(end:-1:startIndx,2)']';
fill(indx,indx3,'k', 'FaceAlpha', 0.1, 'EdgeColor', 'none' );
xlabel('Time, hrs'); ylabel('Time-to-Failure, hrs');
legend(hndl,'True TTF','Bayesian Estimate','OLS Estimate','Population-
based TTF');
title('True and Estimated Time-to-Failure');
return
```

VITA

Alexander Usynin was born on February 4, 1973 in the former USSR. He entered Moscow Institute of Physics and Engineering (Obninsk, Russia) in 1990 and received a Bachelor of Science and a MS degree in Automated Control Systems in 1994 and 1996, respectively. After graduating from Moscow Institute of Physics and Engineering he worked at a nuclear power plant (Balakovo, Russia) as a systems analyst from 1996 to 2002.

He entered the Nuclear Engineering graduate program at the University of Tennessee in 2003. In the fall of 2005, he worked at Sun Microsystems, Inc as a graduate student intern in the physical sciences center.

The following is a list of publications pertinent to the contributions made in the dissertation.

Usynin, A., Hines, J.W., "Prognostics-Driven Optimal Control for Equipment performing in Uncertain Environment", submitted to the *2008 IEEE Aerospace Conference*, Big Sky, MT, March 2008

Usynin, A., Hines, J.W., and Urmanov A.M., "Uncertain Failure Thresholds in Cumulative Damage Models", submitted to *the Annual Reliability and Maintainability Symposium (RAMS)*, Las Vegas, NV, January 2008

Hines, J.W., Usynin,A., "Current Computational Trends in Equipment Prognostics", to appear in *International Journal of Computational Intelligence Systems*, December 2007

Usynin, A. and Hines, J.W., "Uncertainty Management in Shock Models Applied to Prognostic Problems", *The 2007 AAAI Fall Symposium on Artificial Intelligence for Prognostics*, Arlington, VA, November 2007

Usynin, A., Hines J.W., Rasmussen B., “Use of Linear Growth Models for Remaining Useful Life Prediction”, *Proc. of Maintenance and Reliability Conf.* (*MARCON*), Knoxville, TN, May 2007

Usynin, A., Hines, J.W., Urmanov, A., "Formulation of Prognostics Requirements", *Proc. of the 2007 IEEE Aerospace Conference*, Big Sky, MT, March 2007

Hines, J.W., Usynin, A., Urmanov, A., "Prognosis of Remaining Useful Life for Complex Engineering Systems", *5th International Topical Meeting on Nuclear Plant Instrumentation Control, and Human Machine Interface Technology, (NPIC&HMIT)*, Albuquerque, NM, November 2006

Usynin, A., "Model-Fitting Approaches to Reliability Assessment and Prognostic Problems", *Journal of Pattern Recognition Research*, Vol.1, No.1, January 2006